Technische Universität Berlin
School VI Planning Building Environment | Dept. of Civil Engineering
Chair of Water Resources Management and Modelling of Hydrosystems
Prof. Dr.-Ing. R. Hinkelmann

Paul Schütz

Assessing the effectiveness and resilience of Low Impact Development (LID) in a large urban area in Berlin

Master Thesis

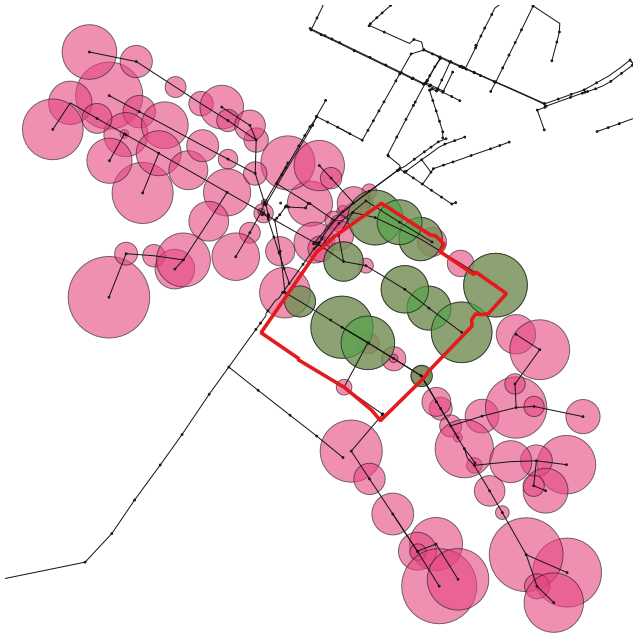

First examiner:	Prof. Dr.-Ing. R. Hinkelmann
Second examiner:	Dr. A. Matzinger
Advisor:	Dr. M. Riechel

March 2022

Declaration of Authorship

I declare that this thesis was composed by myself and that the work contained herein is my own except where explicitly stated otherwise by reference or acknowledgment.

Berlin, March 21, 2022 

Acknowledgments

Many people and projects have contributed to the success of this study. I would especially like to thank my two supervisors at the Kompetenzzentrum Wasser Berlin (KWB), Andreas Matzinger and Mathias Riechel. Both of them gave me advice and support in numerous discussions and meetings and were able to help me with their experience and knowledge, especially in modelling and R, when new problems, questions or results emerged.
I would also like to thank Prof. Hinkelmann, who guided the study in the right direction with his constructive criticism and comments.
Furthermore, I would like to express my special thanks to the Berliner Wasserbetriebe (BWB), which made it possible to carry out the work in the first place by providing data and models which were used in this study. Special mention should be made here of Michel Gunkel, who provided ideas and input for the project in numerous meetings and workshops.
Finally, I would also like to thank the research project *netWORKS4* and the borough of Pankow, whose preliminary work made the actual basis of the study possible.

Abstract

The increasing sealing of formerly natural surfaces in urban areas causes a change in the water balance. The consequences are far-reaching for humans, animals and the environment. For example, urban heat islands arise, but also the drainage systems of the cities are overloaded by the reduced infiltration and evaporation capacities. In order to relieve the system, water masses are discharged via combined sewer overflows into adjacent water bodies, causing additional damage to the affected ecosystems. A remedy for this can be decentralised stormwater management measures, also called Low Impact Developments (LIDs). These help to infiltrate or evaporate the precipitation on site and thus, ensure greater resilience of the converted areas. In the Berlin borough of Pankow, an urban redevelopment area is planned which was accompanied by the *netWORKS4* research project and which should support the participatory implementation of LIDs. In order to make the most suitable selection of LIDs, the concerns and needs of the residents were taken into account. This study examines the effectiveness of these planned LID measures. For this purpose, the urban redevelopment area including the LID measures was digitally mapped in the rainfall-runoff-routing model *SWMM*. A total of 10 scenarios were set up which were examined with regard to their surface runoff, resulting combined sewer overflows and their resilience according to the *Resilience Index*. These scenarios included the construction measures in the urban redevelopment area with and without LID measures but also eight failure scenarios that simulate the maintenance neglect of the LID measures. This work showed that within the urban redevelopment area, a reduction of over 90 % of the surface runoff into the sewage system could be achieved. Furthermore, the Berlin discharge limit of 10 l/s·ha could be maintained throughout. In the sewer catchment area of the urban redevelopment area, a surface runoff reduction of 16 % was achieved with a connected impervious area of 20 %. The combined sewer overflows could also be strongly reduced, some overflow events could be completely prevented. The combined sewer volume could be reduced by 23 %. The simulation of the failure scenarios also showed that neglecting the LID measures consistently leads to an increase in the surface runoff and combined sewer overflow volume. However, all failure scenarios still achieved significantly better results in terms of surface runoff volume, combined sewer volume and resilience than the urban redevelopment area without LID measures. The results of this study once again illustrate the effectiveness of the LID measures and the resulting increase in resilience to rain events.

Kurzzusammenfassung

Die zunehmende Versiegelung von vormals natürlichen Flächen in urbanen Gebieten sorgt für eine Veränderung der Wasserbilanz. Die Folgen daraus sind für Mensch, Tier und Umwelt weitreichend. Es entstehen beispielsweise urbane Hitzeinseln, aber auch die Entwässerungssysteme der Städte werden durch die verminderten Versickerungs- und Verdunstungskapazitäten überlastet. Zur Entlastung der Systeme werden anfallende Wassermassen über Mischwasserüberläufe in angrenzende Oberflächengewässer geleitet. Dies verursacht zusätzlichen Schaden für die betroffenen Ökosysteme. Abhilfe dafür können dezentrale Regenwasserbewirtschaftungsmaßnahmen, auch Low Impact Development (LID) genannt, sein. Diese ermöglichen das Versickern oder Verdunsten des anfallenden Niederschlags vor Ort und sorgen dadurch für eine höhere Resilienz der betroffenen Gebiete. Im Berliner Bezirk Pankow ist ein Stadtumbaugebiet geplant, welches vom Forschungsprojekt *netWORKS4* begleitet wird und die partizipative Umsetzung von LIDs fördern soll. Diesbezüglich wurden die Belange und Bedürfnisse der Bewohner berücksichtigt, um eine möglichst passende Auswahl an LIDs zu treffen. Diese Forschungsarbeit untersucht die Wirksamkeit ebendieser geplanten LID Maßnahmen. Hierzu wurde das Umbaugebiet samt LID Maßnahmen digital in dem Oberflächenabflussmodel *SWMM* abgebildet. Für diese Arbeit wurden insgesamt zehn Szenarien aufgestellt, welche hinsichtlich ihres Oberflächenabflusses, der resultierenden Mischwasserüberläufe und ihrer Resilienz nach dem *Resilienz Index* untersucht wurden. Diese Szenarien beinhalteten zum einen die Baumaßnahmen im Stadtumbaugebiet mit und ohne LID Maßnahmen, aber auch acht Ausfallszenarien, welche die Pflege Vernachlässigung der LID Maßnahmen simulieren. Durch dieser Arbeit konnte aufgezeigt werden, dass innerhalb des Stadtumbaugebietes eine Reduktion von über 90 % des Oberflächenabflusses erzielt werden konnte. Des weiteren konnte die Berliner Einleitebeschränkung von 10 l/s·ha durchgehend eingehalten werden. Im Pumpwerkeinzugsgebiet des Umbaugebietes konnte eine Oberflächenabflussreduktion von 16 % bei einer angeschlossenen versiegelten Fläche von 20 % erzielt werden. Auch die Mischwasserüberläufe konnten stark reduziert werden. So konnten für den Untersuchungszeitraum einige Überlaufevents komplett verhindert und das Mischwasservolumen um 23 % reduziert werden. Die Simulation der Ausfallszenarien hat außerdem gezeigt, dass eine Vernachlässigung der LID Maßnahmen durchgehend zu einer Erhöhung des Oberflächenabflusses und Mischwasserüberlaufvolumens führt. Jedoch erzielten alle Ausfallszenarien immer noch deutlich bessere Ergebnisse hinsichtlich des Oberflächenabflussvolumens, Mischwasservolumens und der Resilienz als die Umsetzung ohne LID Maßnahmen. Die Ergebnisse dieser Arbeit verdeutlichen einmal mehr die Wirksamkeit der LIDs und die dadurch erhöhte Resilienz gegenüber Regenereignissen.

Contents

List of Figures

List of Tables

List of Abbreviations

approx.	approximately	**KWB**	Kompetenzzentrum Wasser Berlin
BlnXI	Sewer Catchment BlnXI	**LID**	Low Impact Development
BWB	Berliner Wasserbetriebe	**NSE**	Nash-Sutcliffe Efficiency
CSO	Combined Sewer Overflow	**PS**	partially sealed
CSS	Combined Sewer System	**Res**	Resilience
e.g.	exempli gratia	**Sev**	Severity
EGR	Extensive Green Roof	**SSS**	Separated Sewer System
Fig.	Figure	**SW**	Service Water
FR	Flat Roof	**SWMM**	Storm Water Management Model
FS	fully sealed	**Tab.**	Table
IGR	Intensive Green Roof	**TTE**	Trough-Trench Element
IS	Infiltration Swale	**URA**	Urban Redevelopment Area
IW	Irrigation Water	**WC**	Water Concept

1. Introduction & Research Questions

The imperviousness of urban areas has a strong impact on the local water balance. The construction of buildings and roads shifts the water balance from the natural state, which is characterised by a large share of evaporation and infiltration, to a water balance in which surface runoff becomes dominant [Sieker, 2022c]. This has a direct impact on humans, animals and the climate. The urban heat island effect, for example, which is characterised by a significantly higher temperature in the city compared to rural areas, has direct consequences for young children, elderly and vulnerable people and can cause higher mortality rates, caused by the reduced evaporation share [Norton et al., 2015]. Furthermore, the usual drainage systems in cities are reaching their limits due to high surface runoff during large and extreme rain events. As a result, the water is discharged into neighbouring water bodies via emergency outlets. The consequences for the ecosystem and its inhabitants range from fish mortality due to contaminated water, to altered riverbeds or even bathing bans for people [Riechel et al., 2020; Locatelli et al., 2019]. These negative side effects of impervious urban areas are likely to be aggravated in the future due to the effects of climate change with more intense rain events and longer heat spells, as well as urbanisation and urban redensification [Westra et al., 2014; Zhou et al., 2018].

Being recognised by politics in Berlin, rainwater discharge restrictions have been passed. These state that rainwater must be managed sustainably so that the consequences of climate change are prevented and natural and harmless drainage conditions are guaranteed in surface waters. This results in the goal of disconnecting 1 % of Berlin's sealed surface area from the existing sewer systems per year and a sewer discharge limit of $< 10\,\mathrm{l/s{\cdot}ha}$ for the connected areas [SENUVK, 2022]. These discharge restrictions and negative effects such as heat islands can be met and counteracted by decentralised rainwater management measures, also called Low Impact Developments (LIDs) [Gill et al., 2007]. LIDs can be implemented in various forms, such as green roofs, troughs, infiltration trenches or green facades in the city [Pallasch, 2021; Riechel et al., 2016].

The research project *netWORKS4* has set itself the goal of learning how LID measures can be integrated in a participatory process. One case study was located in a Berlin borough, in which a large housing construction project is planned. Through an individual selection of LIDs, the needs of all stakeholders are intended to be met. To achieve this, LID measures for various local areas were decided upon with the residents as well as with urban planners, and some of them have already been implemented [Nenz et al., 2020]. However, the effectiveness and impact of these measures still needs to be assessed.

Specifically, the impact on local surface runoff and the resulting impact on the Combined Sewer Overflows (CSO) are of importance at city scale, being an important goal of the EU Water Framework Directive [SEVGUV, 2009]. Several studies indicate the positive impact of decoupling stormwater on CSO occurrence [Riechel et al., 2016; Riechel et al., 2020]. However, the impacts of realistically planned measures that are limited to an urban redevelopment area, is unknown. Moreover the investigation of coupled stormwater measures at catchment scale lack research. These questions can be investigated through digital modelling, for example by using the software *Storm Water Management Model (SWMM)*. Although decentralised stormwater management is more and more common, there are still reservations regarding their functionality if these measures become a dominant element of urban drainage concepts. Therefore, the question of how susceptible to damage and failure the LID measures are and how this affects their performance will be investigated. For this purpose, specific failure scenarios were set up with the help and expertise of the local water operators and were simulated using *SWMM*.
Since resilience to climate change is a common goal among cities, the present work aims at assessing the resulting change in the resilience of the area on the basis of a quantitative evaluation. For this purpose, the elusive concept of resilience is to be quantified using a *Resilience Index*.

This results in the following research questions for this thesis:

- Performance of a realistic implementation of LIDs in an urban redevelopment area:
  - How do the LID measures affect the study site in terms of surface runoff?
  - Can the discharge restrictions of the federal state of Berlin be met by implementing the LID measures in the study site?
  - How do the LID measures affect the whole catchment area in terms of surface runoff and discharge restrictions?
  - How does the Combined Sewer Overflow of the catchment area change and therefore how can negative effects on the environment be reduced?
- Performance of LIDs:
  - How does the performance of the LID measures react to partial failure caused by neglect of maintenance?

- Resilience assessment:
  - Can resilience of these scenarios be assessed and what are the potential of this assessment?

To answer these questions, the study is divided into five sections covering the theoretical background of this thesis, the material and methods used, the presentation of the results and the conclusion that can be drawn.
This introduction is followed by the theoretical part of the study in Sec. 2, which includes the calculation approaches of the *SWMM* software used for modelling, the various stormwater management possibilities and the fundamentals of resilience assessment. In Sec. 3, the data, materials and methods used are considered, including the urban redevelopment area investigated, the data basis for *SWMM*, as well as the compilation of the various model scenarios simulated. Afterwards, the results are discussed in Sec. 4, which include the model transfer from *InfoWorks* to *SWMM*, the plausibility test of the LID chains and the analysis of the model scenarios. Here, the main focus is on the analysis of the different scenarios and the effects to be observed with regard to the surface runoff and combined sewer overflow. Finally in Sec. 5, a conclusion is made and an outlook for further possible research questions is given.

2. Theory

2.1. Rainfall-Runoff Models

Rainfall-runoff models are used in water management to simplify the representation of hydrological processes taking place in reality in a simplified way. A precipitation event, such as rainfall or snowfall, is used as an input signal and the model responses with a runoff, the output signal. This takes place in a previously defined area, so called catchment area. The primary goal is to simulate the models respond as accurate as possible, based on the input signal.Therefore it is necessary to create a model which represents the properties of the catchment area as simple as possible, but as complex as needed [Funke, 2019].

Models come with different possibilities to calculate processes, spatial resolutions and simplicity grades. Resulting from that, models can be classified differently. Here a short classification of Sitterson et al. (2018) is shown, where the models were classified based on their model structure:

- **Empirical models**, also called data-driven models, use non-linear statistical relationships between inputs and outputs. Resulting from that, empirical models are best used, when other outputs are not needed, *e.g.*, the distribution of runoff values between upstream and downstream areas cannot be calculated with this model type. Positive aspects are that empirical models need very few parameters and are easy to use, since they have no physical connection to the catchments. This leads to simplicity of implementation, fast computational times, and cost effectivenes [Sitterson et al., 2018].
- **Conceptual models** interpret runoff processes by connecting simplified components in the overall hydrological process. Reservoir storages and simplified physical equations of the processes provide a conceptual idea of the behaviour in the catchment. Conceptual models need a range of parameters and meteorological input data. Advantages of conceptual models are easy usage, easy calibration and low computational time. A disadvantage is the coarse representation of catchments. Often conceptual models are called semi-physical models, since they are based on water balance equations [Sitterson et al., 2018].
- **Physical models** are based on the understandings of the physics related to hydrological processes. General physic laws and principles are used, including water balance equations, conservation of mass and energy, momentum, and kinematics.

One of the greatest strength of physical models is the connection between model parameters and physical catchments characteristics, which makes them more realistic. Resulting from that, most physical models give a three-dimensional view of the water exchange within the soil, surface, and air. Physical models are best used when precise data is available, physical properties of the hydrological processes are accurately understood, and application on small scales, due to computational time, is done. A disadvantage is the oftentimes resulting high computational time [Sitterson et al., 2018].

2.1.1. SWMM 5.1.015

In this work, the *EPA Storm Water Management Model (SWMM) Version 5.1.015* was used to simulate surface runoff and LID measures in various scenarios. *SWMM* is a dynamic rainfall-runoff simulation model for single event or long-term simulation, used for runoff quantity or quality purposes. It classified as a semi-physical model, since it is physically based and employs principles of conservation of mass, energy and momentum wherever appropriate, but conceptualises in other parts, such as the surface runoff. The software is available freely and was first developed in 1971 by the U.S. Environmental Protection Agency. Through the years it has undergone several major updates and today is used widely in the world of planning, analysis and design related to any water systems in urban areas [Rossman et al., 2015].

2.1.2. SWMM Calculation Approaches

Various processes, as seen in Fig. 2.1, can be modelled in *SWMM*. The different calculation approaches of the significant processes used in this work, such as surface runoff, evaporation, infiltration, hydraulic routing, and LID representation are explained in detail in the following.

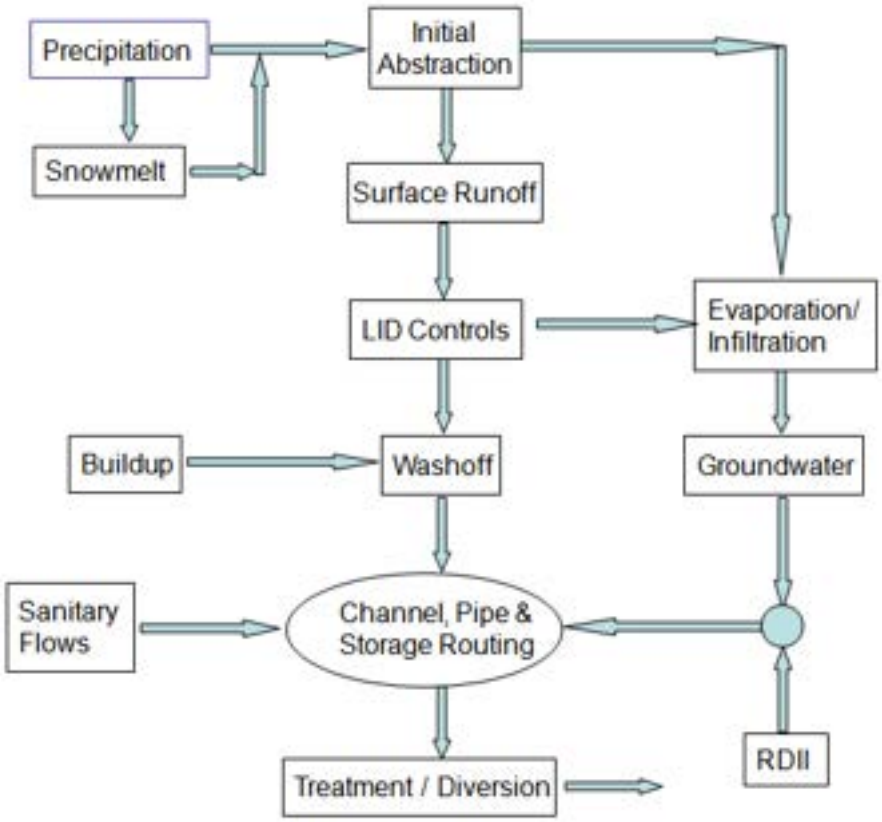

Figure 2.1: Processes in *SWMM* [Rossman et al., 2015]

2.1.2.1. Surface Runoff

SWMM designs subcatchments as rectangular surfaces, which are provided with a constant slope S and width W that drain to a single outlet channel (Fig. 2.2). Overland flow is generated by modelling the subcatchment as a nonlinear reservoir. Subcatchments can receive inflow via precipitation (rainfall and snowfall) and losses can be generated via infiltration or evaporation. The excess stores on top of the subcatchment surfaces to a depth d. Water which exceeds the depression storage d_s becomes runoff (Fig. 2.2).

Surface ponding, interception by flat roofs, vegetation and surface wetting all account as depression storage d_s [Rossman et al., 2015].

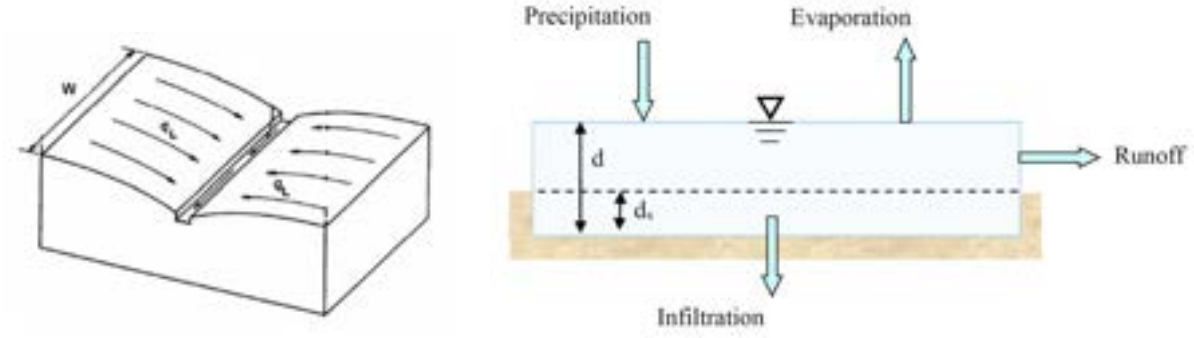

Figure 2.2: Idealised representation of a subcatchment and conceptual view of surface runoff [Rossman et al., 2015]

To express the explained processes in an equation, the law of conservation of mass is used. The net change in depth d per unit of time t is simply the difference between inflow and outflow rates over the subcatchment:

$$\frac{\partial d}{\partial t} = i - e - f - q \tag{2.1}$$

where i (m/s) is the rate of rainfall + snowmelt, e (m/s) is the surface evaporation rate, f (m/s) is the infiltration rate and q (m/s) is the runoff rate.
Assuming that the discharge on the subcatchment surface behaves uniformly as in a channel with width W, height $d - d_s$, and slope S the surface runoff Q (cm/s) is calculated according to the Manning-Strickler equation:

$$Q = \frac{1.49}{n} S^{1/2} R^{2/3} A \tag{2.2}$$

where n is the surface roughness coefficient (s/m$^{1/3}$), S is the average slope of the subcatchment (m/m), A the area across the subcatchment's width through which the runoff flows (m^2) and R is the hydraulic radius associated with this area (m) [Rossman et al., 2015].

2.1.2.2. Evaporation

SWMM can use evaporation rates from different sources, such as (i) a single constant value, (ii) a set of monthly average values, (iii) a user-defined time series of daily values,

(iv) daily values read from an external climate file, or (v) daily values computed from the daily temperatures in an external climate file. The data can be used for evaporation simulation for:

- standing water on subcatchment surfaces
- subsurface water in groundwater aquifers
- open channel water flow
- water in storage units
- water held in LIDs, such as green roofs or infiltration swales.

Evaporation from LID measures (see Sec. 2.1.2.5) is calculated for each layer that can evaporate (surface layer, soil layer). The potential evaporation is covered by the available water of the layers starting from the top, the surface layer. If the demand of potential evaporation is not covered any longer, water from the next layer, the storage layer is evaporated [Rossman et al., 2015].

2.1.2.3. Infiltration

Various simplification approaches have been developed to model infiltration. Since there are different opinions about which approach is the best, the *SWMM* user can chose between the following infiltration methods:

- Horton's Method
- Modified Horton Method
- Green-Ampt Method
- Modified Green-Ampt Method
- Curve Number Method

In this work the *Modified Horton Method* was used, where Horton proposed the following exponential equation to predict the reduction in infiltration capacity over time:

$$f_p = f_\infty + (f_0 - f_\infty)\, e^{-k_d t} \tag{2.3}$$

where f_p is the infiltration capacity into soil (m/s), f_∞ is the minimum or equilibrium value of f_p (at t = ∞) (m/s), f_0 is the maximum or initial value of f_p (at t = 0) (m/s), t is time from beginning of the precipitation (s) and k_d is the decay coefficient (s^{-1}). Graphically shown (see Fig. 2.3), the infiltration capacity decreases with time t due to the saturated soil, resulting from that, the runoff is increasing [Rossman et al., 2015].

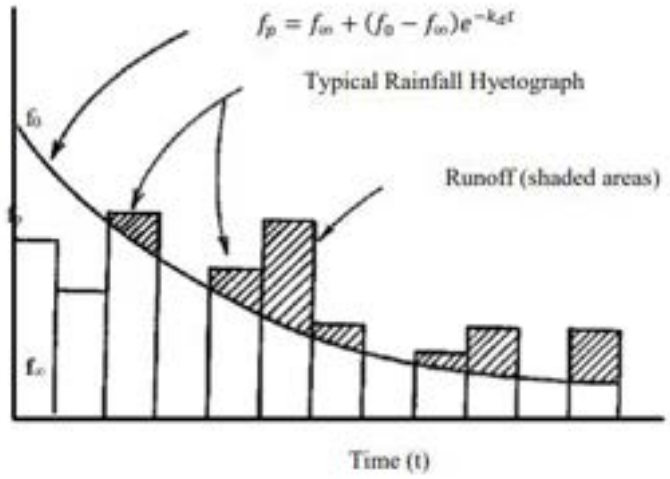

Figure 2.3: Horton infiltration curve [Rossman et al., 2015]

2.1.2.4. Hydraulic Routing Models

The hydraulic routing for channel and pipe flow in *SWMM* can be simulated based on three different approaches. The *Steady Flow* for preliminary analysis and the *Kinematic Wave* and *Dynamic Wave* approaches for further simulation. It must be added, that partial pipe flow is treated as channel flow, if pressurised flow occurs the Hazen-Williams or Dary-Weisbach equation can be used.

Steady Flow

Steady Flow routing is the simplest form of flow calculation. Here, the discharge is calculated uniformly and continuously in each computational time step. It transfers the inflow hydrograph at the upstream end of a conduit to the downstream end of the conduit with no delay or change in shape. Many hydraulic processes in sewer networks, such as backwater effects, initial losses, reversed flow directions, or flow under pressure cannot be modelled. For these reasons, the method should only be used for a rough preliminary analysis of long-term continuous effects [Rossman et al., 2015].

Kinematic Wave

The *Kinematic Wave* routing is derived from a simplified form of the St. Venant equation and uses the continuity equation and the uniform flow equation to calculate the flow in the channels. Thereby the water surface has the same inclination as the conduit and only a full non-pressurised discharge is possible. Compared to steady flow routing, the discharge in the channel can vary both spatially and temporally, allowing attenuated or delayed hydrographs. Numerical stability can be maintained with time steps of 1 to 5 minutes. It is not possible to model pressurised flow, reverse flow or backwater effects [Rossman et al., 2015].

Dynamic Wave

The *Dynamic Wave* routing uses the complete form of the St. Venant flow equations and therefore is the most accurate method. It can account for channel storage, backwater effects, entrance/exit losses, flow reversal and pressurised flow. It is the method of choice for systems subjected to significant backwater due to downstream flow restrictions and with flow regulation via weirs and orifices. Resulting from that, small time steps have to be used to maintain numerical stability. For the discharge in the sewer network, the continuity equation (2.4) and the momentum equation (2.5) are applied:

$$\frac{\partial A}{\partial t} + \frac{\partial Q}{\partial x} = 0 \tag{2.4}$$

where A is the flow across sectional area (m^2), t is the time (s), Q is the flow rate (cm/s) and x is the distance (m).

$$\frac{\partial Q}{\partial t} + \frac{\partial \left(Q^2/A\right)}{\partial x} + gA\frac{\partial H}{\partial x} + gAS_f = 0 \tag{2.5}$$

where x is the distance (m), t is the time (s), A is the flow across sectional area (m^2), Q is the flow rate (cm/s), H is the hydraulic head of water in the conduit (Z+Y)(m), Z is the conduit invert elevation (m), Y is the conduit water depth (m), S_f is the friction slope (head loss per unit length) and g is the acceleration of gravity (m/s^2).
The water level in the junctions is calculated via the volume continuity equation (2.6):

$$\frac{\partial H}{\partial t} = \frac{\sum Q}{A_{SN} + \sum A_{SL}} \tag{2.6}$$

where H is the head (m), t is the time (s), $\sum Q$ is the net flow into the node assembly (inflow - outflow) (cm/s), A_{SN} is the storage node surface area (m^2) and $\sum A_{SL}$ is the surface area contributed by the connected link (m^2) [Rossman et al., 2015].

2.1.2.5. Low Impact Developments (LID)

For the analysis of Decentralised Stormwater Management measures (Sec. 2.2.2), *SWMM* has the advantage of already implemented *Low Impact Development (LID)* units. Those are represented as a combination of individual layers and can be customised through different parameter values for the representation of various LID measures. A typical LID structure, which was used for the representation of all LIDs in this work, is the three-layer structure of a bio-retention cell. As seen in Fig. 2.4 the surface layer (top layer) can receive water via precipitation and runon from other areas and lose water through infiltration to the soil layer underneath, via evapotranspiration and by overflow if the LID units soil is saturated. The soil layer (middle layer) can only receive water from the surface layer, but can lose water through infiltration into the storage layer and via evapotranspiration. The storage layer (bottom layer) can only receive water through the soil layer above and lose water by infiltration into the ground and an underdrain system if selected [Rossman et al., 2015].

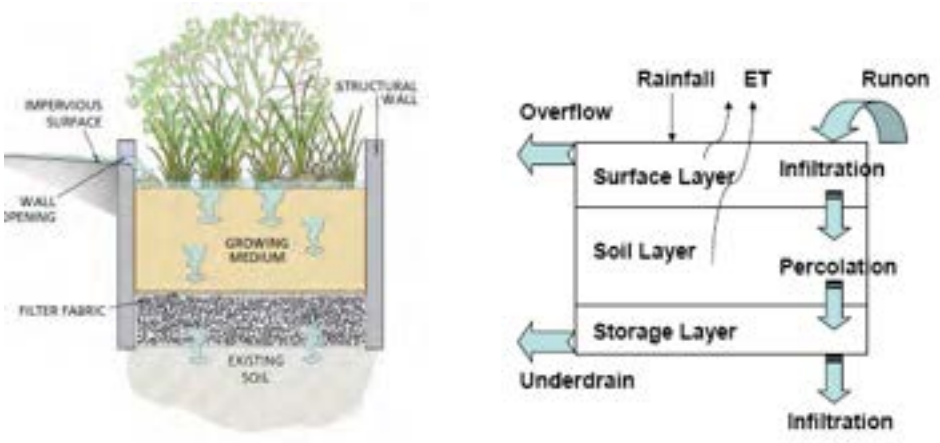

Figure 2.4: LID structure in *SWMM* [Rossman et al., 2015]

To simplify the calculation of the hydrologic performance of the LID units, some assumptions are made:

- The cross-sectional area of the unit remains constant throughout its depth
- Flow through the unit is one-dimensional in the vertical direction

- Inflow to the unit is distributed uniformly over the top surface
- Moisture content is uniformly distributed throughout the soil layer
- Matric forces within the storage layer are negligible so that it acts as a simple reservoir that stores water from the bottom up

With these assumptions LID units can be modelled by solving a set of simple flow continuity equations. Each equation describes the change in water content in a particular layer over time as the difference between the inflow and the outflow water flux rates that the layer receives, expressed as volume per unit area per unit time. This results in Equation 2.7 for the *Surface Layer*, Equation 2.8 for the *Soil Layer* and Equation 2.9 for the *Storage Layer* [Rossman et al., 2015].

$$\phi_1 \frac{\partial d_1}{\partial t} = i + q_0 - e_1 - f_1 - q_1 \tag{2.7}$$

where ϕ_1 is the void fraction of any surface volume, d_1 is the depth of water stored in the surface (m), i is the precipitation rate falling directly on the surface layer (m/s), q_0 is the inflow to the surface layer from runoff captured from other areas (m/s), e_1 is the surface evapotranspiration rate (m/s), f_1 is the infiltration rate of surface water into the soil layer (m/s) and q_1 is the surface layer runoff or overflow rate (m/s).

$$D_2 \frac{\partial \theta_2}{\partial t} = f_1 - e_2 - f_2 \tag{2.8}$$

where D_2 is the thickness of the soil layer (m), θ_2 is the soil layer moisture content (volume of water / total volume of soil), f_1 is the infiltration rate of surface water into the soil layer (m/s), e_2 is the soil layer evapotranspiration rate (m/s) and f_2 is the percolation rate of water through the soil layer into the storage layer (m/s).

$$\phi_3 \frac{\partial d_3}{\partial t} = f_2 - e_3 - f_3 - q_3 \tag{2.9}$$

where ϕ_3 is the void fraction of the storage layer (void volume/ total volume), d_3 is the depth of water in the storage layer (m), f_2 is the percolation rate of water through the soil layer into the storage layer (m/s), e_3 is the storage layer evapotranspiration rate

(m/s), f_3 is the exfiltration rate of water from the storage layer into native soil (m/s) and q_3 is the storage layer underdrain outflow rate (m/s) [Rossman et al., 2015].

2.2. Stormwater Management

There are several ways to manage stormwater in urban areas. Generally, stormwater management can be divided into two fields, *Centralised* and *Decentralised Stormwater Management*. Within the *Centralised Stormwater Management* it can be differentiated between *Combined* and *Separated Sewer Systems*, as seen in Fig. 2.5. The different management possibilities and consequences for environment and people are presented in the following.

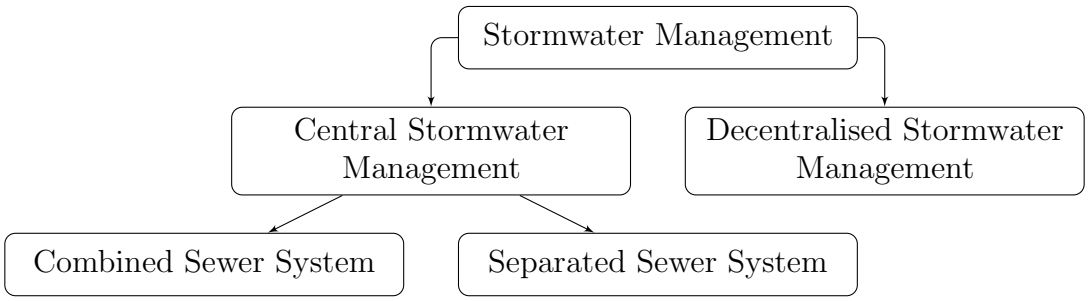

Figure 2.5: Stormwater management practices

2.2.1. Central Stormwater Management

The concept of *Centralised Stormwater Management* is based on the rapid discharge of accumulating precipitation via conduits. A distinction is made between *Combined Sewer Systems* and *Separated Sewer Systems*.

2.2.1.1. Combined Sewer System (CSS)

The *Combined Sewer System (CSS)* is a historically grown drainage method and is found today mainly in older settlements and inner cities. In the *CSS*, wastewater and rainwater are discharged in a single sewer (see Fig. 2.6), treated in a wastewater treatment plant and released through an outfall into close by water bodies. During dry weather, the cross-sections of the sewers are only slightly utilised, whereas in rainy weather, the cross-sections of the sewers, pumping stations and sewage treatment plants are quickly overloaded. To counteract this overload, *Combined Sewer Overflows* are installed at various locations in the system. The system can discharge into nearby water bodies

through these overflows, however in this case wastewater diluted with rainwater enters the environment and pollutes it (see Tab. 2.1) [Gujer, 2007].

2.2.1.2. Separated Sewer System (SSS)

The *Separated Sewer System (SSS)*, which is the current standard of stormwater management, discharges wastewater and rainwater in separate channels (see Fig. 2.6). Here, wastewater includes households and businesses, while rainwater includes runoff from roofs, streets and other sealed surfaces. Rainwater is partially treated and fed to close by water bodies, while foul water is fed to wastewater treatment plants and then returned to water bodies through the outfall of the wastewater treatment plant [Gujer, 2007].

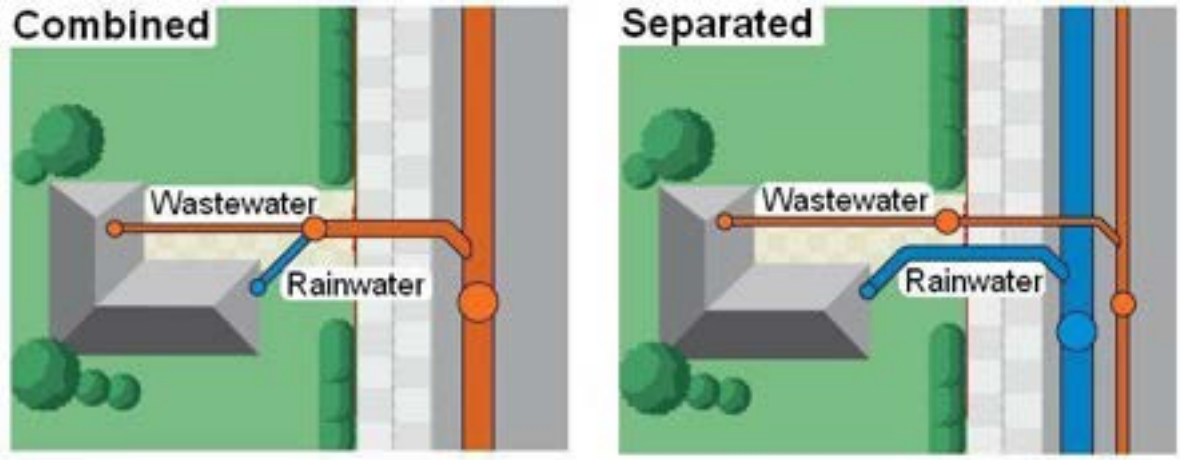

Figure 2.6: Comparison of combined and separated sewer system [FBG, 2022]

2.2.1.3. Effects of Central Stormwater Management

Effects on Water Balance

In recent decades, the sealing of formally natural surface by house and road construction has increased progressively. Increasing impervious surfaces have caused the amount of stormwater runoff to rise. Fig. 2.7 shows how the water balance is changing with increasing urbanization. Evaporation and infiltration decrease, while surface runoff increases significantly. This shift in the water balance has the effect of lowering groundwater levels due to reduced infiltration and increasing heat stress for people in urban areas resulting of a lack of evaporation. Another effect is that centralised stormwater management in form of *CSS* is reaching its capacity limits and is often no longer able to adequately discharge the accumulating precipitation water. Lately this could be observed by residents, *e.g.*,

the extreme rain in June 2017 in Berlin. However, even smaller rainfall events repeatedly lead to an overload of conventional systems. The effects of the resulting overflows will be shown in the following Sec. 2.2.1.3 [Sieker, 2022c].

Figure 2.7: Change of water balance due to urbanisation [Sieker, 2022c]

Effects of Combined Sewer Overflows

A consequence of sealing urban spaces is the increasing surface runoff as described in Sec. 2.2.1.3. This in turn results in an overloading of *CSS*. To relieve *CSS*, overflows are integrated into the system, which discharge into close by water bodies. These discharges cause acute and long term damages for the said water bodies, as shown in Tab. 2.1 [Gantner et al., 2011; Zhou, 2014].

Type of Effect	Type of Exposure	Indicator	Reference Value
acute (hours)	hydraulic	- shear stress - erosion, runoff	single event
	substance	- oxygen deficit - suspending substances - suspended solids, turbidity - toxic substances (NH_3)	single event
	hygienic	- pathogenic bacteria, viruses	single event
	aestethic	- odor, flotsam, coarse material	single event
delayed (days, weeks)	substance	- oxygen depletion (sediment) - toxis substances (NO_2,NH_3) - solids	single event
	hygienic	- bacteria, viruses (sediment)	single event
	aestethic	- floatsam, oil	single event
accumulative, chronic (weeks-years)	hydrological	- flow regime - morphology	Total load of a majority of events, Concentration in the sediment
	substance	- persistent organic compounds - heavy metals - formation of inorganic and organic sediments - oxygen depletion (eutrophic substances)	

Table 2.1: Effects of combined sewer discharges on streams, adapted from Gantner et al. (2011)

2.2.2. Decentralised Stormwater Management

According to Sieker (2022b), *Decentralised Stormwater Management* is based on the following six key components, which can be fulfilled by technical or non-technical measures. Therefore rainwater should be:

- retained locally
- used as drinking water substitute, e.g. service water or irrigation water
- evaporated to improve local climate
- enrich groundwater by infiltration
- treated by passing though soil
- if necessary discharged into a water body or sewage system at a reduced rate.

To be able to fulfil these key components, *Low Impact Development (LID)* measures are used. Ahiablame et al. (2012) defines LIDs as: "A green approach for stormwater management that seeks to mimic the natural hydrology of a site using decentralised micro-scale control measures by achieving water balance." The most common and in

this work used LIDs are introduced in the following sections in terms of their design and expected effects.

2.2.2.1. Extensive Green Roof (EGR) & Intensive Green Roof (IGR)

Green Roofs are a retention-based LID measure, which means that they retain rainwater to reduce the outflow. A distinction must be made between *Extensive Green Roofs (EGR)* and *Intensive Green Roofs (IGR)*.

Functional Description & Design

Extensive Green Roofs (EGR) have a single-layer of substrate with a thickness of 8 - 15 cm and bring a load capacity of 90 - 180 kg/m^2. The height of the vegetation is 10 - 40 cm, which means no tree vegetation is foreseen. They are not intended for residential use and require less maintenance compared to *IGR*. *EGR* can also be installed afterwards due to the thin substrate thickness and resulting low load [Riechel et al., 2017].
Intensive Green Roofs (IGR) have a substrate thicknesses of 15 - 100 cm. These are multi-layered and consist of a vegetation layer, a substrate layer, and a drainage layer. This allows to create garden landscapes with trees, paths, ponds, and swamp zones. Due to the thick substrate layers wide retention of rainwater can be achieved. Therefore, *IGR* can also be used as a compensatory measure in the absence of open spaces [Riechel et al., 2017].

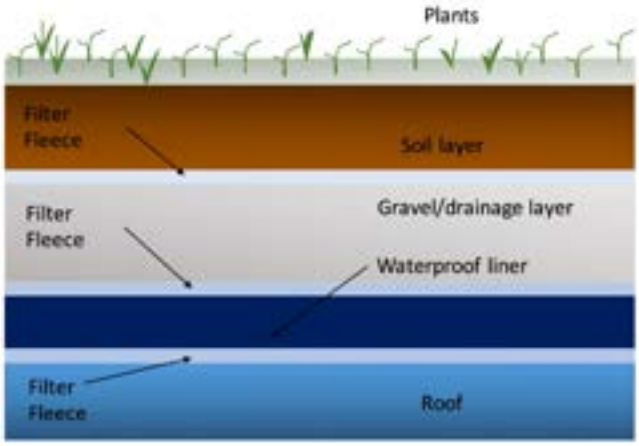

Figure 2.8: Typical cross-section of a green roof [Eckart et al., 2017]

LID Effects

Green Roofs have many positive effects. For this study, the effective runoff reduction is particularly important. Accumulating rainwater is temporarily stored in the various substrate layers or by plants, evaporates or is discharged with delay. This leads to a reduction of *Combined Sewer Overflows* and therefore less hydraulic stress in water bodies (see Tab. 2.1). Furthermore, the evaporation capacity may have a positive effect on the urban climate and the water balance. In addition, aesthetically pleasing green spaces are created in cities, increasing the biodiversity of fora and fauna [Riechel et al., 2017].

2.2.2.2. Infiltration Swale (IS)

Functional Description & Design

The primary function of an *Infiltration Swale (IS)* is to infiltrate rainwater from roofs, yards and traffic areas. An *IS* consists of an approximately 30 cm thick top layer and a subsoil which has a high infiltration capacity. Through the topsoil passage, a purification of the rainwater takes place before it enriches the groundwater. During heavy rainfall events, the rainwater can accumulate in the swale and run off with a time delay. However, it is important to note that the depth of the *IS* should not be more than 30 cm due to safety issues [Riechel et al., 2017].

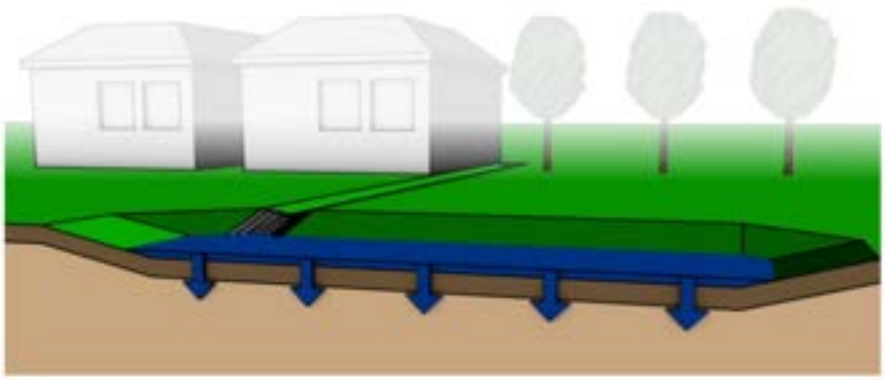

Figure 2.9: Structure of an infiltration swale [Riechel et al., 2017]

LID Effects

The most important aspect of an *IS* is the hydraulic and pollutant relief of water bodies, resulting of the increased infiltration capacity. Furthermore, an *IS* has a positive effect on the urban climate due to its evaporation capacity. In addition, the biodiversity of flora and fauna is promoted [Riechel et al., 2017].

2.2.2.3. Trough-Trench Element (TTE)

Functional Description & Design

Trough-Trench Elements (TTEs) are used to collect rainwater from roof and street surfaces for infiltration into the ground. They are mainly used when the land availability or the infiltration capacity of the soil is too low. The *TTE* has the structure of an *IS* on the surface and therefore offers above-ground retention potential. Below the surface, there are trough elements that provide underground storage space (see Fig. 2.11). Due to this additional storage space, *TTEs* require less space per connected area than *SI* or *IS* [Riechel et al., 2017].

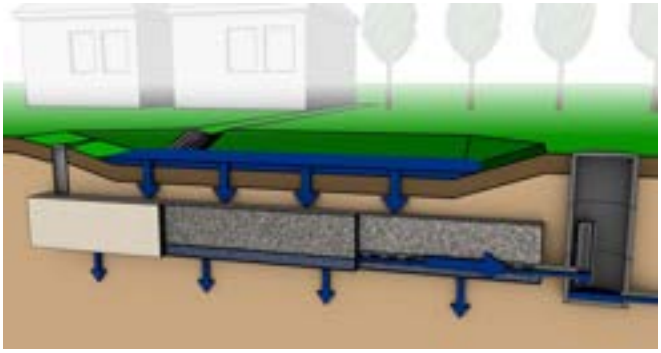

Figure 2.10: Trough-Trench Elements combined to a system [Riechel et al., 2017]

LID Effects

Since the *TTE* generally completely infiltrates the occurring rainwater, water bodies are significantly relieved, hydraulically and pollutionally. The high infiltration results in a considerably increased infiltration rate in terms of the local water balance and groundwater enrichment. Furthermore, the evaporation capacity increases, leading to an improvement of the urban climate. Lastly an improvement in biodiversity of flora and fauna is also achieved [Riechel et al., 2017].

2.2.2.4. Surface Infiltration (SI)

Functional Description & Design

In case of *Surface Infiltration (SI)*, the rainwater from sealed areas is drained into neighbouring green areas, where it infiltrates over a wide area. Infiltration takes place without significant accumulation in side areas. *SI* is used if sufficiently large open areas are available in relation to the connected sealed area. It is particularly suitable for smaller paved open spaces (courtyard areas, driveways, etc.) and small traffic areas with low traffic loads [Sieker, 2022a].

Figure 2.11: Surface infiltration [Sieker, 2022a]

LID Effects

SI has a positive impact on the hydraulic and pollutional relief of water bodies due to its infiltration performance. The increasing evaporation and the small heat capacity of the natural soil positively effects the urban climate. Furthermore, biodiversity can be significantly increased. Other positive aspects are low resource consumption and low investment costs [Sieker, 2022a; Riechel et al., 2017].

2.2.2.5. Permeable Pavement (PP)

Functional Description & Design

Permeable Pavement (PP) serves in its function as a substitute for fully sealed surfaces. *PP* is especially used in low-traffic streets, parking lots, sidewalks and bicycle paths. *PP* can be built in various designs, for example as water-bound surface layers, seepage paving, joint paving or grass pavers. However, the structure is always similar, consisting of a frost protection layer, a base layer, jointing material and the previously mentioned different pavements (see Fig. 2.12) [Riechel et al., 2017].

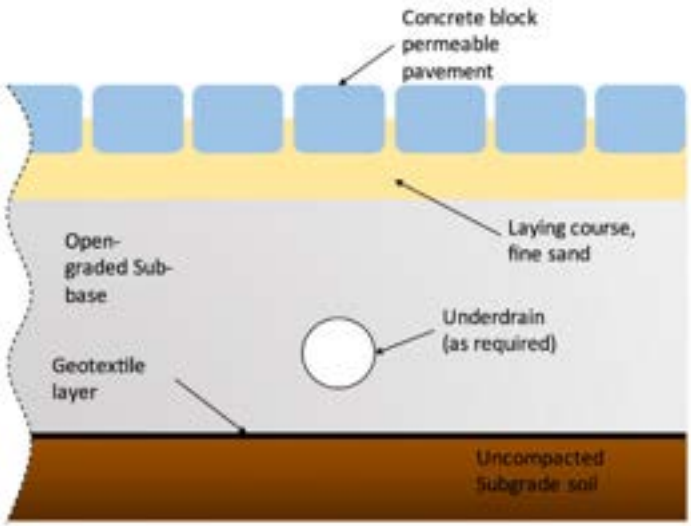

Figure 2.12: Structure of a permeable pavement [Eckart et al., 2017]

LID Effects

The effects of *PP* can be seen in the hydrological and pollutant relief of surface waters. In particular, this is made possible by the increased infiltration capacity, which also leads to a groundwater recharge. Despite the treatment capacity, a substance discharge into the groundwater cannot be completely ruled out. The effect can vary greatly due to the different design types and the different joint proportions of *PP*. Resulting of the increased evaporation rate, a slight reduction in heat stress and a reduction in tropical nights can be expected [Riechel et al., 2017].

2.2.2.6. Rainwater Usage as Service Water (SW) & Irrigation Water (IW)

Functional Description & Design

As previously described in Sec. 2.2.2, the substitution of drinking water by rainwater is also a part of *Decentralised Stormwater Management*. For this purpose, rainwater from roofs or traffic areas is collected. This water must first be mechanically filtered and then subjected to sedimentation in the collection basins. If the water is heavily polluted, flocculation, biological processes or ultraviolet disinfection can also be used for treatment. The water, which is usually collected underground in cisterns, is then transported to the place of use via a separate network of pipes. The cisterns are equipped with an emergency overflow for excessive amounts of water. Usage can be irrigation, toilet flushing or cleaning purposes [Riechel et al., 2017].

Figure 2.13: Rainwater usage [Riechel et al., 2017]

LID Effects

Rainwater harvesting can significantly reduce the volume of drinking water and wastewater. The use of rainwater also reduces operating costs and runoff. The pollution of surface waters can be reduced slightly to moderately by treating the rainwater beforehand. The initial investments vary widely, but the median is moderate. Since the cisterns are placed mostly underground, many aspects such as the urban climate, biodiversity or open space quality remain unaffected [Riechel et al., 2017].

2.3. Resilience Assessment

2.3.1. Resilience Background & Evolution

The idea of the resilience concept originates from the ecological field from the 1970s. There, resilience was understood as the capacity of an ecosystem to survive, adapt and grow in the case of unforeseen changes. In this definition, a resilient ecosystem can stay in a stable state when facing a stressor or can adapt and enter a new stable state, *e.g.*, change the structure while maintaining its functionality, which guarantees its existence [Juan-García et al., 2017].
Through time, other research fields where influenced by the original idea of resilience, for example the social-ecological field, where resilience is defined as: "The capacity of a system to absorb disturbance and re-organize while undergoing change so as to still retain essentially the same function, structure, identity and feedbacks" [Walker et al., 2003].

2.3.2. Resilience in Engineering & Urban Water Management

Resilience in engineering must be viewed slightly different compared to the original ecological view. Schulze (1996) states, that: "Engineering systems are designed to provide specified services and should be efficient, continuously working and predictable." Resulting from that, entering a new steady state, as it might occur in a natural ecosystem, is unacceptable, and human intervention is required to return the system to the original steady state [Schulze, 1996].

Based on this definition the resilience of an engineered system can not be judged on the ability to enter a new stable state, but on the ability to overcome certain unplanned events and come back to original planned functional state. To quantify this ability, Juan-García et al. (2017) defined *Resilience Assessment Elements*:

- **Stressors:** Pressure on the system, caused by human activities (increase of pollution) or natural events (drought, extreme rainfall, floods)
- **Properties:** Features that allow the system to withstand, respond and adapt to stressors, such as: robustness, redundancy, resourcefulness and flexibility
- **Metrics:** Quantify the properties, either qualitatively, quantitatively or through recovery time and failure magnitude compared to the required performance level of the system

- **Interventions:** Improve the system performance, which alters its properties, such as real-time control or increasing of system capacities

Fig. 2.14 shows, how the mentioned *Resilience Assessment Elements* impact and influence engineered systems and its properties. All these elements can be found again in the calculation of the *Quantitative Resilience Index* (Sec. 2.3.3) developed by Matzinger et al. (2018).

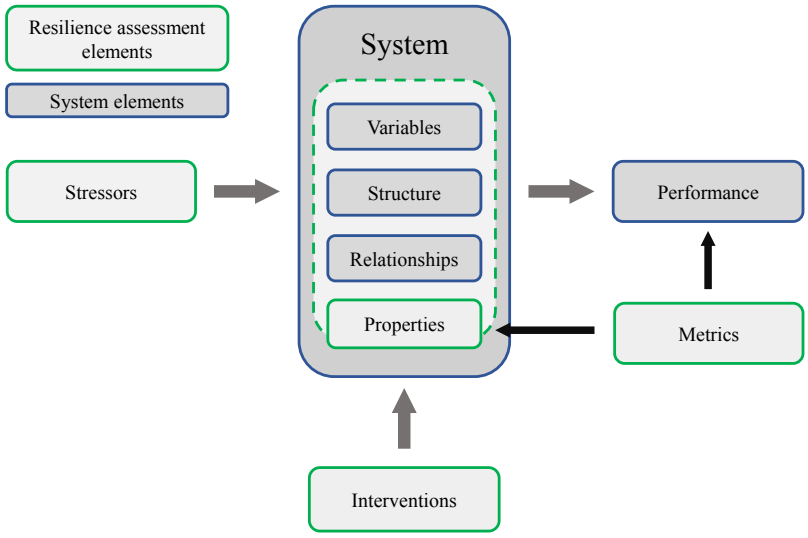

Figure 2.14: Conceptual scheme of system resilience key concepts [Juan-García et al., 2017]

2.3.3. Quantitative Resilience Index

In Matzinger et al. (2018), the *Quantitative Resilience Index* was continued on the previous work of Mugume et al. (2015) and Sweetapple et al. (2017). In Mugume et al. (2015) a *Resilience Index* (Res_0) between 0 and 1 was introduced for the functionality of urban drainage in case of acute disturbances due to extreme rainfall:

$$Res_0 = 1 - Sev \tag{2.10}$$

in this equation, Sev indicates the severity of the loss of performance caused by a disturbance. The calculation approach for Sev was supplemented by Matzinger et al. (2018) by the inclusion of an acceptable performance P_a:

$$Sev = \frac{1}{P_a - P_{max}} x \frac{1}{t_n - t_0} x \int_{t_0}^{t_n} P_a - P\,(t)\,dt \tag{2.11}$$

$$with\ P(t) = \begin{cases} P_a, & \frac{P_a - p(t)}{P_a - P_{max}} < 0 \\ P(t), & \frac{P_a - P(t)}{P_a - P_{max}} \geq 0 \end{cases} \tag{2.12}$$

Sev corresponds to the integral of the performance $P(t)$ over a time interval t_o to t_n, where only periods are integrated in which $P(t)$ is worse than the threshold P_a (see Fig. 2.15). The integral gets bounded by the difference between P_a and a previously specified maximum damage P_{max} and the time interval. For Res_0, this results in a value of 0, if the maximum damage P_{max} occurs over the entire time interval and a value of 1, if P_a is always observed [Matzinger et al., 2018].

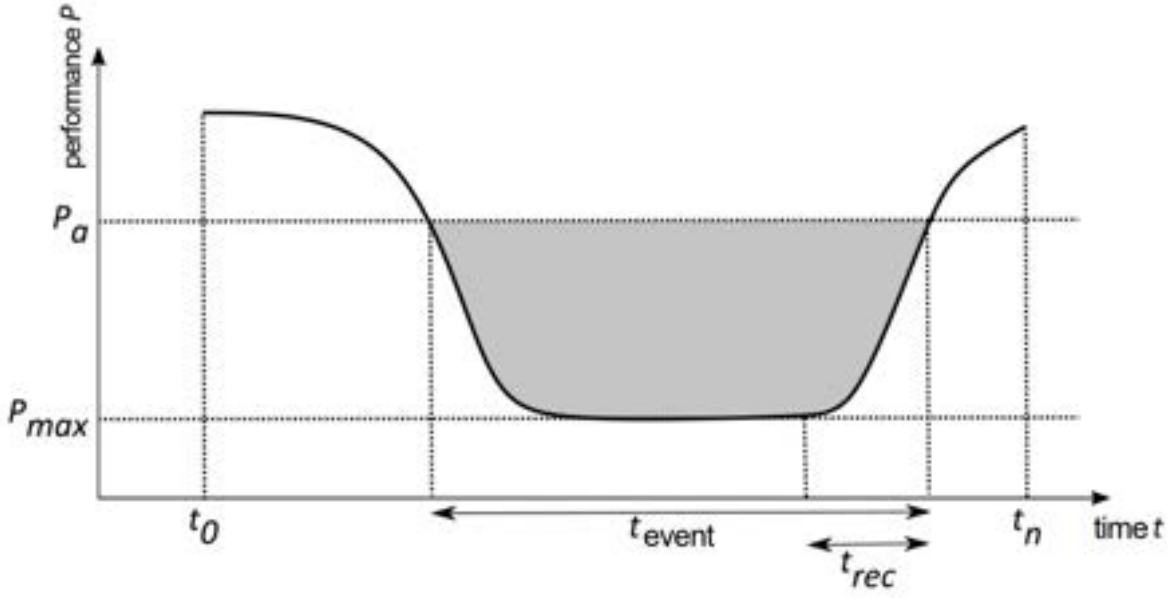

Figure 2.15: Scheme of the calculation approach. Gray shows the integral in Equation 2.11 [Matzinger et al., 2018]

3. Material & Methods

3.1. Study Site

3.1.1. Research Project netWORKS4

The Urban Redevelopment Area (URA) *Michelangelostraße* considered in this study is part of current new construction and redevelopment planning by the city of Berlin, accompanied by the research project *netWORKS4*. The aim of this project is to implement sustainable and attractive stormwater management measures in a participatory manner with stakeholders. The URA *Michelangelostraße* is to become more climate-friendly and resilient through newly built water infrastructure [netWORKS, 2021]. To achieve this, a combination of the following types of water-related infrastructure is planned:

- **Grey Infrastructure** refers to technical structures such as dams, roads, pipes, cisterns, pumps or basins
- **Blue Infrastructure** refers to elements with visible water, like rivers, canals, ponds, wetlands, floodplains or water treatment facilities
- **Green Infrastructure** refers to elements with visible "green", such as green roofs, trees, rain gardens and permeable pavement that can capture, evaporate and infiltrate rain where it occurs [Fletcher et al., 2015]

In order to integrate these different water infrastructure types in the URA, the research team defined six different Focal Areas (FA). The FAs each represent a typical type of urban structure and use (see details Sec. 3.1.3). For the six FAs separate stakeholder workshops were organised to select tailor-made combination of measures (grey, blue, green infrastructure) [Trapp et al., 2019]. The workshops involved both local stakeholders from the URA as well as urban water managers and urban planners at borough or city scale in the participative process. The FAs are marked in Fig. 3.1 and are presented in detail in Sec. 3.1.3. Furthermore, the geographical location, climate, hydrology and sewer system of the URA are presented in the following.

3.1.2. Urban Redevelopment Area Michelangelostraße

3.1.2.1. Geographical Location

The URA is found in the southern part of the Berlin borough of Pankow. More precisely, in the district Prenzlauer Berg. The area has a size of 76 hectares and is bordered by Kniprodestraße in the east, the Ringbahn in the south, Greifswalderstraße in the west and Gürtelstraße and the Jewish cemetery Weißensee in the north (Fig. 3.1). In terms of building structures, the URA can be divided into three areas: (i) the southern area near the Ringbahn, where four-story residential buildings with large, green courtyards can be found, (ii) the middle section of the area, which is primarily built up with eleven-story residential buildings with large courtyards, and (iii) the northern part, bordering on Gürtelstraße, where residential buildings in cellular construction from the post-war period are characteristic.

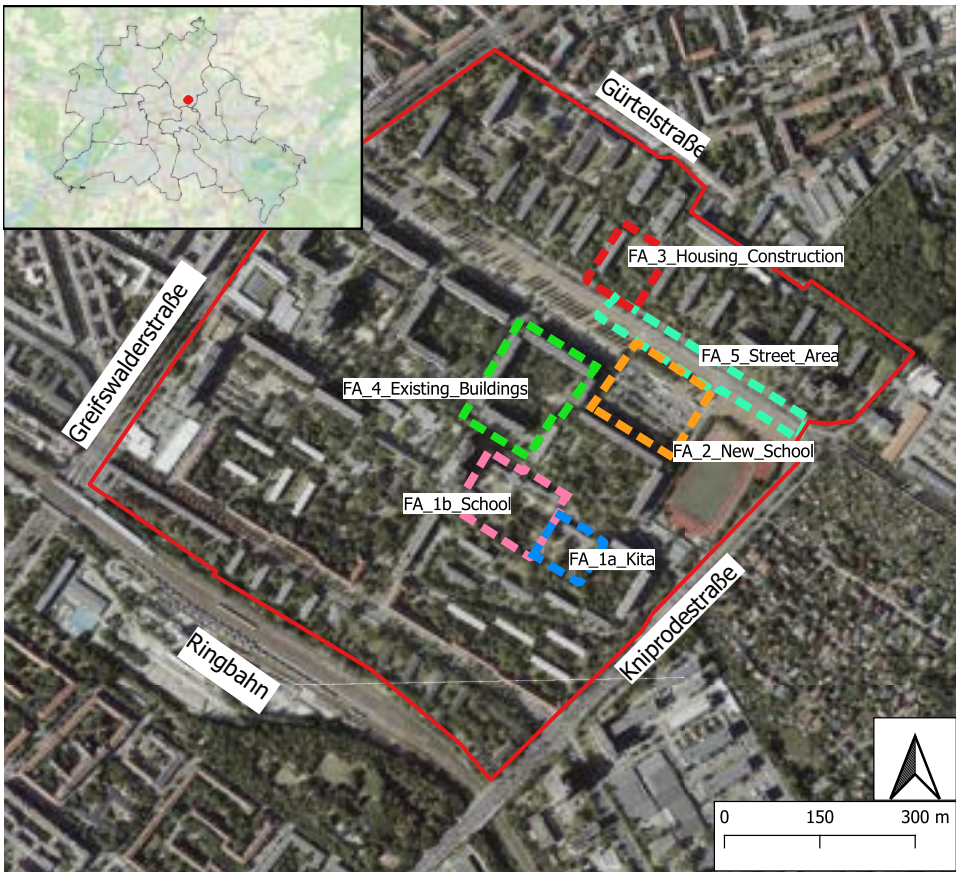

Figure 3.1: URA of *netWORKS4*, adapted from FISBroker (2021)

As can be seen from the building structures, the area is predominantly residential with social infrastructure such as schools and daycare centers, and with little commercial and

industrial development. This is also reflected in the fact that almost 10,000 people live in the URA. Almost 10 % of the neighborhood is classified as green space, but only 7 of the 666 buildings have a green roof, which is only 1 % of the buildings. Five main aims were selected together with stakeholders, which refer to particular needs of the neighborhood. These include environmental aims (biodiversity, surface water protection and groundwater protection) and societal aims (amenity value and environmental education). Furthermore the residents have to deal with two significant stresses. On he one hand heavy air pollution, which results from the major roads that border the neighborhood. On the other hand, vulnerable people are exposed to a high thermal load [Nenz et al., 2020].

3.1.2.2. Climate

From a climatic point of view, Berlin is located at the transition between maritime and continental climate. In the average the temperature for the climate reference station Berlin Dahlem is 9.2 °C. The monthly maximum in average temperature is reached in July with 18.4 °C. The minimum is reached in January with 0.5 °C (see Fig. 3.2). The precipitation distribution is subject to a strong seasonality just like the temperature distribution. Precipitation is highest in July and lowest in April (see Fig. 3.3). The long-term average annual precipitation is 578 mm.

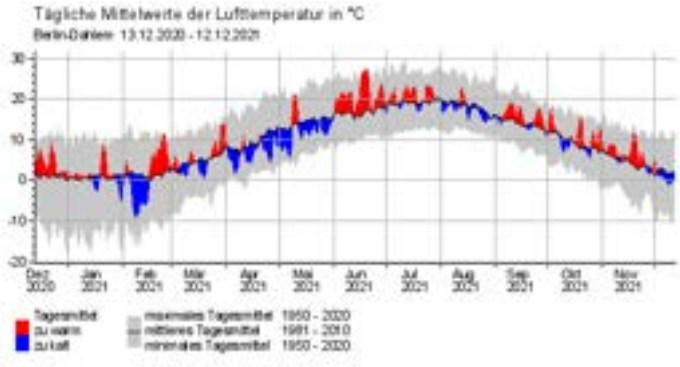

Figure 3.2: Daily mean of the air temperature in Berlin Dahlem [DWD, 2021]

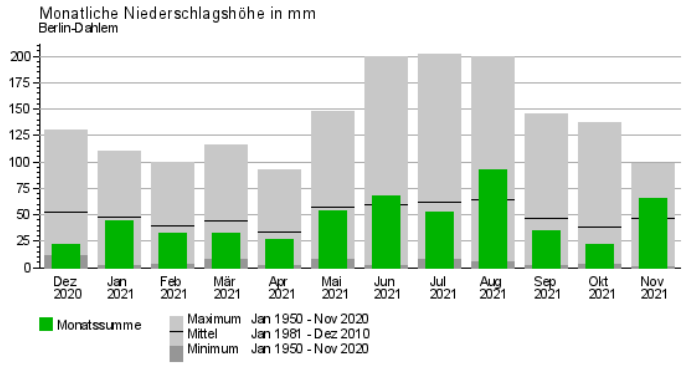

Figure 3.3: Mean of monthly precipitation in Berlin Dahlem [DWD, 2021]

However, it must be noted that both temperature and precipitation vary within Berlin. This is mainly due to the local topography and settlement structure. For example, the Grunewald and the upper Barnim plateau receive the most precipitation in Berlin. The temperature maximum of Berlin, on the other hand, is located in the city center around the Berliner Tiergarten. The URA in this study has an average temperature of 9.5 - 10 °C and thus belongs to the slightly warmer areas within Berlin [Funke, 2019; DWD, 2021]. In the URA, the average annual precipitation is 577 mm, similar to the Dahlem situation. Fig. 3.4 serves as a spatial classification of the places just mentioned.

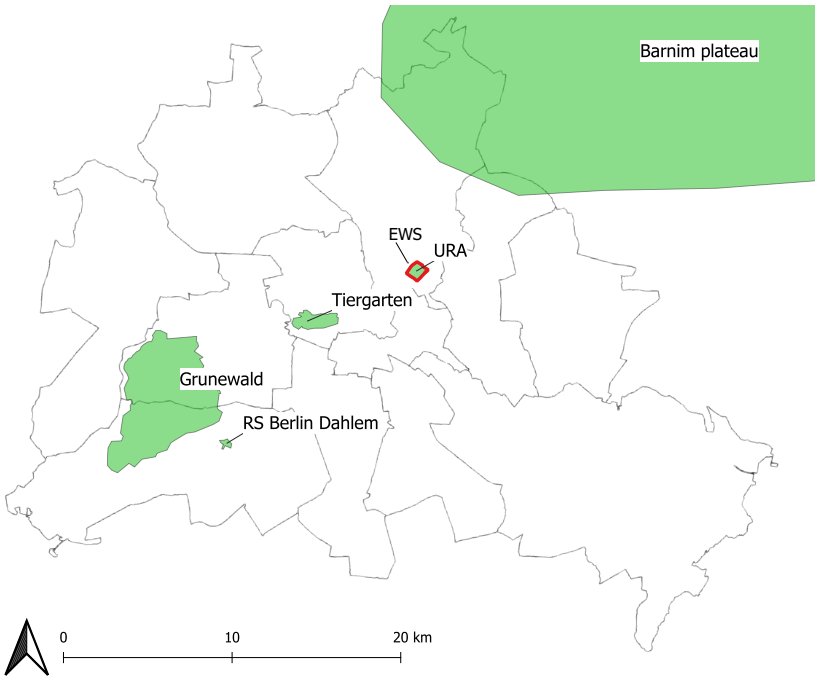

Figure 3.4: Spatial classification of the climatically metioned places, adapted from FIS-Broker (2021)

3.1.2.3. Hydrology and Sewer System

Berlin's surface waters consist of natural watercourses such as the Havel, Spree and Dahme, artificial channels such as the Stadtspree, the Landwehrkanal or the Teltowkanal and a large number of lakes such as the Müggelsee. All the inner city river stretches are strongly modified and regulated for shipping. Due to the low flow velocity and shallow water depths, these waters are ecologically sensitive systems, which react particularly sensitively to nutrient inputs, such as CSOs (Sec. 2.1) [Riechel et al., 2016].

Today, Berlin's sewer system comprises approximately 9600 km of sewers. Of these, almost 4300 km are sewers for wastewater, 3300 km for stormwater and 1900 km are combined sewers. As shown in Fig. 3.5, the center of Berlin is almost exclusively drained by a Combined Sewer System (CSS) and the outlying boroughs by a Separated Sewer System (SSS). The Berlin CSS itself is divided into subareas, here called sewer catchments, in which the water is collected centrally and pumped to the sewage treatment plants via pumping stations. When these pumping stations are overloaded, the water is discharged via CSO outlets into adjacent water bodies.

BlnXI consists of approximately one third CSS and two thirds SSS. The URA considered in this study is fully located in the CSS part within the catchment. The CSO of *BlnXI*, discharges into the River Spree next to the Friedrichsbrücke. In Fig. 3.5 the sewer catchment *BlnXI* is highlighted [BWB, 2012].

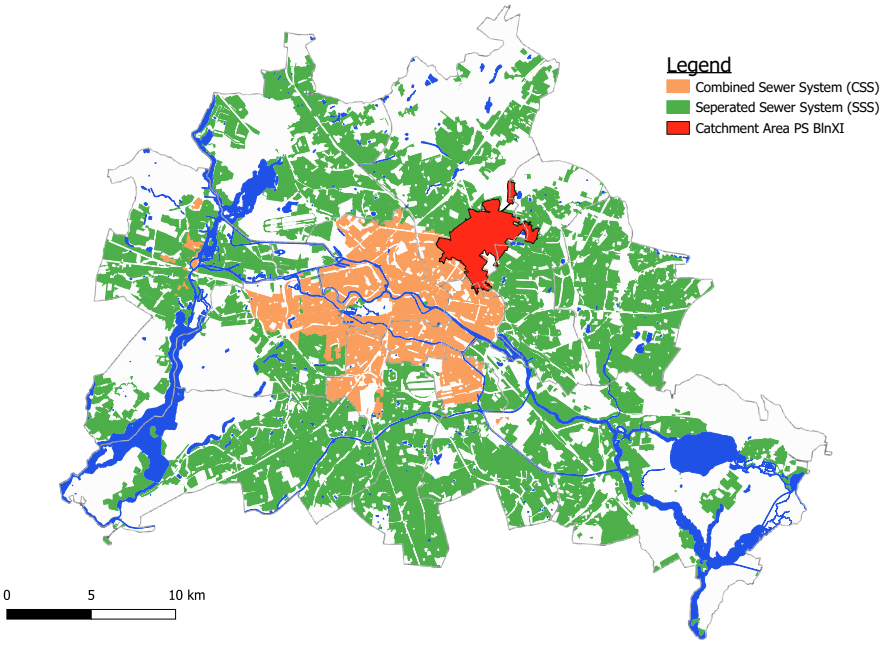

Figure 3.5: Map of the Berlin's sewers system, adapted from FISBroker (2021)

3.1.3. Area Types and their Characteristics

As mentioned in Sec. 3.1.2.1 and shown in Fig. 3.1, the research group of *netWORKS4* identified different FAs in the URA *Michelangelostraße*. Those represent important urban constellations of the city, such as social infrastructure, public open spaces or street areas. In the *FAs*, different combinations of grey, blue and green infrastructure measures were selected by stake holders [Nenz et al., 2020]. These measures are connected to each other and thus result in different chains, called LID chains. The six different *FA*-types, including their infrastructure measures and the resulting chains, are presented below. An overview is given in Table 3.1.

	FA_1a Kita	FA_1b School	FA_2 New_School	FA_3 Housing_Construction	FA_4 Existing_Buildings	FA_5 Street_Area
Flat Roof (FR)	x	x	-	-	x	-
Extensive Green Roof (EGR)	x	x	x	x	x	-
Intensive Green Roof (IGR)	-	-	x	x	x	-
Infiltration Swale (IS)	-	-	x	x	-	x
Trough-Trench Element (TTE)	x	x	x	-	x	-
Cistern	x	x	x	x	x	-
Fully Sealed (FS)	-	x	x	x	x	x
Partially Sealed (PS)	x	x	x	x	x	x
Surface Infiltration (SI)	x	x	x	x	x	x

Table 3.1: Occurring LID measures in the respective Focal Areas

3.1.3.1. FA_1a_Kita

FA_1a_Kita, which reflects the construction and expansion of social infrastructure, features a number of LID measures. Newly built roofs are covered with an *Extensive Green Roof (EGR)*, roof runoff is stored in *Cisterns* and reused as *Service (SW)* and *Irrigation Water (IW)*. In addition, *Fully Sealed (FS)* areas are converted into *Partially Sealed (PS)* areas and *Trough-Trench Elements (TTE)* are built to infiltrate cistern overflow. These individual LID measures result in the LID chains LC1 (Sec. 3.3.2.1) and LC11 (Sec. 3.3.2.11).

3.1.3.2. FA_1b_School

FA_1b_School, which also reflects the construction and expansion of social infrastructure, differs only minimally from FA_1a_Kita. Parts of the building roofs are provided with an *EGR* and rainwater is collected in *Cisterns*. The use of rainwater as *SW* and *IW* is planned. In addition, *FS*-areas will be partially converted into *PS*-areas. *TTE* are built

to infiltrate the excess water. These individual LID measures result in the LID chains LC2 (Sec. 3.3.2.2) and LC6 (Sec. 3.3.2.6).

3.1.3.3. FA_2_New_School

FA_2_New_School, which is intended to strengthen the social infrastructure through a new school building and a sports field, is characterised primarily by buildings which are completely provided with *EGR* and *Intensive Green Roof (IGR)*. Here, too, the rainwater is stored in *Cisterns* and used as *SW* and *IW*. Furthermore, only a small part is *FS*-area, mainly for access roads. The larger part of the open space is *PS*. There are also *IS* and *TTE* on the site. These LID measures result in the LID chains LC3 (Sec. 3.3.2.3), LC4 (Sec. 3.3.2.4), LC6 (Sec. 3.3.2.6), and LC7 (Sec. 3.3.2.7).

3.1.3.4. FA_3_Housing_Construction

FA_3_Housing_Construction represents the new housing development in the city, in form of multi-story residential buildings. Due to the new construction of the buildings, it is possible to design the buildings roofs completely vegetated with *EGR* and *IGR*. Here, too, the rainwater is collected in *Cisterns* and used for *SW* and *IW*. The open spaces are mostly *PS*-areas, only access roads are *FS*. In addition, *Infiltration Swales (IS)* and *TTEs* will be built. These LID measures lead to the LID combinations LC3 (Sec. 3.3.2.3) and LC8 (Sec. 3.3.2.8).

3.1.3.5. FA_4_Existing_Buildings

In FA_4_Existing_Buildings, the redesign of open spaces is a matter of priority. Green roofs are difficult to implement here because the eleven-story buildings were not structurally designed for this purpose. For this reason, mainly the lighter *EGR* are used here and only small buildings are equipped with the heavier *IGR*. The rainwater occurring is collected in *Cisterns* and used as *SW* and *IW*. A large part of the *FS*-areas will be unsealed and is now to be assigned to the *PS*-areas. Furthermore, *TTEs* will be built. This results in the LID chains LC3 (Sec. 3.3.2.3), LC9 (Sec. 3.3.2.9) and LC11 (Sec. 3.3.2.11).

3.1.3.6. FA_5_Street_Area

FA_5_Street_Area includes the redesign of main roads for public transport (tram route), motorised and non-motorised traffic. This includes a reduction of *FS*-areas to *PS*-areas. Furthermore, the construction of a tram line with track bed greening results in open spaces for *Surface Infiltration (SI)*. Precipitation water is to be purified by soil filter

elements and infiltrated in equal parts through *IS* and discharged into the *Sewer System (SS)*. This leads to the LID chains LC10 (Sec. 3.3.2.10) and LC12 (Sec. 3.3.2.12).

3.2. Dynamic Rainfall-Runoff-Routing Model of BlnXI

A calibrated Dynamic Rainfall-Runoff-Routing Model for *BlnXI* was available in model software *InfoWorks*, based on a coarse sewer approximation, as described in Riechel et al. (2016). Since *SWMM* offers some advantages over *InfoWorks*, such as control via *R*, open source availability or a better LID integration, it was decided to run the simulations via *SWMM*. As a result, the Dynamic Rainfall-Runoff-Routing Model used in this study had to be transferred first from *InfoWorks* to *SWMM* (Sec. 3.2.1). In this process, the model had to be parameterised and calibrated (Sec. 3.2.1.1). The transfer results and the calibration assessment of the model *BlnXI* are shown in Sec. 4.1.

3.2.1. Model Transfer InfoWorks to SWMM

3.2.1.1. Parameterization

From *InfoWorks* the model has been exported as a *SWMM* compatible *.inp*-file. However, some settings that were not exported had to be added via *R* afterwards. The following presented parameters had to be configured manually. The bold written parameters were used for calibration and continuously adjusted during the process.

- Precipitation & Evaporation data
- Conduit Shapes
- Dry Weather Inflow (DWI)
- Time Patterns for DWI
- **Real Time Control (RTC) rules for pumps**
- **Infiltration Parameters**
- **Manning's n (Roughness)** for:
  - Impervious Surfaces
  - Pervious Surfaces
  - Conduits

3.2.2. Transfer Assessment Parameters

In order to adequately assess the transfer and calibration of the model *BlnXI*, two indicators were used. These were the measured *Volume* and the *Nash-Sutcliffe Efficiency (NSE)* at different locations in the model:

3.2.2.1. Volume

Volumes for the entire simulation period (as described in Sec. 3.2.3.2) or for single events were assessed at various points in the model: surface runoff volume, flow volume in sewer, pump volume at main pumping station as well as CSO volume.

3.2.2.2. Nash-Sutcliffe Efficiency (NSE)

The *Nash-Sutcliffe-Efficiency (NSE)* is a goodness-of-fit index, which can be applied for the calibration of a variety of hydrological model types. The *NSE* is calculated as one minus the ratio of the error variance of the modelled time-series divided by the variance of the observed time-series (Eq. 3.1):

$$NSE = 1 - \frac{\sum_{t=1}^{n}(X_{s,t} - X_{o,t}i)^2}{\sum_{t=1}^{n}(X_{o,t} - \mu_o)^2} \tag{3.1}$$

where n is the total number of steps, $X_{s,t}$ is the simulated value at time-step t, $X_{o,t}$ is the observed value at time step t and μ_o is the standard deviation of the observed values. Therefore, a perfect model with an estimation error variance equal to zero has a *Nash-Sutcliffe-Effiency* of 1 (NSE = 1). Resulting from that, a model that produces a large error variance equal to the variance of the observed time series, results in a *Nash-Sutcliffe-Efficiency* of 0 (NSE = 0) [Gupta et al., 2009; McCuen et al., 2006].

The transfer results and the calibration assessment of the model *BlnXI* are shown in Sec. 4.1.

Figure 3.6: *SWMM*-model of *BlnXI*, where the circles in the southern part represent the CSS, the areas in the north represent the SSS, the dots represent the junctions and the lines represent the conduits of the system

3.2.3. Data Basis

3.2.3.1. Sewer Network

The model of the sewer catchment *BlnXI* (Fig. 3.6) consists of an area of roughly 1255 ha. This area divides up in 371 ha of *Combined Sewer Subcatchments* and 884 ha of *Stormwater Subcatchments*. As mentioned before, only the *Combined Subcatchments* were used for this simulation. In total the *BlnXI*-model consists of:

- **Subcatchments:** 114
- **Nodes:** 542
- **Conduits:** 554
- **Storage Units:** 5
- **Pumping Stations:** 1
- **Weirs:** 7
- **Outfalls:** 2

3.2.3.2. Precipitation

The precipitation data in this study were provided by *Berliner Wasserbetriebe (BWB)*. The *BWB* maintains rain gauging stations at each of its pumping stations in the respective catchment areas. The rainfall data used in this study were collected at *Erich-Weinert-Straße (EWS)* in Berlin, Pankow (see Fig. 3.4). The precipitation series used, covers six months and starts in May 2017 and ends in October 2017. The temporal resolution is five minutes. In order to use the precipitation data in *SWMM*, they were previously converted to a *SWMM* compatible *.txt* format using *R*. Within the model, all areas were forced with this precipitation series.

During the time period considered in this study (May 2017 to October 2017), precipitation was above average, totalling 527 mm. In particular, individual extreme rain events on 29. June 2017 and 20. July 2017 occurred and led to considerable flooding in Berlin [Matzinger et al., 2019].

With 2017, an extreme year was used to test LIDs for a large range of rain events. This has to be kept in mind when discussing scenario results. A graphical representation of the precipitation data can be seen in Fig. A.1.

3.2.3.3. Evaporation

The potential evaporation rate $h_{v_p(j)}$ (mm) was calculated by a simplified approach based on a modified evaporation Eq. 3.2 by Brandt [Stapf, 2011].

$$h_{vp(j)}[mm] = 1.34 \left(\frac{4}{3} + \sin(\frac{2\pi j}{365 - \frac{\pi}{2}}) \right) \tag{3.2}$$

where j is the day of the precipitation event, starting with 1 for 1. January. The potential evaporation rate was calculated for each day of the period 01. May 2017 to 31. October 2017 and stored in a *SWMM* compatible time series. The occurring evaporation rate is graphically illustrated in the appendix under Fig. A.2.

3.2.3.4. LIDs

All configurations used in this study for the occurring LID measures, as shown in Tab. 3.1, originate from the documentation by Kliewer (2015). This manual contains parameters for all common ground types, such as permeable pavements or asphalt, and LID measures such as *EGR* and *TTE*. The parameter settings are also used as the basis of the DWA-model *WABILA* and thus consider German standards [Henrichs et al., 2016]. The LID measures are all constructed in the form of *Bio-Retention Cells* as described in Sec. 2.1.2.5. The exact values of each LID measure can be viewed in Tab. A.1 and Tab. A.2.

3.3. Modelling

The following section covers the model structure of the *BlnXI*-model, which includes the representation of the URA in the *SWMM*-model, the upscaling of the FAs, an explanation of the LID chains that occur and the implementation of the LID chains in the *SWMM*-model. Furthermore, the model scenarios and failure scenarios simulated in this work are presented.

3.3.1. Model Setup

Since the previously calibrated *BlnXI*-model is a coarse network, which does not include any LIDs and therefore only roughly represents local conditions within the region, the model must be further refined for simulation in areas, where LIDs are planned. On the other hand, LIDs planned for the single FAs are foreseen for the entire URA [Trapp et al., 2020]. For this, an upscaling of the individual FAs to the entire URA had to be done. In order to be able to do this, preliminary steps had to be taken.

3.3.1.1. Representation of the URA in the SWMM-Model

In order to be able to realistically represent the URA *Michelangelostraße* in the *SWMM*-model of *BlnXI*, an area comparison had to be made in advance. Since all subsequently determined area shares of LID measures are determined via *ALKIS*, the comparison must be carried out between *ALKIS* and the *SWMM*-model. The *Amtliche Liegenschaftskatasterinformationssystem (ALKIS)* provides rough information on building areas, parcel boundaries, but also land use types. Therefore, *ALKIS* maps were loaded as a digital maps to *QGIS*, which is a free geographic information system to create, edit and analyse geographic data [QGIS, 2022]. On the one hand, *ALKIS* does not aim at an assessment of imperviousness. The coarse-grid *SWMM*-model, on the other hand, represents areas in a conceptional, simplified manner. In short, both *ALKIS* and the *SWMM*-model are inprecise estimates of reality, regarding different connectivities and imperviousness of areas. For the comparison, the impervious areas of the sewer catchment *BlnXI* were determined via *ALKIS* and via the *SWMM*-model.

	ALKIS (ha)	**SWMM-model (ha)**	**Factor**
Impervious Area of Sewer Catchment BlnXI	194.11	230.19	1.186

Table 3.2: Difference in impervious areas between *ALKIS* & *SWMM*

The results in Tab. 3.2 show, that the impervious area in *ALKIS* is slightly smaller with 194.11 ha compared to the 230.19 ha determined for the *SWMM*-model, therefore the impervious areas in the *SWMM*-model are larger by a factor of 1.186. This factor must be taken into account in the later determined area shares via *ALKIS*.
In the next step, the impervious area of the URA was determined via *QGIS*, based on the *ALKIS* data. This showed that, in the actual state, 33.08 ha of the URA are impervious. This value was now multiplied by the previously determined factor of 1.186 in order to represent the same proportion of impervious area of the URA in the *SWMM*-model. Consequently, 39.23 ha of the total of 230.19 ha, respectively 17.04 %, of the impervious area in the *SWMM*-model had to be selected to realistically represent the URA.
This approach is illustrated in Fig. 3.7. The *SWMM*-model of the sewer catchment *BlnXI* is shown in both figures. The URA area is shown by a red border. To enable a spatial representation in the system, the 39.23 ha of the total of 230.19 ha conceptional, impervious areas within *SWMM* were selected to lie within the shown URA. These areas shown in green therefore represent the URA *Michelangelostraße* in the *SWMM*-model.

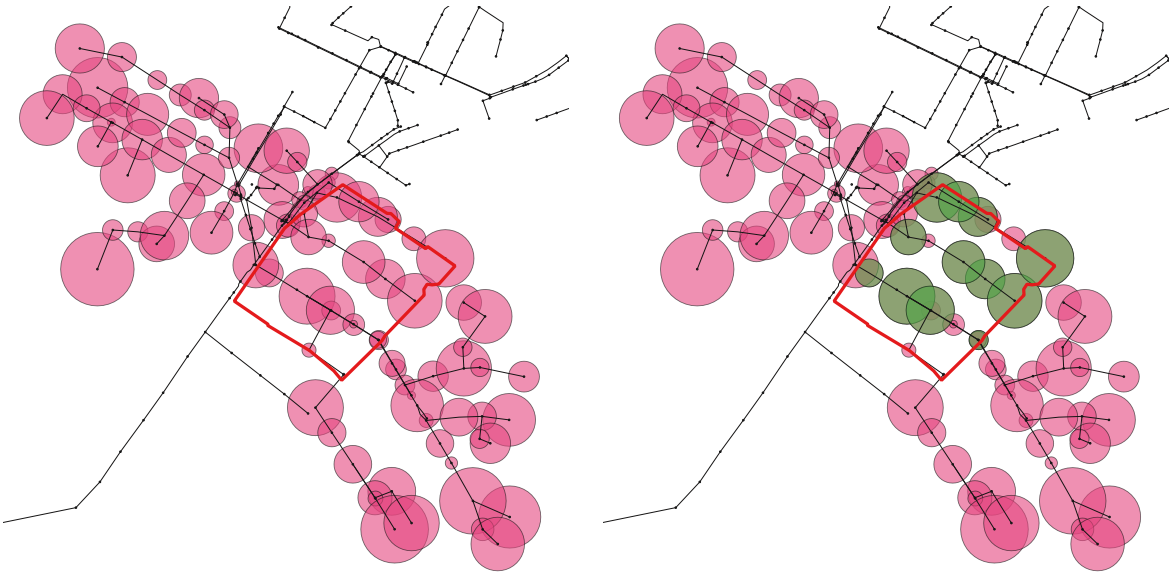

Figure 3.7: Representation of the URA in *SWMM*

3.3.1.2. Upscaling of the Focal Areas

In order to assess the effectiveness of the LID measures at URA level as politically planned, the FAs had to be scaled up from their original size (see Fig. 3.1) to the entire URA of *Michelangelostraße*. This upscaling took place in cooperation with the *Berliner Wasserbetriebe (BWB)*. Various aspects were considered:

1. Current planning of the borough of Pankow were considered for the six FAs. This includes coarse planning information, tangible planning, *e.g.* on positions of new building blocks, as well as changes during actual implementation of the first *FA_1a_Kita*.

2. Similar structures to the original FAs had to be identified in the URA, *e.g.*, all kindergartens were identified and assigned to *FA_1a_Kita*.

3. Local infiltration capacities were observed and taken into account in the upscaling (see Fig. A.9), this led to adaptations in the infiltration systems applied for the LID combinations.

4. Local conditions, such as safety precautions in schools and kindergartens were considered.

Taking all this information into account, the map of the final upscaling in Fig. 3.8 was created. It can be seen that the *FA_1a_Kita* has a total of four locations.

Figure 3.8: Final upscaling of FAs in URA *Michelangelostraße*, adapted from FISBroker (2021)

FA_3_Housing_Construction occupies almost the entire north of the URA and thus roughly represents a quarter of the URA. *FA_4_Existing_Buildings*, which occupies the entire middle and lower part of the URA, is the largest FA with over 50 % of the URA. *FA_5_Street_Area* is composed of the two crossing roads in the north and south. In addition, it must be mentioned that the white areas in Fig. 3.8 did not correspond to any FA due to their structure. For this reason, they were not considered in any further calculations, unless explicitly mentioned.

After the graphical upscaling of the FAs, the corresponding area shares had to be determined. Therefore the previously mentioned *ALKIS* was used as data basis via *QGIS*. The values determined from *QGIS* were multiplied by the previously calculated factor of 1.186 to compensate for the difference between *ALKIS* and the *SWMM*-model. The result of the determined area shares (incl. the factor) can be seen in Tab. 3.3. This

area composition is the basis for the set up of the scenarios and is used for the further calculations of this study.

	Impervious Building Area of FA in (%)	Undeveloped Impervious Area of FA in (%)	Pervious Area of FA in (%)	Total FA area in (ha)	FAs Portion of URA in (%)
FA_1a Kita	16.87	33.29	49.84	2.87	3.26
FA_1b School	19.04	55.73	25.23	2.66	3.04
FA_2 New_School	11.43	36.54	52.03	5.46	6.24
FA_3 Housing_Construction	21.70	34.46	43.84	20.92	23.89
FA_4 Existing_Buildings	16.09	42.14	41.77	49.70	56.77
FA_5 Street_Area	-	54.70	45.30	5.962	6.81
Mean in (%)	16.16	40.93	42.91	87.56	

Table 3.3: Area composition of the URA by the FAs after upscaling

3.3.2. LID Chains Composed of LID Measures

The FAs scaled up in the previous section are represented by LID chains. These chains are composed of the LID measures that occur in the respective FAs. The different measures could be abstracted to 12 different LID chains for inclusion in the *SWMM*-model. These are divided into *Building-Chains* (LC1 - LC5), which have a stormwater runoff generating roof as the starting point and *Area-Chains* (LC6 - LC12), which have Fully Sealed (FS) or Partially Sealed Area (PS) as the starting point. The respective area shares in the individual LID chains differ in the later model depending on their relative shares in the FAs.

3.3.2.1. LID Chain 1

The LID Chain 1 (LC1) (Fig. 3.9) is composed of a *Flat Roof (FR)* and an *Extensive Green Roof (EGR)*. The generated runoff drains to a *Cistern* where *Service Water (SW)* and *Irrigation Water (IW)* is taken from. The overflow of the *Cistern* runs into an *Trough-Trench Element (TTE)*. The remaining water from the *TTE* flows into a *Sewer System (SS)*.

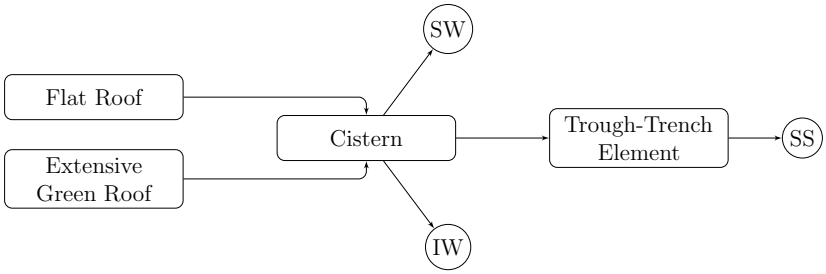

Figure 3.9: LID Chain 1

3.3.2.2. LID Chain 2

The LID Chain 2 (LC2) (Fig. 3.10) is composed of a *Flat Roof (FR)* and an *Extensive Green Roof (EGR)*. The generated runoff drains to a *Cistern* where *Service Water (SW)* and *Irrigation Water (IW)* is taken from. The overflow of the *Cistern* runs into an *Infiltration Swale (IS)*. The remaining water from the *IS* flows into a *Sewer System (SS)*.

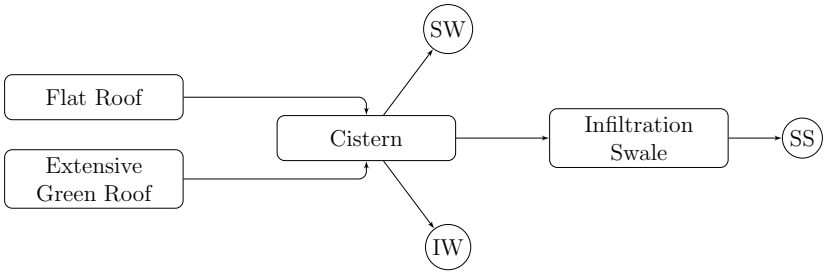

Figure 3.10: LID Chain 2

3.3.2.3. LID Chain 3

The LID Chain 3 (LC3) (Fig. 3.11) is composed of an *Extensive Green Roof (EGR)* and an *Intensive Green Roof (IGR)*. The generated runoff drains to a *Cistern* where *Service Water (SW)* and *Irrigation Water (IW)* is taken from. The overflow of the *Cistern* runs into an *Infiltration Swale (IS)*. The remaining water from the *IS* flows into a *Sewer System (SS)*.

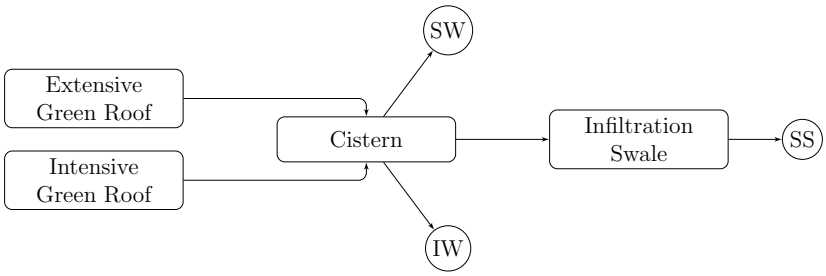

Figure 3.11: LID Chain 3

3.3.2.4. LID Chain 4

The LID Chain 4 (LC4) (Fig. 3.12) is composed of an *Extensive Green Roof (EGR)* and an *Intensive Green Roof (IGR)*. The generated runoff drains to a *Cistern* where *Service Water (SW)* and *Irrigation Water (IW)* is taken from. The overflow of the *Cistern* runs into a *Trough-Trench Element (TTE)*. The remaining water from the *TTE* flows into a *Sewer System (SS)*.

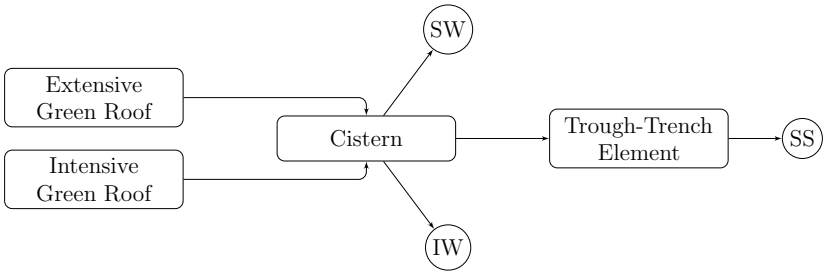

Figure 3.12: LID Chain 4

3.3.2.5. LID Chain 5

The LID Chain 5 (LC5) (Fig. 3.13) is composed of 76 % *Flat Roof (FR)*, 20 % *Extensive Green Roof (EGR)* and 4 % *Intensive Green Roof (IGR)*. The generated runoff drains to 20 % into *Surface Infiltration (SI)*. The other 80 % drain into a *Cistern* where *Service Water (SW)* and *Irrigation Water (IW)* is taken. The overflow of the *Cistern* runs into an *Trough-Trench Element (TTE)*. The remaining water from the *TTE* flows into a *Sewer System (SS)*.

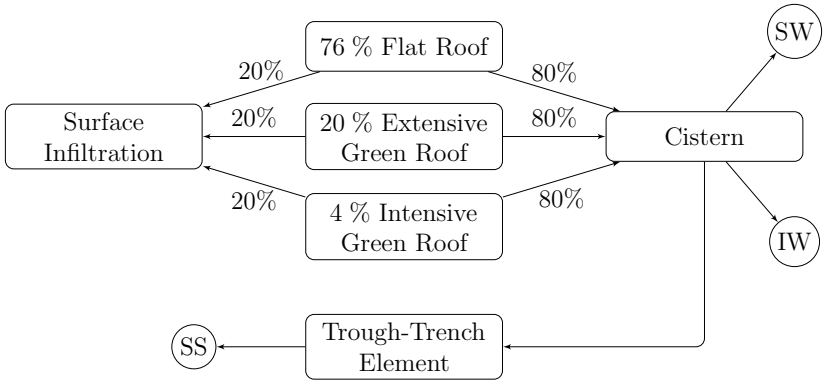

Figure 3.13: LID Chain 5

3.3.2.6. Linkage 6

The Linkage Chain 6 (LC6) (Fig. 3.14) is composed of a *Fully Sealed Area (FS)* and a *Partially Sealed Area (PS)*. The generated runoff drains to an *Infiltration Swale (IS)*. The overflow of the *IS* runs into a *Sewer System (SS)*.

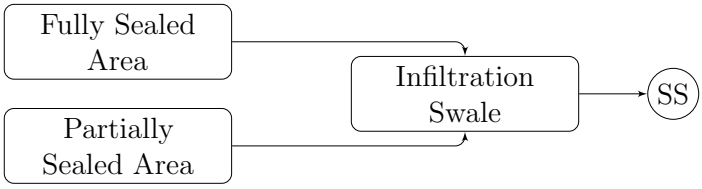

Figure 3.14: LID Chain 6

3.3.2.7. LID Chain 7

The LID Chain 7 (LC7) (Fig. 3.15) is composed of a *Fully Sealed Area (FS)* and a *Partially Sealed Area (PS)*. The generated runoff drains to a *Trough-Trench Element (TTE)*. The overflow of the *TTE* runs into a *Sewer System (SS)*.

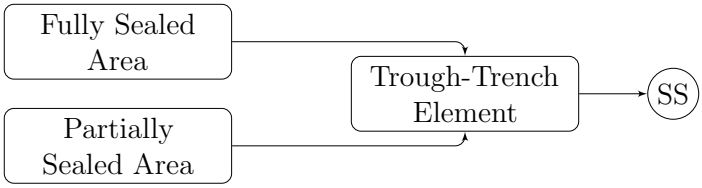

Figure 3.15: LID Chain 7

3.3.2.8. LID Chain 8

The LID Chain 8 (LC8) (Fig. 3.16) is composed of a 100 % *Fully Sealed Area (FS)*. The generated runoff drains to an *Infiltration Swale (IS)*. The overflow of the *IS* runs into a *Sewer System (SS)*.

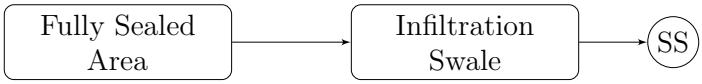

Figure 3.16: LID Chain 8

3.3.2.9. LID Chain 9

The LID Chain 9 (LC9) (Fig. 3.17) is composed of a 100 % *Fully Sealed Area (FS)*. The generated runoff drains to a *Trough-Trench Element (TTE)*. The overflow of the *TTE* runs into a *Sewer System (SS)*.

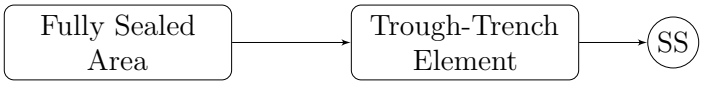

Figure 3.17: LID Chain 9

3.3.2.10. LID Chain 10

The LID Chain 10 (LC10) (Fig. 3.18) is composed of a 100 % *Fully Sealed Area (FS)*. The generated runoff drains to 50 % into an *Infiltration Swale (IS)* and to 50 % directly into a *Sewer System (SS)*.

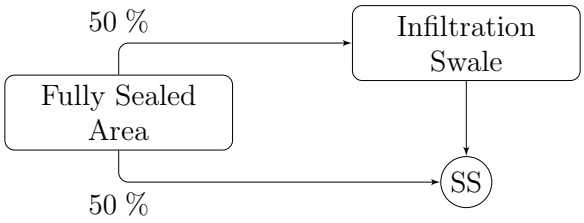

Figure 3.18: LID Chain 10

3.3.2.11. LID Chain 11

The LID Chain 11 (LC11) (Fig. 3.19) is composed of a 100 % *Partially Sealed Area (PS)*. The generated runoff drains to a *Surface Infiltration (SI)*. The overflow of the *SI* runs into a *Sewer System (SS)*.

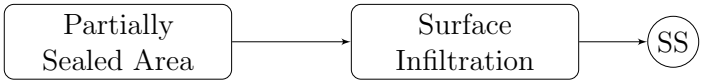

Figure 3.19: LID Chain 11

3.3.2.12. LID Chain 12

The LID Chain 12 (LC12) (Fig. 3.20) is composed of a 100 % *Partially Sealed Area (PS)*. The generated runoff drains to an *Infiltration Swale (IS)*. The overflow of the *IS* runs into a *Sewer System (SS)*.

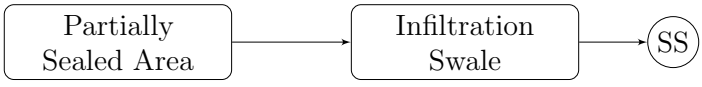

Figure 3.20: LID Chain 12

3.3.3. Test of LID Chains

In order to get a better understanding of the effects of the individual chains and to check their plausibility, the LID chains were tested individually before the implementation in the later used *SWMM*-model *BlnXI*.
With the intention to establish a standardised comparison of the effects and to check the plausibility, all LID chains runoff is stated as l/s·ha. For the test, area shares of the runoff generating areas, such as *Roofs* or *Sealed Areas*, are always equally divided, *e.g.*, if the effective runoff area consists of *EGR* & *IGR*, the area shares are 50/50. The only exception is Linkage Chain 5 (LC5), where the area division is described as in Sec. 3.3.2.5. For the test (as for the upscaling), the *Cistern* volume was calculated by taking the mean value of resulting m^3 due to connected runoff area from the upscaling in Sec. 3.3.1.2. The same applies to the consumption of *Service Water (SW)* and *Irrigation Water (IW)*. The subsequent infiltration measures, such as *Infiltration Swale (IS)* and *Trough-Trench Element (TTE)*, always correspond to 10 % of the effective runoff area. The reference area for the Building-Chains is a Fully Flat Roof (Reference FR) and for the Area-Chains a Fully Sealed Area (Reference FS). The rain events used to test the LID chains are briefly presented graphically with the results of the test and in terms of their most important properties in Sec. 4.2.

3.3.4. Implementation of LID Chains in SWMM-Model

After the previously described test of the LID chains, these had to be implemented in the existing *SWMM*-model in order to be able to map and quantify the effects of the LID measures. For this purpose, the areas previously selected in Fig. 3.7, which represent the URA in the *SWMM*-model, were replaced by LID chains. Fig. 3.21 shows an example of how several LID chains occurring in the respective FA replace an earlier selected area. In this way, the entire previously defined URA *Michelangelostraße* could be replaced by LID chains in the *SWMM*-model. As outlined above, LID chains can also contain fully sealed areas, depending on planning in the FAs. A representation of the *SWMM*-model before implementation is shown in the appendix Fig. A.3.

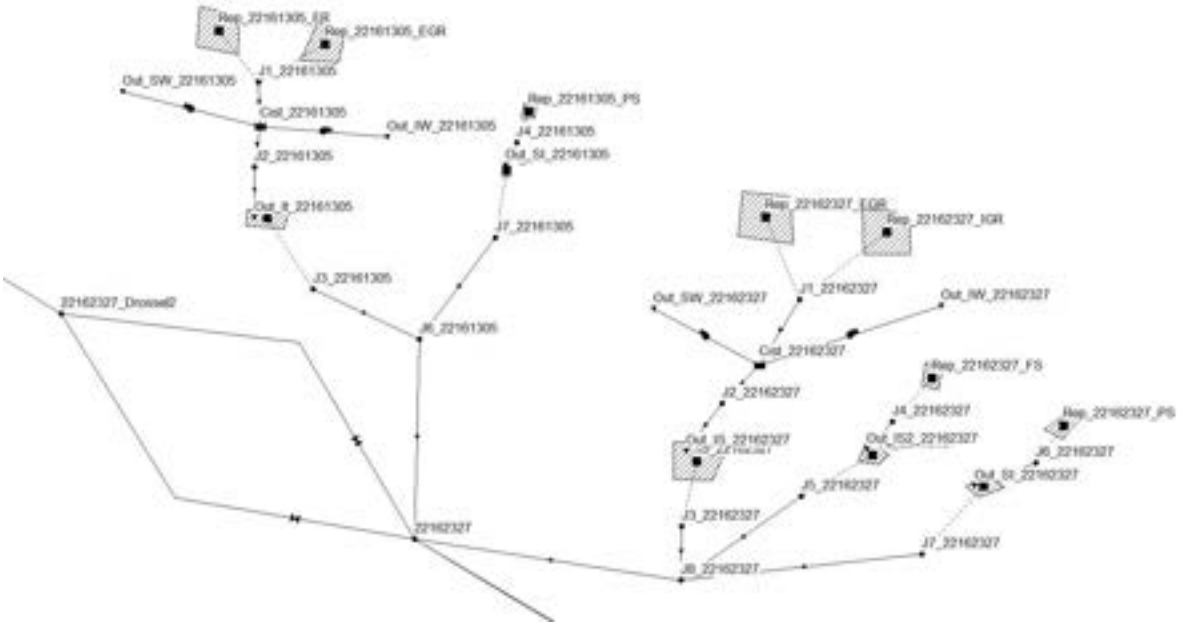

Figure 3.21: Representation of the LID chains in *SWMM*-model

3.3.5. Failure Incidents & Severity of Failure

In order to observe the behaviour of the system and to be able to assess it on the basis of resilience, various failure scenarios were set up for this work. Like the upscaling in Sec. 3.3.1.2, these failure scenarios were created in cooperation with the *Berliner Wasserbetriebe (BWB)*. Experience values of the *BWB* maintenance teams responsible for the LIDs were taken into account and included. Furthermore, empirical values from previous implementations of LID measures were considered in order to be able to create scenarios that are as realistic as possible. This has resulted in the following failure incidents:

- **Cisterns**
  - *Pump Failure* represents the decrease in pumping capacity of cistern pumps due to a lack of maintenance
  - *Silting* represents the decrease in the volume of the cisterns due to sludge input from green roofs or other surfaces
- **Green Roofs**
  - *Substrate Erosion* represents the reduction in the thickness of green roofs due to wind, washout or physical damage

- **Infiltration**
  - *Colmation* represents the reduction of permeability in infiltration measures due to entrained fine material
  - *Sedimentation* is an overall term for all damage that reduces the volume and infiltration performance of infiltration systems. This includes classic sedimentation, accumulation of plant material, littering and parked cars.

In order to simulate failure scenarios of varying intensity, two degrees of failure severity were introduced for the modelling. Based on interviews with BWB, LIDs are maintained between 1 and 6 times per year, which leaves them at high performance level. For the failure scenarios it is assumed that less frequent maintenance will lead to partial failure of the LIDs. These failures are labelled in this study as *Light-Scenario* and *Strong-Scenario* and are defined as the following:

- **Light-Scenario** represents that care and maintenance of the LID measures is done, but too infrequently and sporadically, only about every 2 years.
- **Strong-Scenario** represents a complete neglect of care and maintenance of the LID measures over a period of approximately 10 years.

A total of eight different failure scenarios were compiled from the *Failure Incidents* and *Severities* just listed. These cover the failures separately by LID type (*Cisterns*, *Green Roofs*, *Infiltration*) as well as a combination of all these, called *Total Failure*. Each of these four scenarios is calculated as a *Light-* and *Strong-Scenario*. A detailed explanation of the changed and adjusted parameters can be found in Sec. 3.4.

3.4. Model Scenarios

A total of ten different model representations of the sewer catchment *BlnXI* were simulated in *SWMM*. These are the *01 - Construction without Water Concept*, the *02 - Construction with Water Concept* and eight *Failure Scenarios*. Each of these model scenarios is presented below in terms of properties, settings, and their characteristics.

3.4.0.1. 01 - Construction without Water Concept (SC-01)

		01 - Construction without Water Concept (SC-01)
Impervious Area of URA	**ha**	40.97
Impervious Area of URA connected to LIDs	**ha / %**	0.0 / 0.0
Impervious Area of BlnXI	**ha**	231.93
Impervious Area of BlnXI connected to LIDs	**ha / %**	0.0 / 0.0

Table 3.4: Overview *01 - Construction without Water Concept (SC-01)*

01 - Construction without Water Concept (SC-01) represents the planned new housing development in the URA *Michelangelostraße* without taking LID measures into account in the planning. This new development project aims to build 1,200 housing units in the northern part of the URA by 2035. The area required for this is represented by FA_3_Housing_Construction in Fig. 3.8.
SC-01 is intended to show how these housing constructions will affect the sewer catchment *BlnXI* if no LID measures are considered in the planning. Due to these circumstances, the impervious area of the URA increases from 39.23 ha from status quo to 40.97 ha for *SC-01* as a result of the housing construction. Despite the many new housing units, this is only a small increase in impervious area as, many fully sealed parking spaces will be built over. The total area in *BlnXI* also increases from 230.19 ha to 231.93 ha. In *SC-01*, no impervious areas are connected to LID measures. An overview is given in Tab. 3.4.

3.4.0.2. 02 - Construction with Water Concept (SC-02)

		02 - Construction without Water Concept (SC-02)
Impervious Area of URA	**ha**	49.99
Impervious Area of URA connected to LIDs	**ha / %**	49.10 / 98.40
Impervious Area of BlnXI	**ha**	240.97
Impervious Area of BlnXI connected to LIDs	**ha / %**	49.10 / 20.38

Table 3.5: Overview *02 - Construction with Water Concept (SC-02)*

02 - Construction with Water Concept (SC-02) represents the LID upscaling of the FAs that was done in Sec. 3.3.1.2 . *SC-02* therefore combines all LID measures and resulting LID chains from the *netWORKS4* research project. The housing construction, described in *SC-01*, is also included, but in this case the new impervious areas due to construction are connected to LID measures. As can be seen in Tab. 3.5, this results in a further increase in impervious areas. This is due to the fact that a classification of the impervious areas, which also includes partially sealed areas, is carried out in this study. This results in an impervious area for the URA of 49.99 ha. Of this, 98.4 % is connected to LID measures. Only parts of the streets in FA_5_Street_Area are directly connected to the sewer system. For the sewer catchment *BlnXI*, this results in an impervious area of 240.97 ha, through *SC-02* 20.38 % of that are connected to LID measures.
A detailed overview can be found in the following Tab.3.6 where the area shares of each LID chain as well as FAs are listed.

		FA_1a Kita	FA_1b School	FA_2 New_School	FA_3_Housing Construction	FA_4_Existing Buildings	FA_5 Street_Area	Sum in (ha)	Portion of BlnXI in (%)
Building Chains	LID Chain 1	0.4817	-	-	-	-	-	0.4817	0.200
	LID Chain 2	-	0.5068	-	-	-	-	0.5068	0.210
	LID Chain 3	-	-	0.0687	4.5385	-	-	4.6072	1.912
	LID Chain 4	-	-	0.5551	-	-	-	0.5551	0.230
	LID Chain 5	-	-	-	-	7.9977	-	7.9977	3.320
Area Chains	LID Chain 6	-	1.4833	1.5267	-	-	-	3.0100	1.249
	LID Chain 7	-	-	0.4684	-	-	-	0.4684	0.194
	LID Chain 8	-	-	-	1.0838	-	-	1.0838	0.450
	LID Chain 9	-	-	-	-	1.4240	-	1.4240	0.591
	LID Chain 10	-	-	-	-	-	0.8885	0.8885	0.369
	LID Chain 11	0.9506	-	-	6.1232	19.5191	-	26.5929	11.038
	LID Chain 12	-	-	-	-	-	1.4841	1.4841	0.616
	Sum in (ha):	1.4323	1.9901	2.6189	11.7455	28.9408	2.3727	49.1002	20.379

Table 3.6: Area composition in ha of *02 - Construction with Water Concept (SC-02)*

3.4.0.3. 03 - Cistern - Light

Failure Scenario	LID - Measure	Incident	SWMM LID Parameter	Initial Value	Adjusted Value	% of Initial Value
03 - Cistern - Light	Cistern	Pump Failure	Pump Curve	Individual	Individual	-10 %
		Silting	Storage Max. Depth	3 m	2.25 meter	-25 %

Table 3.7: Adjusted parameters - 03 - Cistern - Light

03 - Cistern - Light represents the first failure scenario. It combines the two incidents *Pump Failure* and *Silting*. The *Light*-Variant is assumed, *i.e.*, a neglect of maintenance over a period of approximately 2 years. For this, the *Pump Capacity* is reduced by 10 % to simulate the *Pump Failure* and the *Storage Max. Depth* is reduced by 25 % to simulate *Silting*.

3.4.0.4. 04 - Cistern - Strong

Failure Scenario	LID - Measure	Incident	SWMM LID Parameter	Initial Value	Adjusted Value	% of Initial Value
04 - Cistern - Strong	Cistern	Pump Failure	Pump Curve	Individual	Individual	-25 %
		Silting	Storage Max. Depth	3 m	1.50 m	-50 %

Table 3.8: Adjusted parameters - 04 - Cistern - Strong

04 - Cistern - Strong combines the same two incidents as *03 - Cistern Light*, *Pump Failure* and *Silting*. The difference in this failure scenario is the severity of the incidents as it is the *Strong*-Variant. The *Pump Capacity* is reduced by 25 % to simulate *Pump Failure* and the *Storage Max. Depth* is reduced by 50 % to simulate *Silting*.

3.4.0.5. 05 - Green Roofs - Light

Failure Scenario	LID - Measure	Incident	SWMM LID Parameter	Initital Value	Adjusted Value	% of Initial Value
05 - Green Roof - Light	Extensive Green Roof	Substrate Erosion	Soil Thickness	100 mm	90 mm	-10 %
	Intensive Green Roof	Substrate Erosion	Soil Thickness	250 mm	225 mm	-10 %

Table 3.9: Adjusted parameters - 05 - Green Roof Light

05 - Green Roofs - Light combines the two incidents *Substrate Erosion* and *Consolidated Flow Paths*. The *Soil Thickness* was reduced by 10 % to simulate the *Substrate Erosion*

and the *Field Capacity* was reduced by 25 % to simulate the *Consolidated Flow Paths*. This applies to both *Extensive Green Roofs* and *Intensive Green Roofs*.

3.4.0.6. 06 - Green Roofs - Strong

Failure Scenario	LID - Measure	Incident	SWMM LID Parameter	Initital Value	Adjusted Value	% of Initial Value
06 - Green Roof - Strong	Extensive Green Roof	Substrate Erosion	Soil Thickness	100 mm	75 mm	-25 %
	Intensive Green Roof	Substrate Erosion	Soil Thickness	250 mm	187.5 mm	-25 %

Table 3.10: Adjusted parameters - 06 - Green Roof Strong

06 - Green Roofs - Strong combines the same two incidents as *05 - Green Roofs - Light*, *Substrate Erosion* and *Consolidated Flow Paths*. The difference in this failure scenario is the severity of the incidents, as it is the *Strong*-Variant. *Soil Thickness* is reduced by 25 % to simulate *Pump Failure* and the *Field Capacity* is reduced by 50 % to simulate *Consolidated Flow Paths*.

3.4.0.7. 07 - Infiltration - Light

Failure Scenario	LID - Measure	Incident	SWMM LID Parameter	Initial Value	Adjusted Value	% of Initial Value
07 - Infiltration - Light	Infiltration Swale	Colmation	Soil Conductivity	3600 mm/hr	3420 mm/hr	-5 %
		Sedimentation	Surface Berm Height	300 mm	270 mm	-10 %
			Soil Conductivity	3600 mm/hr	3240 mm/hr	-10 %
	Trough-Trench Element	Colmation	Soil Conductivity	180 mm/hr	171 mm/hr	-5 %
		Sedimentation	Surface Berm Height	300 mm	270 mm	-10 %
			Soil Conductivity	180 mm/hr	162 mm/hr	-10 %

Table 3.11: Adjusted parameters - 07 - Infiltration - Light

07 - Infiltration - Light includes the incidents *Colmation* and *Sedimentation*. However, a distinction must be made here between two areas of responsibility. For the *Infiltration Swales* and *Trough-Trench Elements* in the public street space, *i.e.*, partly in FA_4_Existing_Buildings and completely in FA_5_Street_Area, the *Berliner Wasserbetriebe (BWB)* are in charge for care and maintenance. As the discussions with *BWB* showed, that these infiltration measures are taken care of up to six times a year, no superficial deterioration is to be expected. The adjusted LID parameters of the *Sedimentation* therefore only come into effect in the remaining FAs. However, even the *BWB* cannot completely

prevent *Colmation* which takes place underground, despite maintenance. This results in a reduction for the parameters *Surface Berm Height* and *Soil Conductivity* by 10 % for the incident *Sedimentation* for all FAs, except FA_5_Street_Area. In FA_5_Street_Area, only *Colmation* occurs. This is simulated by reducing the parameter *Soil Conductivity* by 5 %.

3.4.0.8. 08 - Infiltration - Strong

Failure Scenario	LID - Measure	Incident	SWMM LID Parameter	Initial Value	Adjusted Value	% of Initial Value
08 - Infiltration - Strong	Infiltration Swale	Colmation	Soil Conductivity	3600 mm/hr	3420 mm/hr	-5 %
		Sedimentation	Surface Berm Height	300 mm	150 mm	-50 %
			Soil Conductivity	3600 mm/hr	2700 mm/hr	-25 %
	Trough-Trench Element	Colmation	Soil Conductivity	180 mm/hr	171 mm/hr	-5 %
		Sedimentation	Surface Berm Height	300 mm	150 mm	-50 %
			Soil Conductivity	180 mm/hr	135 mm/hr	-25 %

Table 3.12: Adjusted parameters - 08 - Infiltration - Strong

08 - Infiltration - Strong also consists of *Colmation* and *Sedimentation*. Here, again, a distinction is made between the areas of responsibility of the *BWB* and private owners. For infiltration measures in the private sector, the result is that *Colmation* is modelled with a reduction of 25 % for the *Soil Conductivity*. *Sedimentation* is modelled with a 25 % reduction of the *Soil Conductivity* and a 50 % reduction of the *Surface Berm Height*. For the infiltration measures in the public space, *Sedimentation* is again omitted and only *Colmation* is modelled by reducing *Soil Conductivity* by 5 %.

3.4.0.9. 09 - Total Failure - Light

Failure Scenario	LID - Measure	Incident	SWMM LID Parameter	Initital Value	Adjusted Value	% of Initial Value
09 - Total Failure -Light	Cistern	Pump Failure	Pump Curve	Individual	Individual	-10 %
		Silting	Storage Max. Depth	3 m	2.25 m	-25 %
	Extensive Green Roof	Substrate Erosion	Soil Thickness	100 mm	90 mm	-10 %
	Intensive Green Roof	Substrate Erosion	Soil Thickness	250 mm	225 mm	-10 %
	Infiltration Swale	Colmation	Soil Conductivity	3600 mm/hr	3420 mm/hr	-5 %
		Sedimentation	Surface Berm Height	300 mm	270 mm	-10 %
			Soil Conductivity	3600 mm/hr	3240 mm/hr	-10 %
	Trough-Trench Element	Colmation	Soil Conductivity	180 mm/hr	171 mm/hr	-5 %
		Sedimentation	Surface Berm Height	300 mm	270 mm	-10 %
			Soil Conductivity	180 mm/hr	162 mm/hr	-10 %

Table 3.13: Adjusted parameters - 09 - Total Failure - Light

09 - Total Failure - Light is a combination of all the incidents that occur in this study. The reduction of the parameters is the same as in all other *Light*-Variant scenarios described above.

3.4.0.10. 10 - Total Failure - Strong

Failure Scenario	LID - Measure	Incident	SWMM LID Parameter	Initital Value	Adjusted Value	% of Initial Value
10 - Total Failure -Strong	Cistern	Pump Failure	Pump Curve	Individual	Individual	-25 %
		Silting	Storage Max. Depth	3 m	1.5 m	-50 %
	Extensive Green Roof	Substrate Erosion	Soil Thickness	100 mm	75 mm	-25 %
	Intensive Green Roof	Substrate Erosion	Soil Thickness	250 mm	187.5 mm	-25 %
	Infiltration Swale	Colmation	Soil Conductivity	3600 mm/hr	3420 mm/hr	-5 %
		Sedimentation	Surface Berm Height	300 mm	150 mm	-50 %
			Soil Conductivity	3600 mm/hr	2700 mm/hr	-25 %
	Trough-Trench Element	Colmation	Soil Conductivity	180 mm/hr	171 mm/hr	-5 %
		Sedimentation	Surface Berm Height	300 mm	150 mm	-50 %
			Soil Conductivity	180 mm/hr	135 mm/hr	-25 %

Table 3.14: Adjusted parameters - 10 - Total Failure - Strong

10 - Total Failure - Strong also contains all incidents occurring in this work. The reduction of the parameters is the same as in all other *Strong*-Variant scenarios described above.

3.5. Data Analysis of Model Scenarios

The following section describes the data analysis carried out in this study. The comparison of the different model scenarios is structured consistently. First, the runoff of the *Urban Redevelopment Area (URA)* is considered, then the runoff of the entire *Sewer Catchment (BlnXI)* is observed, and finally, the *Combined Sewer Overflow (CSO)* of *BlnXI* is viewed. A distinction is made between the model analysis, which includes consideration according volume and peak rates, and the resilience analysis, which includes consideration according to the *Resilience Index*.

3.5.0.1. Model Analysis

The general model analysis was carried out using various parameters and events. The total volume and the peak rates were always considered. For the consideration of the total simulation period as presented in Sec. 3.2.3.2 and the individual events, the volume and the peak rates were always considered. For a consistent comparison of the individual scenarios, four events were selected in advance and repeatedly considered for the comparison. The selected rain events are briefly presented graphically and on the basis of their most important characteristic values in Fig. 3.22. It should be mentioned here that these are not always all shown, but can be viewed in full for each analysis in the appendix under A.

3.5.0.2. Resilience Analysis

In order to be able to establish the resilience assessment according to the *Resilience Index* (Sec. 2.3), different thresholds were set in advance for the investigation of the surface runoff and CSO:

- **Surface Runoff Volume**, the discharge restriction of the federal state of Berlin of 10 l/s·ha is used as the threshold
- **CSO Discharge**, the threshold of >0.001 m^3/s is used to identify an event

The following presented parameters were considered in the resilience assessment:

- **Number of Events** that exceed the predefined threshold
- **Total Event Duration** of the events that exceed the threshold
- **Mean Event Duration** of the events that exceed the threshold

- **Mean trec of Events**, mean recovery time which is needed after the event peak to fall below the set threshold
- **Total Severity of Events** that exceed the threshold
- **Total Resilience of Events** that exceed the threshold

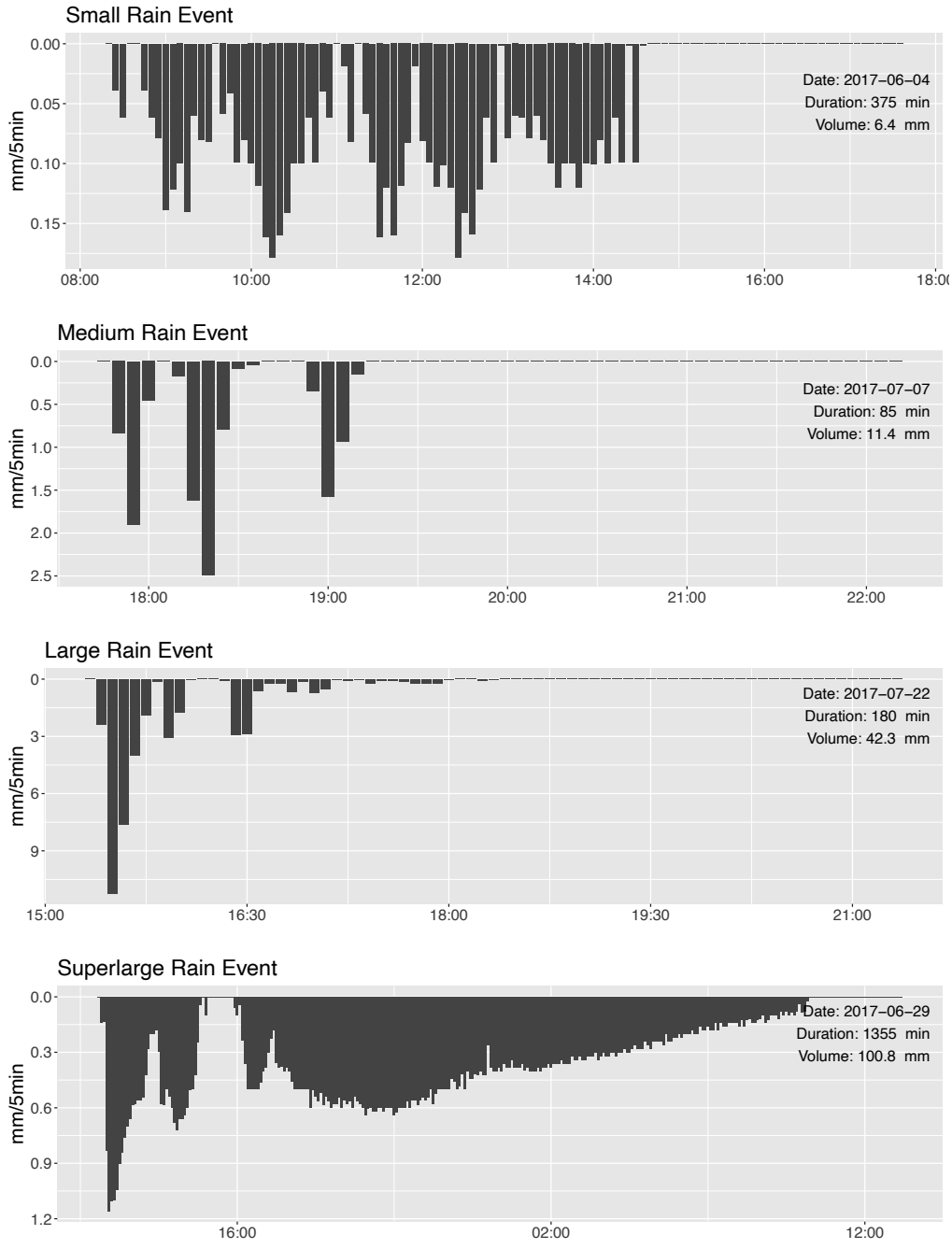

Figure 3.22: Selected rain events to enable consistent comparison

4. Results & Discussion

4.1. Calibration Assessment of BlnXI SWMM-Model

As described in Sec. 3.2, the calibration was done indirectly, by comparing the model performance to the calibrated *InfoWorks*-model. The two parameters, *Volume* and *Nash-Sutcliffe Efficiency (NSE)*, were validated for various significant points or simulated values in the model (Sec. 3.2.2). These points included (i) the system *Surface-Runoff*, (ii) the *Pumping Station*, (iii) the *Combined Sewer Overflow*, (iv) a *Combined Sewer Conduit*, (v) the runoff of a *Pervious Catchment*, and (vi) the runoff of an *Impervious Catchment*.

Measurement	Volume InfoWorks (m^3)	Volume SWMM (m^3)	%-Difference	NSE
BlnXI Surface Runoff	1,068,482	1,051,560	- 1.58	-
Pumping Station	3,184,854	3,058,156	-3.98	0.914
Combined Sewer Overflow	560,646	555,591	- 0.91	0.864
Combined Sewer Conduit	796,297	708,672	- 11.00	0.914
Runoff Pervious Catchment	6,255	6,379	1.93	0.754
Runoff Impervious Catchment	30,267	29,451	- 2.77	0.889

Table 4.1: Assessment of model transfer

As can be seen in Tab. 4.1, the *BlnXI*-model could be sufficiently calibrated to the existing *InfoWorks*-model. This is reflected in the different measured *Volumes*, where a deviation of < 4 % is reached. Especially the *Combined Sewer Overflow Volume*, which is of importance for this study, shows a satisfactory value with a deviation of < 1 %, this is shown graphically in Fig. 4.2. Only in the case of the *Combined Sewer Conduit*, the *Volume* differs by > 10 %. The excellent calibration of the model is also reflected in the *NSE*-values. Here, except for the runoff of the *Pervious Catchment*, satisfactory values of $NSE > 0.85$ could be achieved. The parameters used for model calibration are marked bold in Sec. 3.2.1.1.

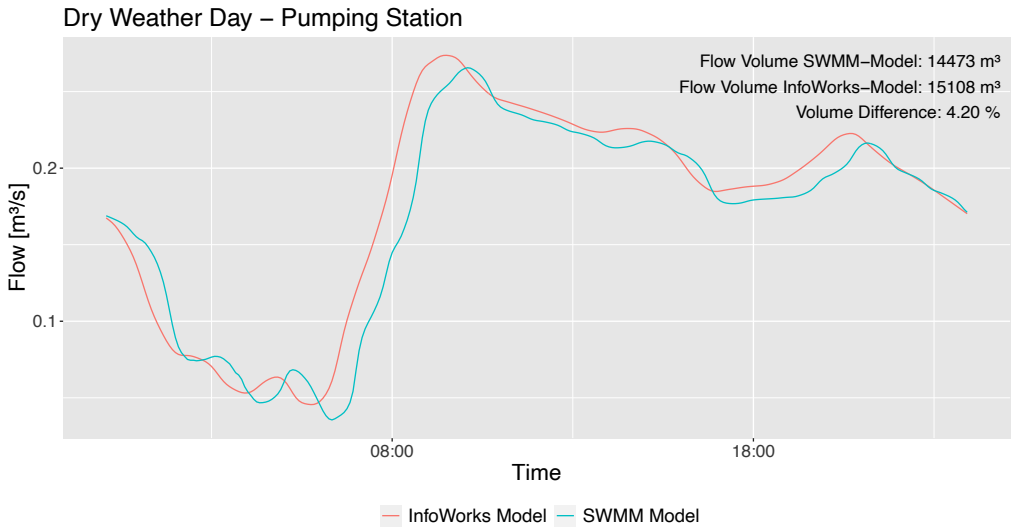

Figure 4.1: Calibration at pumping station for dry weather day

The successful calibration can also be proven graphically at the relevant location of the *Pumping Station* for the sewer satchment *BlnXI*. Fig. 4.1 shows the pumping behaviour on a dry weather day. It can be seen that the *SWMM*-model can process the wastewater in the combined system with a volume difference of < 5 % and a slight time shift.

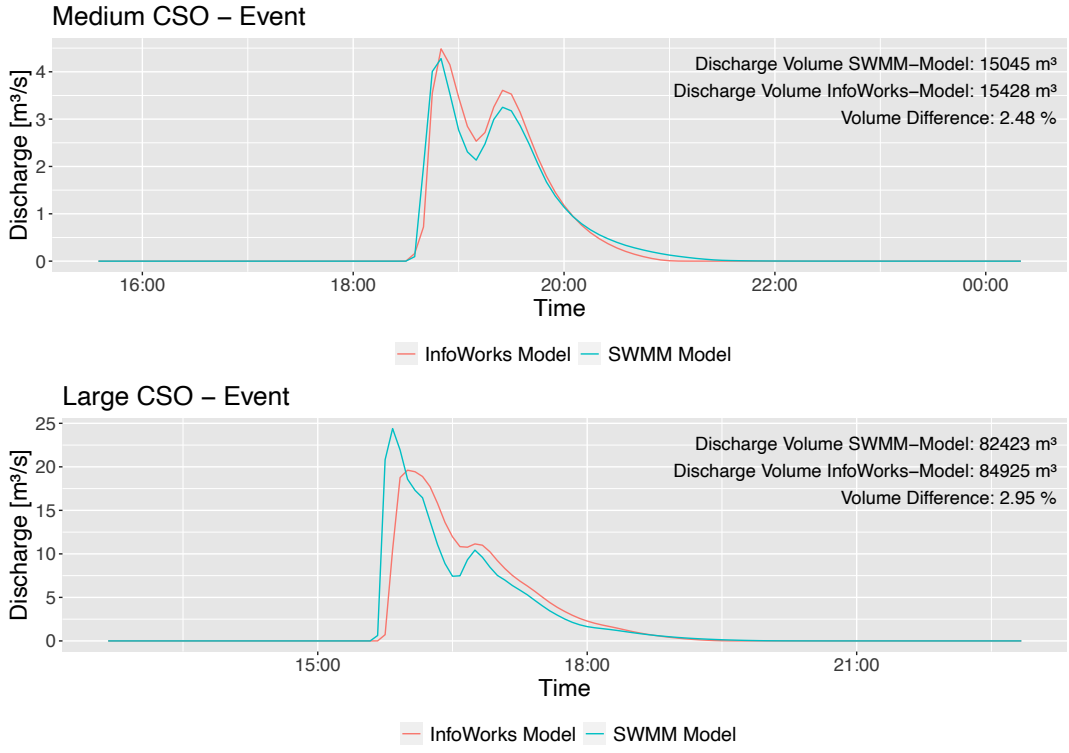

Figure 4.2: Calibration shown for medium & large CSO event

As shown in Fig. 4.2 by two CSO events, the transfer of the *InfoWorks*-model to *SWMM* also achieves excellent CSO results. For the selected *Medium CSO-Event*, both the intensity and the volume were very accurate. For the CSO volume of the event, a difference of 2.48 % was achieved. Also the *Large CSO-Event* was matched well, especially with regard to the volume, with a difference of < 3 %.

In conclusion, the transfer of the *BlnXI*-model from *InfoWorks* to *SWMM* was very satisfactory. Excellent results were achieved especially for the key values of the system that are of great importance for the further investigations, such as the *Pumping Station*-volume, the *Surface Runoff*-volume and the CSO volume. When comparing the models, one has to keep in mind that the *InfoWorks*-model was calibrated for pump volume and CSO volume of different simulation years [Riechel et al., 2016, Riechel et al., 2020]. Runoff from pervious and impervious areas is represented in a simpler way than in *SWMM* and complete agreement between the two models cannot be expected. In general the high level of agreement, particularly for the CSO volume, allows simulation with similar accuracy to the original model. Further graphical representations of the calibration can be found in the appendix in Fig. A.4.

4.2. Effects and Plausibility of LID Chains

The LID chains presented in Sec. 3.3.2 were simulated separately to assess their effectiveness and test plausibility of model representation. The effects of LID chains LC1, LC4 and LC11 are shown exemplarily below. The remaining chains are shown in the appendix under Fig. A.5.
To have a realistic simulation of the LID chains, rain events of different sizes were selected from the rain series from May 2017 to October 2017, which was later used for the modelling of the different scenarios. These differ in terms of their precipitation volume, intensity and duration. The rain events are shown graphically in Fig. 4.3.
For *LID-Linkage-Chain 1*, it can be clearly seen that the runoff volume from the effective runoff area (50 % FR+ 50 % EGR) for the *Small* and *Medium Rain Event* was halved by the conversion compared to the *Reference Area Flat Roof (Reference FR)*. The *Cistern* as the next element in the chain is sufficient to completely retain the occurring runoff. For the *Large Rain Event*, more conclusions can be drawn. Despite the larger rain event, the runoff volume of the *Reference FR* could be halved. Afterwards, however, the *Cistern* quickly fills up due to the large runoff volume. However, the overflowing water of the *Cistern* can be completely retained by the *Trough-Trench Element (TTE)* in

the last stage. For the three rain events shown, this means complete disconnection.This is plausible also from a practical point of view. *TTE* are typically designed to retain rain events up to an annuity of five years, which includes the three standard rain events examined in this study.

For *LID-Linkage-Chain 4*, we see that by converting the *Reference FR* into 50 % *EGR* and 50 % *IGR*, the *Small* and *Medium Rain Event* can already be completely eliminated and no runoff occurs. For the *Large Rain Event*, however, roof runoff occurs after a short time despite *EGR* and *IGR*. This leads to runoff to the *Cistern* over a longer period of time, resulting in a smaller but longer overflow than for the reference. This low overflow is completely retained by the *TTE*. Here, again, a complete decoupling can be determined for the three rain events shown.

LID-Linkage-Chain 11 is shown here because it takes up the largest proportion of the URA in the later modelling scenarios. It can be seen that by converting the *Reference Area Fully Sealed (Reference FS)* into *Partially Sealed (PS)* area, complete decoupling can already be achieved for the *Small Rain Event*. For the *Medium* and *Large Rain Event*, a runoff from the *PS-Area* can be seen. This is due to the fact that a lot of precipitation falls in a relatively short time and the infiltration capacity is exceeded. However, as the precipitation subsides, the *PS-Area* is able to infiltrate it again. Nevertheless, the runoff is completely retained in the final stage by the *Surface Infiltration*. In conclusion, it can be stated that the expected effects could be achieved for all LID chains used in this study. For the rain events used in this test, complete decoupling was achieved for all LID chains except for *LC10*, which is only half connected to LID measures. This shows that the LID chains are properly designed to deal with rain events of annuities < 5 years.

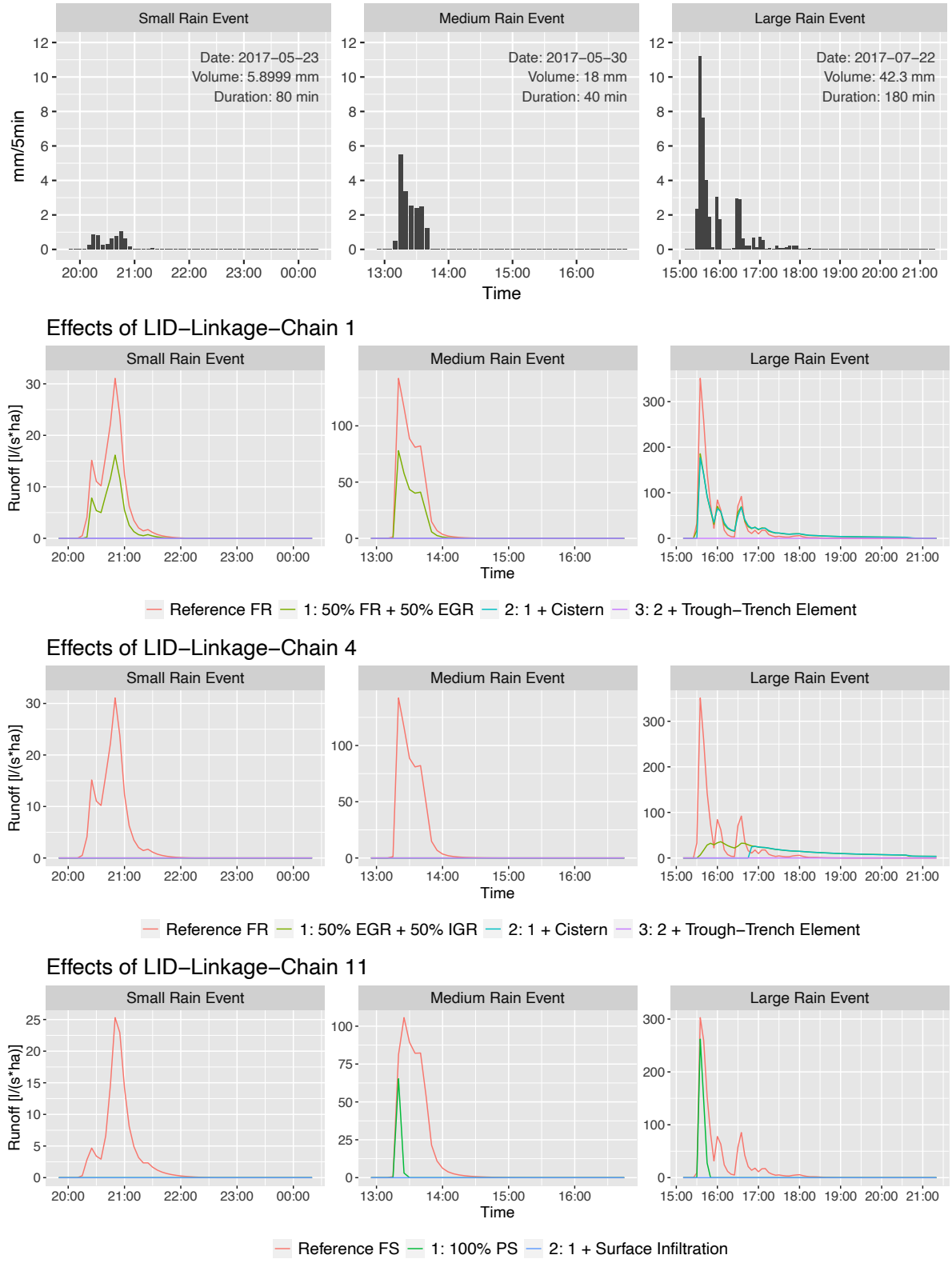

Figure 4.3: Flow simulation through LID chains

4.3. Model Scenarios

4.3.1. 01 & 02 - Construction without/with Water Concept

In the following, the scenarios *01 - Construction without Water Concept (SC - 01)* and *02 - Construction with Water Concept (SC - 02)* are compared. The two concepts have already been presented in Sec. 3.4; Tab. 4.2 lists the most important characteristics once again.

		01 - Construction without Water Concept (SC-01)	**02 - Construction with Water Concept (SC-02)**
Impervious Area of URA	**ha**	40.97	49.99
Impervious Area of URA connected to LIDs	**ha / %**	0.0 / 0.0	49.10 / 98.40
Impervious Area of BlnXI	**ha**	231.95	240.97
Impervious Area of BlnXI connected to LIDs	**ha / %**	0.0 / 0.0	49.10 / 20.38

Table 4.2: Overview - area shares *SC-01* & *SC-02*

4.3.1.1. Surface Runoff URA

		01 - Construction without Water Concept	**02 - Construction with Water Concept**	**Reduction in %**
Runoff Volume - URA				
Surface Runoff of URA	m^3	189,362	17,722	90.64
Surface Runoff of Impervious Area	mm	462.2	35.45	92.33
Surface Peak Runoff Rate	l/s·ha	144.40	5.58	96.13
Resilience URA				
Runoff Events > l/s·ha	n	20	0	100
Total Event Duration	h:min	27:25	00:00	100
Mean Event Duration	min	82	0	100
Mean trec of Events	min	51.5	0	100
Total Severity of Events	-	0.0441	0	100
Total Resilience of Events	-	0.9559	1.00	-4.61

Table 4.3: Runoff URA - *SC-01* & *SC-02*

For the *URA*, the simulation for *SC-01* resulted in a surface runoff volume of 189,362 m^3 or 462.2 mm for the study period May 2017 to October 2017. The peak runoff rate was 144.40 l/s·ha. *SC-02* reduced the surface runoff volume by 90.6 %. In addition, the peak runoff rate could be considerably decreased by 96.1 % to 5.58 l/s·ha.
The surface runoff volume of the *URA* can also be subjected to a plausibility check. In Trapp et al., 2020, rough projections for the effectiveness of the LID measures in

exactly this URA were made based on a *WABILA*-model approach. In order to be able to compare it with the reduction in this study, however, the area of the previously unassignable parts of the URA (marked white in Fig. 3.8) must be added back to the effective runoff area. After including these areas, the runoff volume of *SC-02* increases to 25,050 m^3. This results in a reduction of 86.8 %, even exceeding the estimate of 73 % made in Trapp et al. (2020). The slightly higher decoupling shows that the more detailed analysis done here can supports the assessment (*e.g.*, through actual runoff simulation or through consideration of actual infiltration capacity).

In the resilience assessment, a total of twenty events were identified for *SC-01*, which exceeded Berlin's Rainwater Discharge Restriction of 10 l/s·ha. In total this threshold was exceeded for a duration of 27 h 25 min with a mean event duration of 82 min. On average, it takes an event 51.5 min to fall below the legal requirements after reaching the peak runoff rate. According to the *Resilience Index* (Sec. 2.3), this is resulting in a total severity for the events of Sev = 0.0441 and correspondingly in a resilience of Res = 0.9559 for *SC-01*. For *SC-02* on the other hand, URA surface runoff did not exceed the threshold of 10 l/s·ha once. This rules out further calculation of the parameters and the URA in *SC-02* can be considered as fully resilient (Sev = 0; Res = 1) to the rain events occurring in the summer half-year 2017.

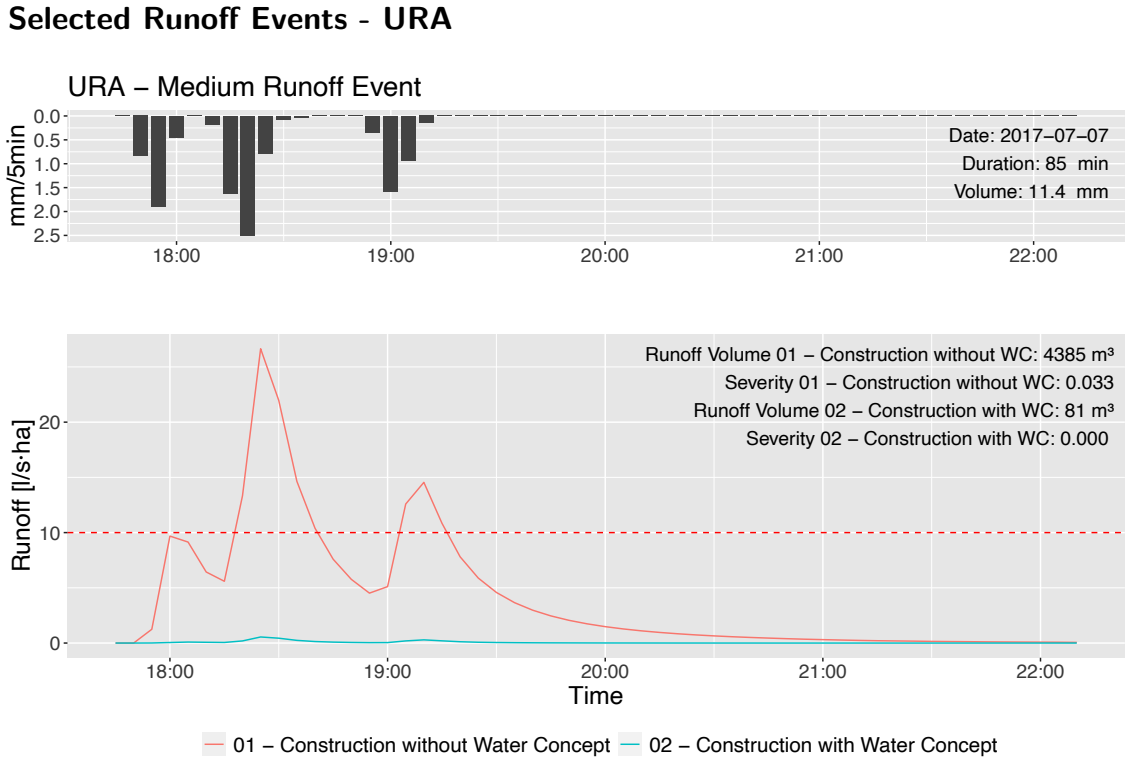

Figure 4.4: URA runoff medium event

The effects of the LID measures of *SC-02* for the runoff of the URA are illustrated for the *Medium Event* (Fig. 4.4). It can be clearly seen that the rain event causes a significant exceedance of the threshold 10 l/s·ha for *SC-01* which causes a runoff volume of 4,385 m^3. By disconnecting the impervious areas, it was possible to achieve that the threshold of < 10 l/s·ha was not nearly reached and the runoff volume was drastically reduced to 81 m^3. This is also reflected in the severity of the *Resilience Index*. Since the threshold is not exceeded, the system is classified as resilient for this rain event and has a severity of Sev = 0.000.

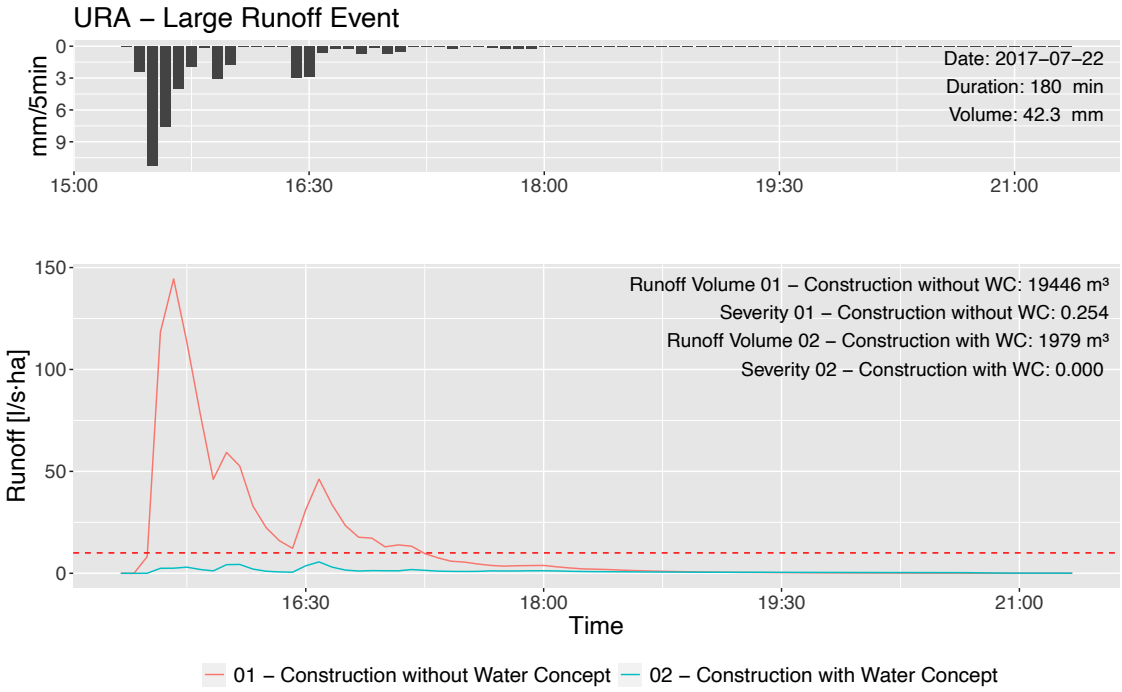

Figure 4.5: URA runoff large event

The effects of the LID measures of *SC-02* can also be shown for a large rain event. During the event on 22.07.2017, shown in Fig. 4.5, the intensity went up to 11.2 mm/5min of precipitation. It can be seen that the discharge restriction set by the state of Berlin was exceeded significantly with a peak runoff of 144 l/s·ha for *SC-01*. In the case of *SC-02*, the limit is not exceeded even during this high-intensity rain event and the runoff volume is reduced by 89 %, from 19,446 m^3 to 1,979 m^3. Resulting from that, *SC-02* is resilient to this large rain event with a severity of Sev = 0.000.

In conclusion, it can be stated that the runoff volume and the peak runoff of the URA could be drastically reduced by the LID measures. Even in an investigation period that was characterised by very high precipitation and extreme rain events, the discharge limits were not exceeded.

Further runoff events of the URA are shown graphically in the appendix in Fig. A.10.

4.3.1.2. Surface Runoff BlnXI

		01 - Construction without Water Concept	02 - Construction with Water Concept	Reduction in %
Runoff Volume - BlnXI				
Surface Runoff of BlnXI	m^3	1,057,770	886,130	16.23
Surface Runoff of Impervious Area	mm	456.0	367.7	19.36
Surface Peak Runoff Rate	l/s·ha	130.53	105.81	18.94
Resilience BlnXI				
Runoff Events > 10 l/s·ha	n	17	13	23.5
Total Event Duration	h:min	26:50	23:30	12.42
Mean Event Duration	min	94.7	108.5	-14.57
Mean trec of Events	min	59.7	68.1	-14.07
Total Severity of Events	-	0.0384	0.0274	28.65
Total Resilience of Events	-	0.9616	0.9726	-1.14

Table 4.4: Runoff *BlnXI - SC-01 & SC-02*

For the runoff of the sewer catchment *BlnXI*, the simulation for *SC-01* resulted in a runoff volume of 1,057,770 m^3. *SC-02* led to a runoff volume of 886,130 m^3, which is a reduction by 16.2 %, with a connection rate of the impervious areas of *BlnXI* to LIDs of 20.4 %. An even greater impact was made for the surface peak runoff rate which was reduced by 18.9 % for the sewer catchment *BlnXI*.

Although only about 20 % of *BlnXI* was connected to LID measures, the total runoff events which exceeded Berlin's restrictions of 10 l/s·ha could be reduced from 17 to 13 events. The smaller number of events is also reflected in the total event duration which decreased by 12.4 % from 26 h 50 min to 23 h 30 min. The mean event duration, on the other hand, is increasing, from previously 94.7 min to 108.5 min as well as the mean recovery time from 59.7 min to 68.1 min. This is not unexpected as the previously mentioned four prevented runoff events by the LID measures are relatively small and short events, and the reduced number of events has a strong impact on the mean values. In addition, the implementation of the measures has reduced the severity of failures, the total event severity could be reduced by 28.7 % from Sev = 0.0384 to Sev = 0.0274. In turn the resilience of *BlnXI* was increased by 1.1 % from Res = 0.9616 to Res = 0.9726. However, it becomes clear that resilience is a parameter that is difficult to classify, as the change takes place in a very small percentage. For the severity, on the other hand, the change is easier to identify.

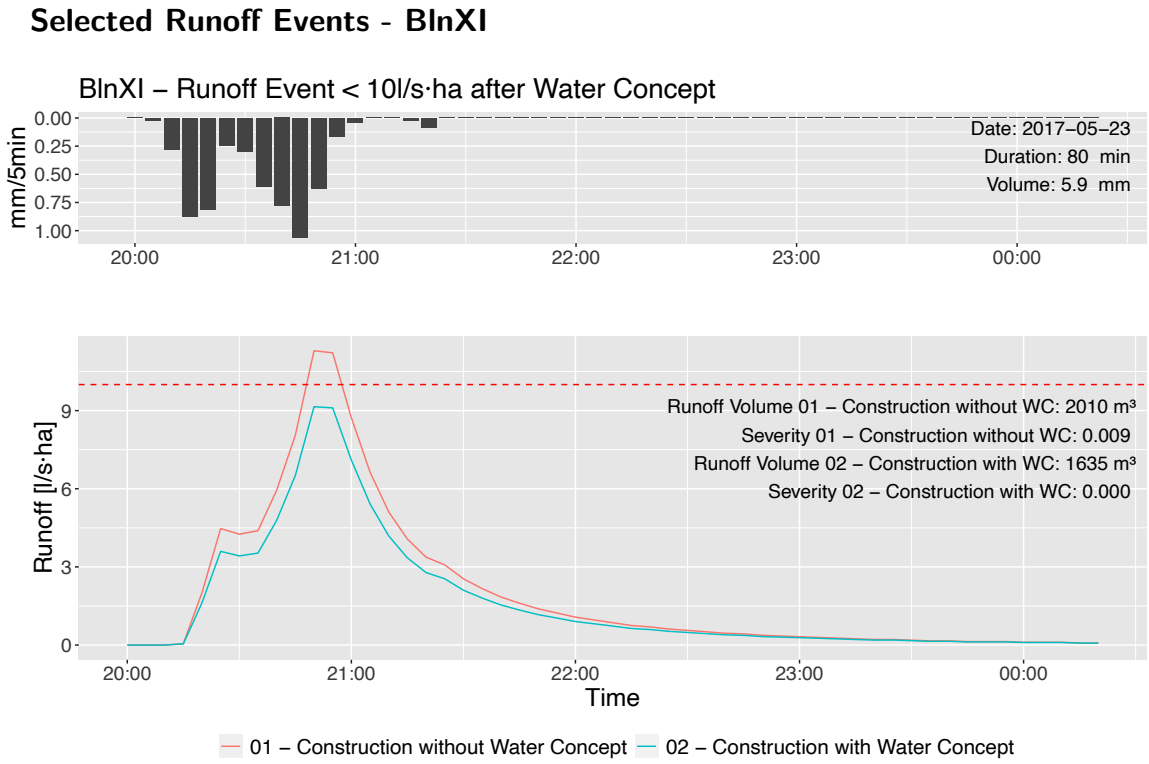

Figure 4.6: *BlnXI* - Runoff < 10 l/s·ha after *SC-02*

The runoff event shown in Fig. 4.6 is one of the four events of the sewer catchment *BlnXI* that could be brought below Berlin's discharge threshold due to LID implementation. For the event, the runoff volume could be reduced by 18.7 % from 2,010 m^3 for *SC-01* to 1,635 m^3 for *SC-02*, which led to a reduction in peak runoff rate from almost 11 l/s·ha to 9 l/s·ha. This results in an event resilience of Res = 1 for *SC-02* from the perspective of the *Resilience Index*.

The events that were brought below the threshold were already small events in *SC-01*, caused by minor (but still CSO producing) rain events. As a result, the threshold was only slightly exceeded before the LID implementation. Major precipitation events, such as the *Large Runoff Event* in Fig. 4.7, have not moved close to Berlin's discharge restriction.

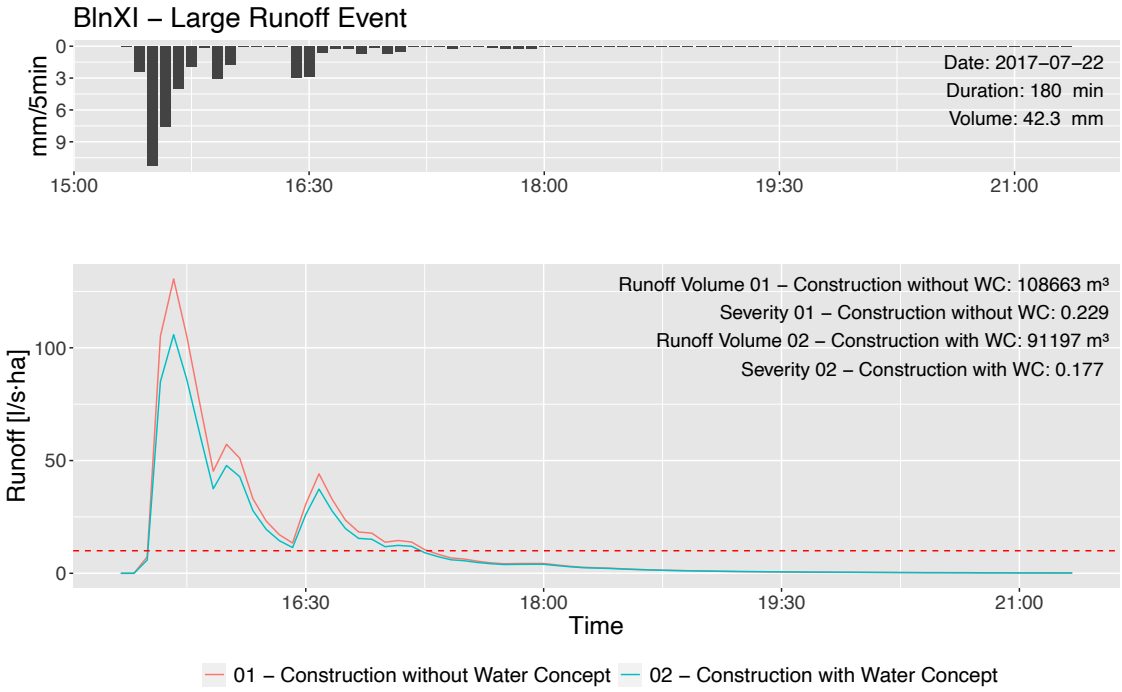

Figure 4.7: *BlnXI* runoff large event

The event peak runoff rate for *SC-01* is 131 l/s·ha and causes a total runoff volume of 108,663 m³. The LID measures can reduce the peak runoff rate by 18.9 % to 106 l/s·ha. The volume can also be reduced by 16.1 % to 91,197 m³. The reduction in volume is also reflected by the severity which could be reduced by 22.7 % from Sev = 0.229 to Sev = 0.177. Conversely, this means that the event resilience was increased from Res = 0.771 to Res = 0.823 by 6.7 %. Nevertheless, it can be stated that the sewer catchment *BlnXI* is not resilient to this large rainfall event regarding the runoff threshold of 10 l/s·ha.

In conclusion, it can be determined that the LID measures are noticeable in the entire sewer catchment *BlnXI*. However, as was to be expected, they have a much smaller effect on the runoff events at *BlnXI*-level compared to the impact in the URA. Despite the fact that the measures were only implemented locally, four small events no longer exceeded the legal requirements. In order to achieve further reductions, measures in the rest of the *BlnXI* catchment would also be needed. Further runoff events of the sewer catchment *BlnXI* are shown graphically in the appendix in Fig. A.11.

4.3.1.3. Combined Sewer Overflows

		01 - Construction without Water Concept	02 - Construction with Water Concept	Reduction in %
CSO Volume				
CSO - Volume	m^3	563,301	430,562	23.56
CSO Peak Discharge Rate	m^3/s	24.72	17.57	28.91
Resilience CSO				
Discharge Events > 0.001 m^3/s	n	26	24	7.7
Total Event Duration	h:min	155:45	136:10	12.6
Mean Event Duration	min	359.4	340.4	5.29
Mean trec of Events	min	309.4	306.6	0.91
Total Severity of Events	-	0.0405	0.0310	23.47
Total Resilience of Events	-	0.9595	0.9690	-0.99

Table 4.5: CSO - *SC-01* & *SC-02*

Regarding CSO, the simulation for *SC-01* resulted in a CSO volume of 563,301 m^3. Comparing Tab. 4.5 with Tab. 4.4, it is noteworthy that about 50 % of surface runoff leaves the sewer system via CSO. This high rate is due to exceptional conditions in summer 2017. Almost 200,000 m^3 of CSO are due to the most extreme event on June 29th. Without the two largest events the share of stormwater runoff that leaves via CSO is reduced to about 35 %.
SC-02 led to a CSO volume of 430,562 m^3 which is a reduction by 23.6 %. As mentioned in 4.3.1.2, 16.2 % of *BlnXI's* surface runoff volume could be reduced, therefore, a ratio of $\sim$ 1.45 between reduced surface runoff volume and reduced CSO volume is achieved. This observation agrees well with the findings of Riechel et al., 2020 who found a factor of $\sim$ 1.5 for a different combined sewer catchment in Berlin.
The CSO peak discharge rate could be reduced by 28.9 % from 24,72 m^3/s for *SC-01* to 17,57 m^3/s for *SC-02*. This reduction in the peak discharge rate can also have an effect on the potential impact on the water bodies in which the discharge occurs. As stated in Riechel et al. (2016), a lower mixing ratio between CSO discharge and river water has a positive impact on the stressed water body, therefore, the CSO volume and peak reduction can both be considered as important achievements.

In the resilience assessment for the CSO discharge, a total of 26 events were identified for *SC-01* which exceeded the set threshold of 0.001 m^3/s. Due to *SC-02*, two events could be completely prevented and total CSO event duration was reduced by 12.6 % to 136 h 10 min. As already mentioned in the previous observations, the impact on the mean parameters is significantly smaller, which can be attributed to the complete

reduction of small events by the LID measures. This is once again evidenced by the mean event duration which was only reduced by 5.3 % to 340.4 min. The LID measures have almost no effect on the recovery time. The total severity was reduced by 23.5 % and thus roughly corresponds to the reduction of the CSO volume. The resilience again shows that despite the very large volume and peak reduction, only a small percentage change can be seen. The system has increased its resilience by 0.99 % from Res = 0.9595 to Res = 0.9690. In the following, the effects of the LID measures are shown graphically using CSO events of different sizes.

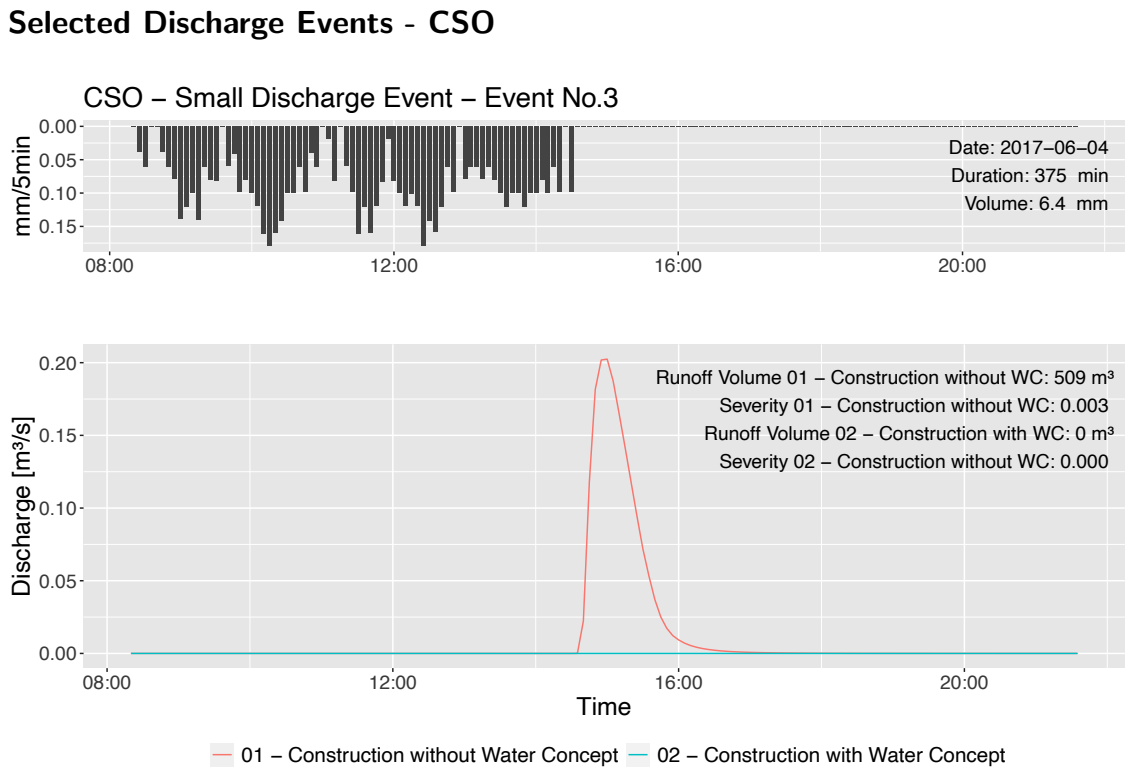

Figure 4.8: CSO small event

The *CSO Discharge Event No.3* shown in Fig. 4.8 is one of the events that could be prevented by the implementation of LID measures in the *URA*. It is caused by a rain event that has a volume of 6.4 mm over a period of over six hours. It is shown that the *SC-01* system is resilient to the event for a long time but with advanced rain duration it could not longer handle the occurring runoff. This is causing a CSO volume for *SC-01* of 509 m^3 and a severity of Sev = 0.003 which indicates that it is a small CSO event. Due to the LID measures in *SC-02*, the sewer system and the pumping station are sufficient to process the occurring runoff. As a result, a CSO overflow can be completely

prevented and the *SC-02* is resilient against this rain event with a Severity of Sev = 0.000. For classification, it is important that the rain event is characterised by a very long duration and therefore, it does not lead to an abrupt overload of the LID measures. This significantly contributes to the prevention of the event.

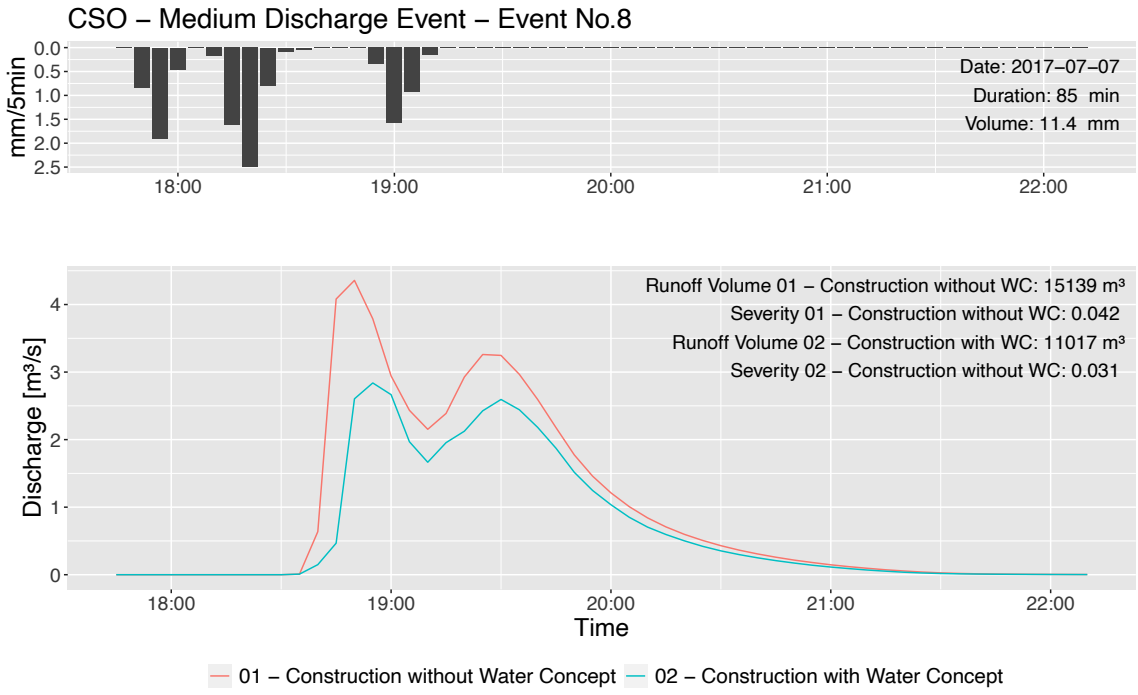

Figure 4.9: CSO medium event

For the *Medium CSO Discharge Event No.8*, shown in Fig. 4.9, it can be seen that the implementation of the LID measures in *02 - Construction with Water Concept (SC-02)* led to a weakening of the CSO discharge intensity. Furthermore, it can be seen that the peak of the discharge can be reduced from > 4 m³/s to < 3 m³/s. This is also reflected in the volume of the event which could be reduced by 27.2 % from 15,139 m³ for *SC-01* to 11,017 m³ for *SC-02*. The quantified severity was also reduced from Sev = 0.042 for *SC-01* to Sev = 0.031 for *SC-02*.

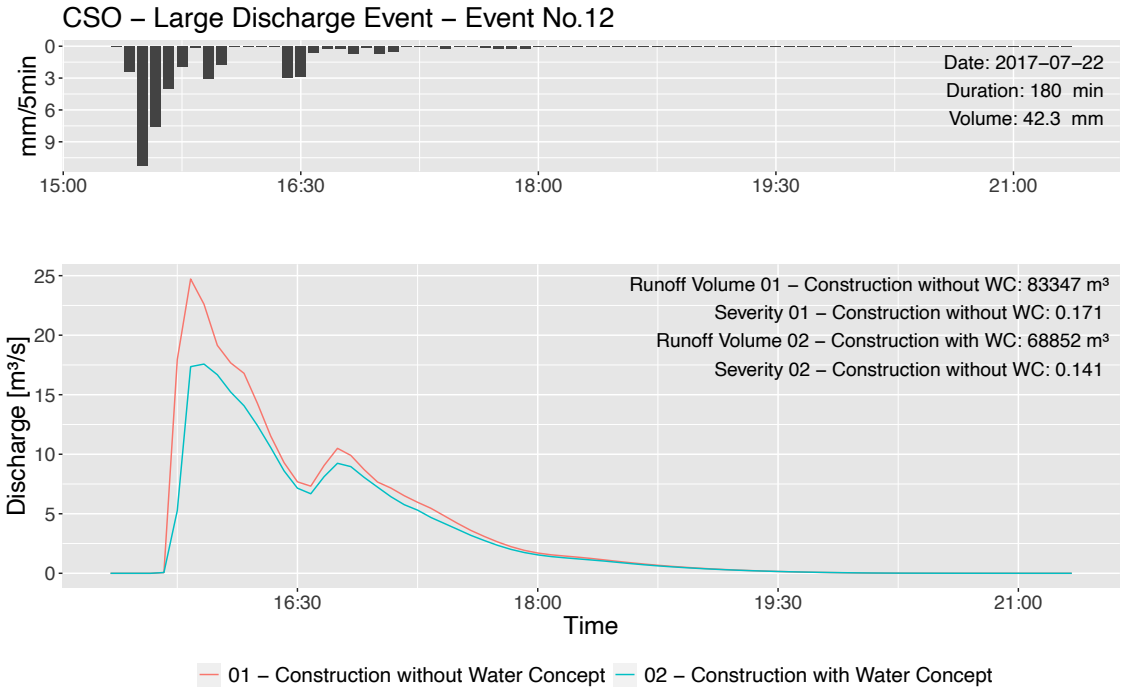

Figure 4.10: CSO large event

Large CSO Discharge Event No.12, shown in Fig. 4.10, clearly demonstrates the effects of implementing the LID measures in the *URA*. Due to the very high intensity of the rain event, the beginning of the overflow cannot be postponed but the intensity can be visibly weakened. *CSO Event No.12* displays the peak discharge rate in the study period for both scenarios. The peak discharge rate could be reduced from 24.72 m^3/s for *SC-01* to 17.57 m^3/s for *SC-02* by 28.9%. The CSO volume could be reduced from 83,347 m^3 to 68,852 m^3 by 17.4%. A trend can be seen here, which is confirmed in Fig. 4.11:
"The larger the volume of the CSO discharge event, the smaller the percentage volume reduction."
The severity could also be reduced, from Sev = 0.171 for *SC-01* to Sev = 0.141 for *SC-02*.

Further CSO discharge events are shown graphically in the appendix in Fig. A.12.

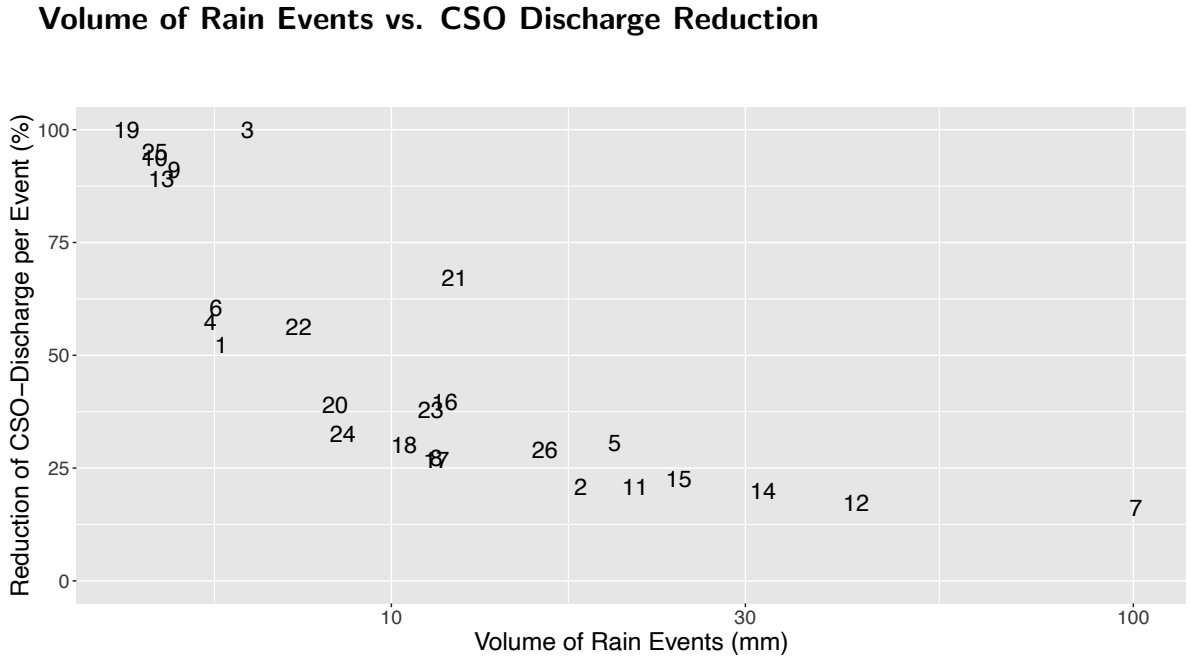

Figure 4.11: Correlation between rain events volume vs. CSO discharge reduction. Numbers are event numbers (compare Tab. A.3 in the appendix)

Fig. 4.11 shows the correlation between the volume of rain events that cause the overflows and the reduction of these overflows between *SC-01* and *SC-02*. It can be seen that as the volume of rain events increases, the percentage of CSO reduction decreases. The previously considered small (*Event No.3*), medium (*Event No.8*) and large (*Event No.12*) events reflect this trend. Two outliers need to be examined more closely.

Firstly, *Event No.7*, which has a precipitation volume of over 100 mm and a duration of over 24 hours. With an event of such volume and duration (annuity $>$ 100a), the simulation of the LIDs and the sewer system may be no longer correct, since processes could play a role that are not represented in the model. Therefore, this event must be considered with special caution. Nevertheless, it is graphically represented in the appendix in Fig. A.12.

Secondly *Event No.21*, despite a precipitation volume of 12.2 mm, a reduction of 67.2 % takes place here and thus does not fit into the correlation trend shown in Fig. 4.11. However, this can be explained by the fact that the rain event has a duration of $>$ 10h and does not have a high precipitation intensity. This means that the LID measures are not suddenly overloaded, can provide a retention of the precipitation and result in a high discharge reduction.

All events listed here can be viewed with regard to their rain volume, duration, CSO-volumes of the scenarios and reduction in Tab. A.3 in the appendix.

4.3.2. Failure Scenarios

The following section takes a closer look at the *Failure Scenarios* introduced earlier in Sec. 3.4. The structure of this section is consistent to the previous section: First, the effects on the *URA* are examined, then the effects on the *Combined Sewer Overflow (CSO)* are considered. The threshold for the resilience assessment are set the same. The effects of the *Failure Scenarios* on the runoff in the sewer catchment *BlnXI* are not presented as the differences were very small.

4.3.2.1. Runoff URA - Failure Scenarios

	URA-Surface Runoff			**URA-Resilience**
	Surface Runoff Volume	Surface Runoff Impervious Area	Peak Runoff Rate	Runoff Events > 10 l/s·ha
	m^3	mm	l/s·ha	n
01 - Construction without Water Concept	189,362	462.20	144.40	20
02 - Construction with Water Concept	17,722	35.45	5.58	-
03 - Citsern - Light	18,247	36.50	5.58	-
04 - Cistern - Strong	18,596	37.20	5.54	-
05 - Green Roof - Light	17,926	35.86	5.61	-
06 - Green Roof - Strong	18,119	36.25	5.63	-
07 - Infiltration - Light	18,021	36.05	5.59	-
08 - Infiltration - Strong	19,296	38.60	9.88	-
09 - Total Failure - Light	18,774	37.56	5.59	-
10 - Total Failure - Strong	20,831	41.67	9.99	-

Table 4.6: URA - Overview Failure Scenarios

As can be seen in Tab. 4.6, all failure scenarios have led to an increase in surface runoff volume as well as surface runoff of the impervious areas in the URA. In addition, the more severe scenarios (*strong*-variants) have led to larger runoff volumes compared to the corresponding *light*-variants which already indicates plausible results. Furthermore, the observation of the peak runoff rates is indicative; it shows that an increase in the peak runoff rates is partly caused by the scenarios, but some scenarios are also slightly below the reference scenario *SC-02*. This minimal undercutting of the peak runoff of *SC-02* can be attributed to simulation errors or model inaccuracies. Despite the massive failures and deteriorations in *08 - Infiltration Strong* and *10 - Total Failure - Strong*, which have the largest peak runoff rate, the threshold of < 10 l/s·ha by the federal state of Berlin

was not exceeded once. This eliminates the need for further resilience calculations and all failure scenarios can be considered resilient regarding the < 10 l/s·ha threshold for the study period, according to the *Resilience Index*.

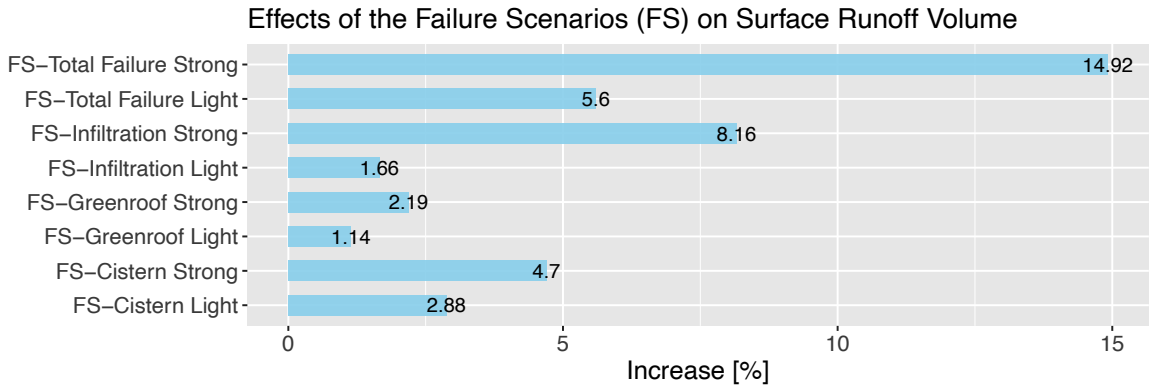

Figure 4.12: Effects of Failure Scenarios on URA - Runoff Volume compared to SC-02

Fig. 4.12 shows the previously mentioned surface runoff volume increase of the individual failure scenarios compared to *SC-02*. Here, it is clearly shown that the strong variants of the scenarios provide a larger increase than the light variants. It can also be seen that the position of the LID measure, which fails in the chain, may have an effect on the URA volume. The closer the LID measure is to the sewer, the more severe the failure appears to be. Further research investigations of this hypothesis could be subject of a follow-up study. In conclusion, it can be stated that, as expected, *10 - Total Failure - Strong*, with just under 15 % volume increase, represents the strongest failure. In this case, a complete neglect of care over a period of 10 years was estimated. In order to put this increase in runoff volume into perspective, Fig. 4.13 compares runoff reductions with *SC-01*.

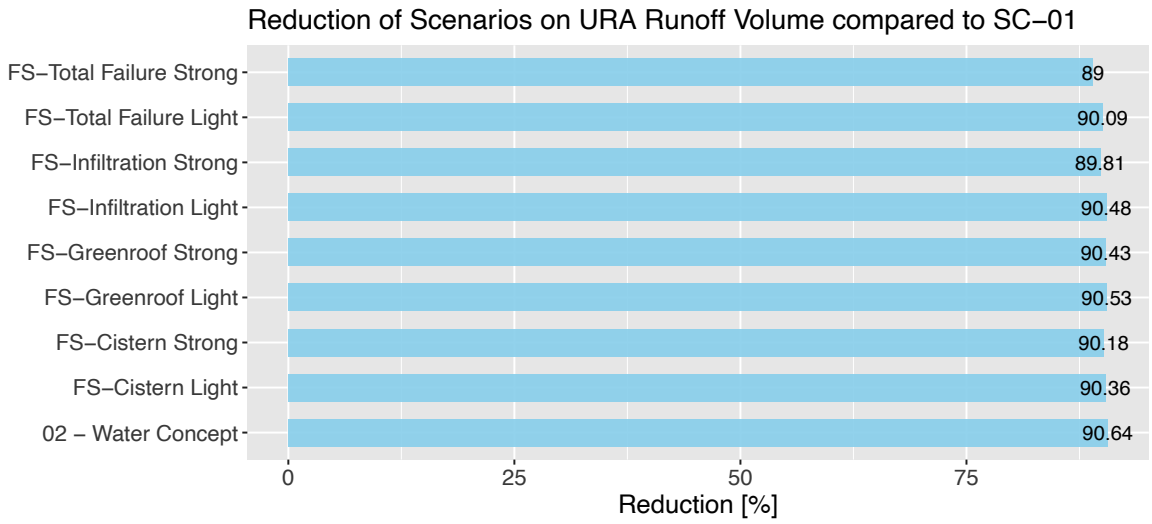

Figure 4.13: Effects of Failure Scenarios on URA runoff volume compared to *SC-01*

The figure shows that even the volume increase of almost 15 % in *10 - Total Failure - Strong* is still a strong improvement compared to *01 - Construction without Water Concept*. Despite the massive failures and the neglect of the maintenance of the LID measures, which are simulated in *10 - Total Failure - Strong*, a reduction of 89 % can still be assumed through this scenario compared to *SC-01*.

In conclusion, it can be stated that despite the neglect of the LID measures, no scenario exceeds the threshold of 10 l/s·ha, therefore, complete resilience is still given. Furthermore, an increase in volume within the URA is to be expected for each of the failure scenarios. However, despite this increase, the scenarios still offer a significant improvement of runoff volume reduction over *SC-01*, by almost 90 %, only 1.6 % less than fully functional LIDs in *SC-02*.

4.3.2.2. CSO - Failure Scenarios

CSO Volume - Failure Scenarios

	CSO-Volume		**Resilience**
	Discharge Volume	Peak Discharge Rate	CSO Events > 0.001 m^3/s
	m^3	m^3/s	n
01 - Construction without Water Concept	563,301	24.72	26
02 - Construction with Water Concept	430,562	17.57	24
03 - Cistern - Light	431,446	18.39	24
04 - Cistern - Strong	431,916	18.40	24
05 - Green Roof - Light	431,402	18.40	24
06 - Green Roof - Strong	431,505	18.41	24
07 - Infiltration - Light	431,558	18.43	24
08 - Infiltration - Strong	432,807	18.77	24
09 - Total Failure - Light	432,051	18.43	24
10 - Total Failure - Strong	434,282	18.79	24

Table 4.7: CSO - Overview Failure Scenarios

Tab. 4.7 shows the effects of the failure scenarios on the combined sewer overflow volume. As can be seen, the CSO volume and the CSO peak discharge rate increased through all simulated scenarios, as expected. Here, it can be seen that despite the failure scenarios, no events have been added in comparison to *SC-02* and all failure scenarios include 24 events that are exceeding the threshold.

CSO Discharge Volume

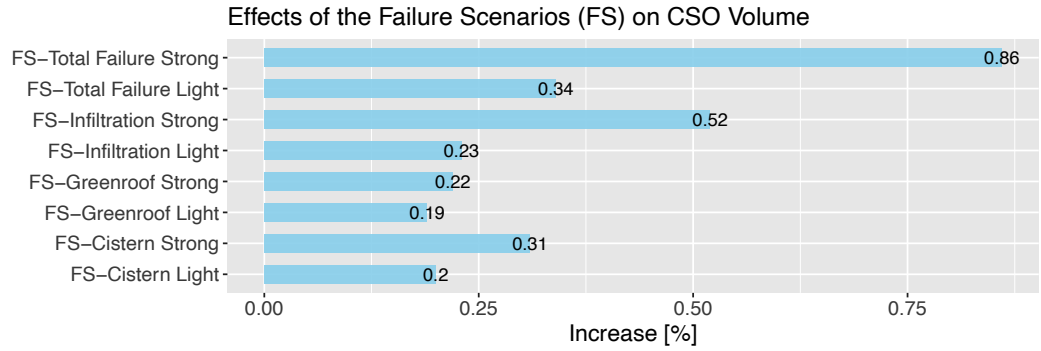

Figure 4.14: Effects of Failure Scenarios on CSO volume compared to *SC-02*

Fig. 4.14 shows the CSO volume increase of the Failure Scenarios compared to *02 - Construction with Water Concept*. The results are consistent with the increase in URA runoff volume, *FS - Total Failure Strong* has the largest increase of about 0.9 %, followed by *FS - Infiltration Strong* and *FS - Total Failure Light*. It can also be seen that all strong variants cause a greater CSO discharge than the light variants as expected.
However, it should be noted that the CSO volume is not completely congruent with the URA surface runoff volume. For example, *FS - Green Roof Strong* has a smaller URA runoff volume but a higher CSO discharge volume than *FS - Infiltration Light*. This can be attributed to the fact that a larger runoff volume does not necessarily lead to a larger CSO volume, since other factors may play a role in the CSO overflow, for example, the occurrence in time, the location in the system or the intensity. On the other hand, differences are very small.

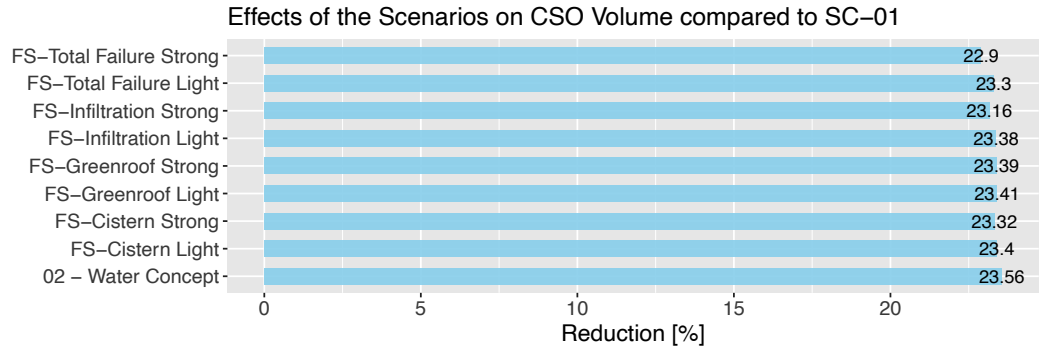

Figure 4.15: Effects of Failure Scenarios on CSO volume compared to *SC-01*

In order to be able to interpret the increases in the CSO discharge of the failure scenarios, it is important to compare them to *01 - Construction without Water Concept*. Here, it

becomes clear once again that even in *FS - Total Failure Strong*, poorly functioning LID measures still reduce the CSO discharge volume by almost 23 % compared to *SC-01*, as can be seen in Fig. 4.15. This confirms the conclusions for URA runoff that even poorly maintained and not completely efficient LID measures still ensure a considerable improvement.

CSO Peak Discharge

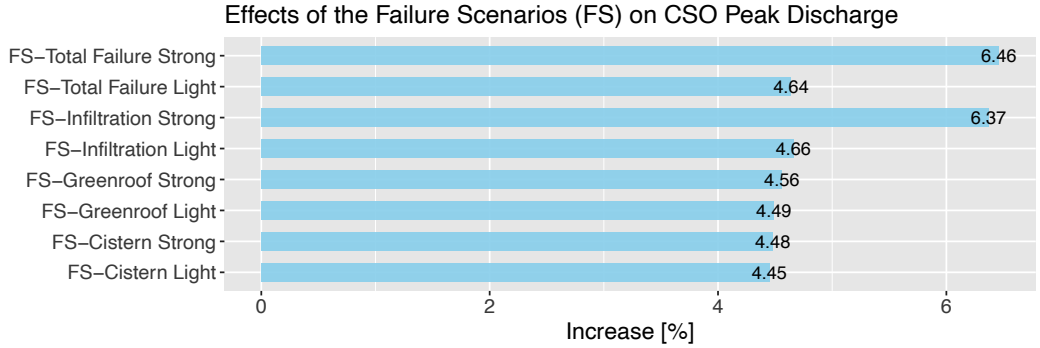

Figure 4.16: Effects Failure Scenarios on CSO peak discharge compared to *SC-02*

Fig. 4.16 shows the increase in CSO peak discharge compared to *02 - Construction with Water Concept*. Here, it can be seen that a peak increase occurs through all scenarios, but *FS - Infiltration Strong* and *FS - Total Failure Strong* in particular stand out. This again confirms the peak runoff rate, which was determined in the URA for the failure scenarios, where SC-08 and SC-10 also had the largest increases. Fig. 4.17 again puts the CSO peak increase in relation to *SC-01*. It is again clear to see that even with the increase due to the failure scenarios, the performance of scenarios with LID measures is still about 24 % below of *SC-01*.

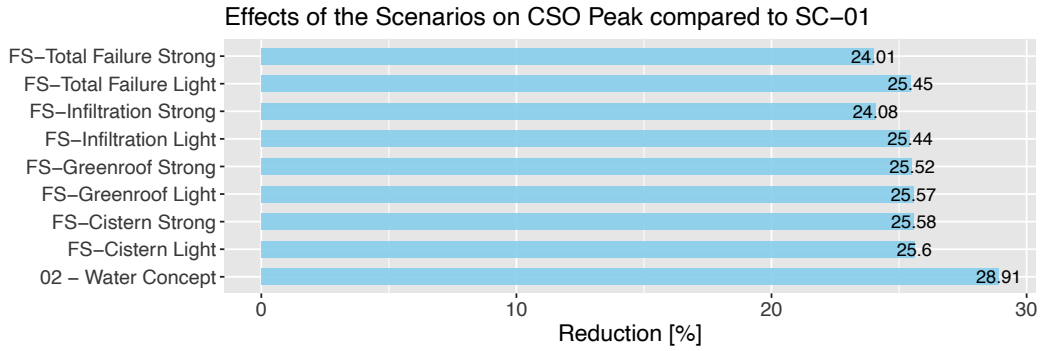

Figure 4.17: Effects Failure Scenarios on CSO peak discharge compared to *SC-01*

Effects of Failure Scenarios on CSO Volume

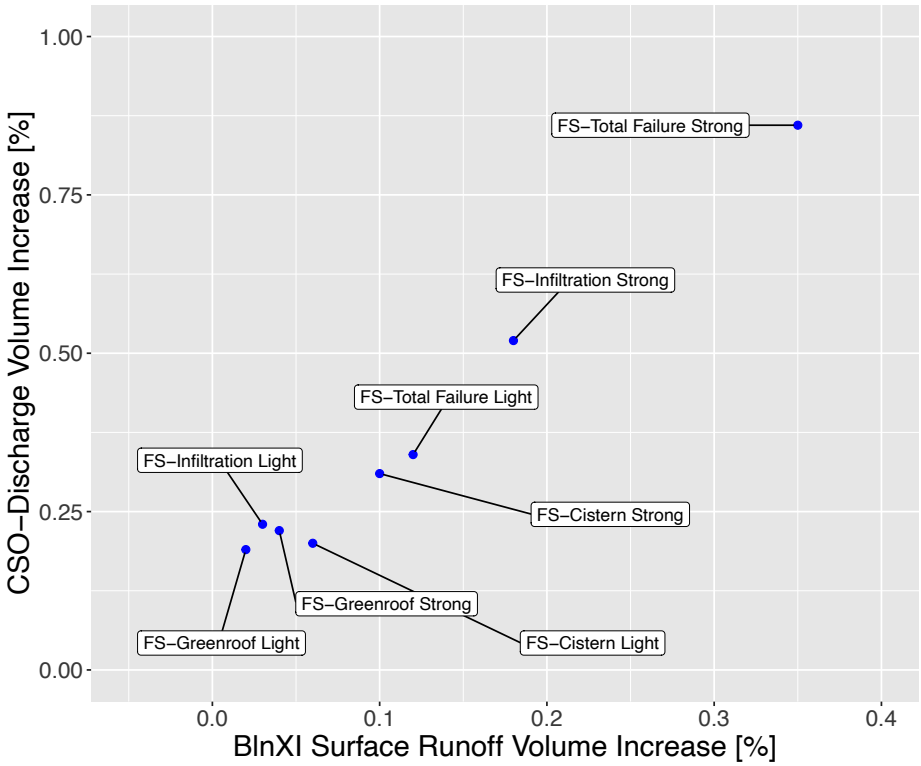

Figure 4.18: Effects of Failure Scenarios on CSO volume

Fig. 4.18 is used to better understand the impact of the failure scenarios on the CSO volume. Here, the relationship between the increase in surface runoff volume of each failure scenario and the increase in the resulting CSO volume is described. It can be seen that the CSO volume increase occurs disproportionately to the URA increase. It is shown, *e.g.*, that for *FS - Infiltration Strong* an increase in the surface runoff in *BlnXI* of 0.18 % results in an increase in CSO volume of 0.52 %, resulting in a factor of 2.8. This observation can be confirmed by *FS - Total Failure Strong*, where a runoff increase of 0.35 % triggers a CSO volume increase of 0.86 %, leading to a factor of 2.46. Factors > 1 were expected from *SC-02*, where reduction in CSO were 1.45 times higher than reduction in stormwater runoff. However, factors for runoff increase (due to LID failures) were clearly higher than for runoff reduction (due to LID establishment). From this it can be concluded that the failure scenarios are by far the better alternative in terms of CSO volume compared to not using LID measures. However, due to the neglect of maintenance and the resulting increase in URA runoff, there is a disproportionate growth in CSO discharge .

CSO Resilience - Failure Scenarios

	Resilience				
	CSO-Events > 0.001 m³/s	**Discharge Volume**	**Total Event Duration**	**Total Event Severity**	**Total Event Resilience**
	n	m³	h:min	-	-
01 - Construction without Water Concept	26	563,281	155:45	0.04054	0.95946
02 - Construction with Water Concept	24	430,562	136:05	0.03101	0.96899
03 - FS - Cistern - Light	24	431,446	135:55	0.03107	0.96893
04 - FS - Cistern - Strong	24	431,916	135:50	0.03110	0.96890
05 - FS - Green Roof - Light	24	431,402	138:45	0.03106	0.96894
06 - FS - Green Roof - Strong	24	431,505	136:05	0.03107	0.96893
07 - FS - Infiltration - Light	24	431,558	138:25	0.03108	0.96892
08 - FS - Infiltration - Strong	24	432,807	141:15	0.03116	0.96884
09 - FS - Total Failure - Light	24	432,051	135:50	0.03113	0.96887
10 - FS - Total Failure - Strong	24	434,282	140:45	0.03126	0.96874

Table 4.8: Resilience Overview of the Failure Scenarios

To conclude the consideration of the failure scenarios, the resilience of the system against these failures will be assessed. As expected from the effects of the failure scenarios on URA runoff and CSO volume shown previously, severity increases and resilience decreases. As can be seen in Tab. 4.8, the differences in the increase in severity are very small, but it can still be seen that *FS - Infiltration Strong* and *FS - Failure Strong* are characterised by the highest severity among the failure scenarios.

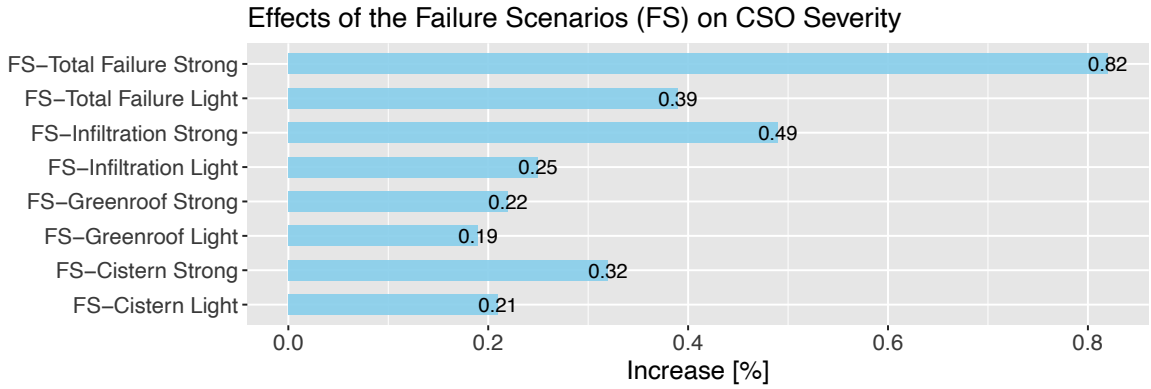

Figure 4.19: Effects of Failure Scenarios on total severity of CSO events compared to *SC-02*

Fig. 4.19 shows the increase in the severity of the failure scenarios compared to *02 - Construction with Water Concept*. Here it can be clearly seen that the scenarios which already have the largest growth in the CSO volume also have the largest increase in severity. In addition to CSO volume and peak discharge, the integrating measure of severity underlines that the *FS - Infiltration Strong* and *FS - Total Failure Strong* have the strongest effects on the resilience of the system. The following Fig. 4.20, however, also puts this into perspective in comparison to *01 - Construction without Water Concept* and again shows that the severity could be consistently reduced by approx. 23 % despite the failures.

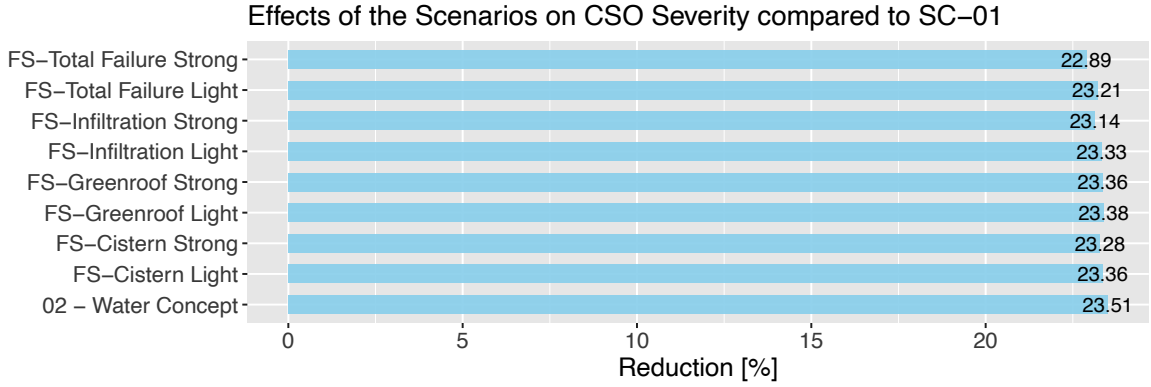

Figure 4.20: Effects of Failure Scenarios on total severity of CSO events compared to *SC-01*

5. Conclusions

In this study, two implementation scenarios and eight failure scenarios were considered for the *URA Michelangelostraße*. For this purpose, the model of the sewer catchment *BlnXI* was first transferred from *InfoWorks* to *SWMM* and afterwards calibrated. The local conditions on site were taken into account to develop different scenarios in order to enable a representation as realistic as possible. This included the needs and demands of the local stakeholders, which were expressed within the framework of the *netWORKS4* research project. These were represented by LID chains composed of different infrastructure measures. For the failure scenarios, the experiences and characteristic values of the *Berliner Wasserbetriebe (BWB)* regarding the failure incidents were used as a basis for the most possible realistic consideration possible. With these scenarios, the effects on the *Surface Runoff URA*, *Surface Runoff BlnXI* and *Combined Sewer Overflow (CSO)* were investigated in terms of discharge volume, discharge peak and quantitative resilience.

5.1. Calibration & Model Setup

Calibration

The transfer from *InfoWorks* to *SWMM* and the subsequent calibration of the *BlnXI*-model can be classified as successful. This was ensured by all parameters relevant for this study, such as CSO discharge volume and surface runoff volume. A deviation from the *InfoWorks*-model of < 1 % for the CSO volume and < 2% for the surface runoff volume was achieved. This is also reflected in the satisfying Nash-Sutcliffe-Efficieny of > 0.85 for all relevant measuring points. Therefore, from the perspective of model quality, large inaccuracies and inconsistencies can be excluded.

Model Setup

Aiming to represent the LID measures occurring of the URA in the *BlnXI SWMM*-model, the existing measures were represented as LID chains. The basis of the parameters of these chains was taken from Kliewer, 2015. The chains were tested in advance for plausibility and effectiveness. No irregularities were found.

In order to be able to represent these areas accurately in the model, a factor was introduced to take into account the previously determined impervious area difference between *ALKIS* and *SWMM*. Consequently a realistic representation of LIDs and area shares can be assumed.

5.2. Effects of 02 - Construction with Water Concept

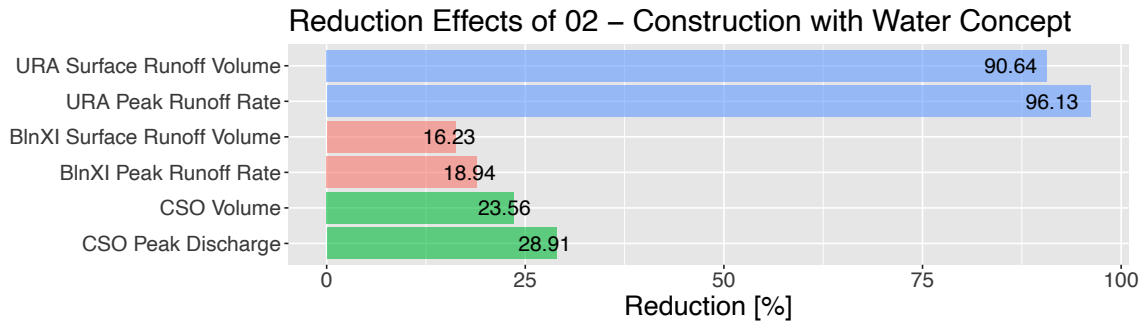

Figure 5.1: Effects of *02 - Construction with Water Concept*

URA Michelangelostraße

As shown in Fig. 5.1, the LID measures in *SC-02* led to a reduction in runoff volume of 90.6 %. The peak runoff rate could be reduced by 96.1 %, which means that the URA can continuously comply with Berlin's discharge restriction of < 10 l/s·ha, even for a summer half-year characterised by extreme rain events. Therefore, the URA can be described as fully resilient through the measures based on the *Resilience Index*. This strong reduction in surface runoff can be attributed to an increased infiltration and evaporation due to the LID measures. These in turn, have a positive effect of approaching the natural water balance and will also have a positive impact on the CSO reduction.

Sewer Catchment BlnXI

The LID measures implemented in *SC-02* also positively affect the sewer catchment *BlnXI*. Thus, as shown in Fig. 5.1, a reduction of the runoff volume by 16.2 % and a reduction of the peak runoff rate by 18.9 % is achieved. It is also possible to bring individual runoff events below the discharge restriction of < 10 l/s·ha. This can also be quantified by the severity of the *Resilience Index*. For the runoff events that took place, the severity was reduced by 28.7 %. However, the converted area is not sufficient to bring a large number of runoff events below this limit and the events which were brought below this threshold are characterised by very small precipitation. In order to achieve a more significant reduction of surface runoff volume, more large-scale LID implementations are needed.

Combined Sewer Overflow (CSO)

As can be seen in Fig. 5.1, the LID measures for *SC-02* were able to reduce the CSO volume by 23.6 %. Compared to the 16.2 % reduction of the surface runoff volume, this is exceeding the effect by a factor of ~ 1.45. It can be concluded that the implementation of LID measures helps to drastically reduce the CSO volume and peak discharge rates or can even retain complete CSO events. This has a positive impact on the consequences of CSO overflows as mentioned in Sec. 2.2.1.3. In addition, it can be determined that the reduction of CSO volume steadily decreases with increasing rain event volume. This can be attributed to the overloading of the individual LID measures due to the increasing rain volume and rain duration.

5.3. Impacts of Failure Scenarios

URA Michelangelostraße

All failure scenerios have led to an increase in surface runoff volume. *SC-08* and *SC-10* also considerably increased the peak runoff rates. Nevertheless, the discharge requirements of < 10 l/s·ha of Berlin were not exceeded once. Even scenario *FS - Total Failure - Strong* still achieves much better results regarding the URA surface runoff than *01 - Construction without Water Concept*.

Therefore, it can be concluded for this modelling that the concerns regarding the functionality of LID measures are unfounded and that even with a complete neglect and discontinuation of the maintenance of LID measures, good results can still be achieved in terms of runoff volume reduction in the *URA*.

Combined Sewer Overflow (CSO)

It can be seen that all failure scenarios lead to an increase in CSO volume and peak discharge rate compared to *02 - Construction with Water Concept*. This is quantified and proven by the severity of the *Resilience Index*. However, if the failure scenarios are compared to *01 - Construction without Water Concept*, it becomes clear that all the failure scenarios still achieve significantly better results in terms of CSO discharge volume and peak discharge rate.

This shows that the resilience of the entire sewer catchment *BlnXI* can be increased even by poorly maintained LID measures. Nevertheless, it should be noted that neglecting maintenance is not recommended as the increase in runoff volume has a disproportionate effect on CSO discharge volume.

5.4. Limitations of the Study

Despite these far-reaching findings and the plausibility of existing work, the following limitations must be considered:

- *SWMM* only offers a simplified approach to calculate evaporation which is why it is not possible to draw up a conclusive water balance and read out an exact distribution between infiltration, evaporation and surface runoff.
- The LID parameters used were not subjected to any parameterisation. Instead, only a simple plausibility check was carried out on the basis of three rain events and the correctness of the values from Kliewer, 2015 was trusted.
- The implementation of the LID measures has been greatly simplified. For example, the *Infiltration Swales*, *Trough-Trench Elements* or *Green Roofs* were implemented as large rectangular areas for the respective FA. This does not correspond to the actual reality and must be taken into account.

5.5. Outlook and Further Research Questions

Through the study presented here, further research questions have arisen that could be explored in future work:

- How do the characteristic values investigated here, such as surface runoff and CSO volume, change when the LID measures are not implemented in a concentrated manner in one URA but are distributed at many locations throughout the sewer system?
- What impact does the position of the LID measure in the associated LID chain have for the failure severity? Can the failures of LID measures further up the chain be better compensated by the subsequent measures?
- A deeper investigation of the relationship between surface runoff and CSO discharge: In addition to the runoff volume, what other roles do the temporal occurrence, the intensity or the location in the system play?

References

Ahiablame, L.M., Engel, B.A., and Chaubey, I. (2012). "Effectiveness of low impact development practices: Literature review and suggestions for future research". In: *Water, Air, and Soil Pollution* 223.7, pp. 4253–4273. doi: 10.1007/s11270-012-1189-2.

BWB, Berliner Wasserbetriebe (2012). *Die Berliner Kanalisation : unsichtbar und unentbehrlich*. Berliner Wasserbetriebe, Unternehmenskommunikation, Catrin Glücksmann (V.i.S.d.p.) url: https://nbn-resolving.de/urn:nbn:de:kobv:109-opus-148660.

DWD (2021). *Deutscher Wetterdienst, Wetterstation Berlin Dahlem*. url: https://www.dwd.de/DE/wetter/wetterundklima_vorort/berlin-brandenburg/berlin_dahlem/_node.html (visited on 12/17/2021).

Eckart, K., McPhee, Z., and Bolisetti, T. (2017). "Performance and implementation of low impact development – A review". In: *Science of The Total Environment* 607-608, pp. 413–432. issn: 0048-9697. doi: https://doi.org/10.1016/j.scitotenv.2017.06.254.

FBG, Fachbereich Geowissenschaften FU Berlin. (2022). *Difference between a combined and a separated sewer system*. url: https://www.geo.fu-berlin.de/en/v/iwrm/Implementation/technical_measures/Wastewater-treatment/Sewer-systems/index.html (visited on 01/07/2022).

FISBroker, SENSW. (2021). *FIS-Broker, Senatsverwaltung für Stadtentwicklung und Wohnen (Hrsg.)* url: https://fbinter.stadt-berlin.de/fb/index.jsp (visited on 12/17/2021).

Fletcher, T.D., Shuster, W., Hunt, W.F., Ashley, R., Butler, D., Arthur, S., Trowsdale, S., Barraud, S., Semadeni-Davies, A., Bertrand-Krajewski, J.-L., Mikkelsen, P.S., Rivard, G., Uhl, M., Dagenais, D., and Viklander, M. (2015). "SUDS, LID, BMPs, WSUD and more – The evolution and application of terminology surrounding urban drainage". In: *Urban Water Journal* 12.7, pp. 525–542. doi: 10.1080/1573062X.2014.916314.

Funke, F. (2019). “Modellierung und Bewertung von Maßnahmen der dezentralen Regenwasserbewirtschaftung anhand aktueller Planungsvarianten in Berlin-Pankow”. MA thesis. Geographische Umweltforschung, Freie Universität Berlin.

Gantner, K. and Barjenbruch, M. (2011). *Reduzierung des Frachteintrags aus Mischwasserentlastungen*. Abschlusspräsentation zum UEP Projekt. Berlin.

Gill, S., Handley, J.F., Ennos, R., and Pauleit, S. (2007). “Adapting Cities for Climate Change: The Role of the Green Infrastructure”. In: *Built Environment* 33, pp. 115–133. doi: 10.2148/benv.33.1.115.

Gujer, W. (2007). *Siedlungswasserwirtschaft : mit 84 Tabellen*. ger. 3., bearbeitete Auflage. Berlin u.a.: Springer. isbn: 9783540343295.

Gupta, H.V., Kling, H., Yilmaz, K.K., and Martinez, G.F. (2009). “Decomposition of the mean squared error and NSE performance criteria: Implications for improving hydrological modelling”. In: *Journal of Hydrology* 377.1-2, pp. 80–91. doi: 10.1016/j.jhydrol.2009.08.003.

Henrichs, M., Langner, J., and Uhl, M. (Jan. 2016). “Development of a simplified urban water balance model (WABILA)”. In: *Water Science and Technology* 73. doi: 10.2166/wst.2016.020.

Juan-García, P., Butler, D., Comas, J., Darch, G., Sweetapple, C., Thornton, A., and Corominas, L. (2017). “Resilience theory incorporated into urban wastewater systems management. State of the art”. In: *Water Research* 115, pp. 149–161. doi: 10.1016/j.watres.2017.02.047.

Kliewer, D. (2015). *WaBiLa – Validierung - Eine Eignungsprüfung des Wasserbilanzmodells WaBiLa mittels SWMM*. IWARU – Institut für Wasser, Ressourcen und Umwelt.

Kriegebaum, S. (2021). “Transformation im urbanen Raum - GIS-basierte Abbildung technischer Randbedingungen dezentraler Regenwasserbewirtschaftungsmaßnahmen als Planungsgrundlage”. MA thesis.

Locatelli, L., Russo, B., and Martinez, M. (Sept. 2019). "Evaluating health hazard of bathing waters affected by combined sewer overflows". In: *Natural Hazards and Earth System Sciences*. doi: 10.5194/nhess-2019-292.

Matzinger, A., Zamzow, M., Riechel, M., Pawlowsky-Reusing, E., and Rouault, P. (2018). "Quantitative Beschreibung der Resilienz urbaner Wassersysteme". In: *Regenwasser in urbanen Räumen - aqua urbanica trifft RegenwasserTage*. Vol. Band 1, (2018), S. 119 – 127. Technische Universität Kaiserslautern, p. 9.

Matzinger, A., Pilger, M. L., Nebauer, M., and Rouault, P. (2019). "Potenzial von Bilddaten aus sozialen Medien für die urbane Überflutungsvorsorge - Versuch einer Anwendung für zwei extreme Starkregenereignisse in Berlin." In: *Aqua Urbanica*, p. 6.

McCuen, R., Knight, Z., and Cutter, A. (Nov. 2006). "Evaluation of the Nash–Sutcliffe Efficiency Index". In: *Journal of Hydrologic Engineering - J HYDROL ENG* 11. doi: 10.1061/(ASCE)1084-0699(2006)11:6(597).

Mugume, S.N., Gomez, D.E., Fu, G., Farmani, R., and Butler, D. (2015). "A global analysis approach for investigating structural resilience in urban drainage systems". In: *Water Research* 81, pp. 15–26. doi: 10.1016/j.watres.2015.05.030.

Nenz, D., Trapp, J.H., Matzinger, A., Rouault, P., Gunkel, M., Anterola, J., and Reichmann, B. (2020). *Planerische Machbarkeitsstudien zur Umsetzung blau-grün-grau gekoppelter Infrastrukturen in Berlin*. Forschungsverbund netWORKS. url: https://repository.difu.de/jspui/handle/difu/579132.

netWORKS, Forschungsverbund (2021). *Forschungsprojekt - netWORKS4*. url: https://networks-group.de/de/networks-4/das-projekt.html (visited on 12/17/2021).

Norton, B.A., Coutts, A.M., Livesley, S.J., Harris, R.J., Hunter, A.M., and Williams, N.S.G. (2015). "Planning for cooler cities: A framework to prioritise green infrastructure to mitigate high temperatures in urban landscapes". In: *Landscape and Urban Planning* 134, pp. 127–138. issn: 0169-2046. doi: https://doi.org/10.1016/j.landurbplan.2014.10.018.

Pallasch, M.G. (2021). "Implementation von dezentraler Regenwasserbewirtschaftung in kommunale Planungsprozesse als Beitrag zu einer wassersensiblen Stadtentwicklung". Doctoral Thesis. Berlin: Technische Universität Berlin. DOI: 10.14279/depositonce-12575.

QGIS (2022). *Official QGIS Website*. URL: https://www.qgis.org/en/site/ (visited on 03/03/2022).

Riechel, M., Matzinger, A., Pawlowsky-Reusing, E., Sonnenberg, H., Uldack, M., Heinzmann, B., Caradot, N., Seggern, D. von, and Rouault, P. (2016). "Impacts of combined sewer overflows on a large urban river - Understanding the effect of different management strategies". In: *Water Research*. DOI: 10.1016/j.watres.2016.08.017.

Riechel, M., Remy, C., Matzinger, A., Schwarzmüller, H., Rouault, P., Schmidt, M., Offermann, M., Strehl, C., Nickel, D., Sieker, H., Pallasch, M., Köhler, M., Kaiser, D., Möller, C., Büter, B., Lessmann, D., von-Tils, R., Säumel, I., Pille, L., Winkler, A., Bartel, H., Heise, S., Heinzmann, B., Joswig, K., Reichmann, B., and Rehfeld-Klein, M. (2017). *Maßnahmensteckbriefe der Regenwasserbewirtschaftung - Ergebnisse des Projektes KURAS. Berlin*. URL: http://www.kuras-projekt.de/index.php?id=78.

Riechel, M., Matzinger, A., Pallasch, M., Joswig, K., Pawlowsky-Reusing, E., Hinkelmann, R., and Rouault, P. (Nov. 2020). "Sustainable urban drainage systems in established city developments: Modelling the potential for CSO reduction and river impact mitigation". In: *Journal of Environmental Management*. DOI: 10.1016/j.jenvman.2020.111207.

Rossman, L.A. and Agency, U.S. Environmental Protection (2015). *Storm Water Management Model User's Manual Version 5.1*. URL: https://www.epa.gov/water-research/storm-water-management-model-swmm-version-51-users-manual.

Schulze, P. (1996). *Engineering Within Ecological Constraints*. The National Academies Press. ISBN: 978-0-309-05198-9. DOI: 10.17226/4919. URL: https://www.nap.edu/catalog/4919/engineering-within-ecological-constraints.

SENUVK (2022). *Begrenzung von Regenwassereinleitungen bei Bauvorhaben in Berlin (BReWa-BE)*. URL: https://www.berlin.de/sen/uvk/umwelt/wasser-und-geologie/regenwasser/rechtliche-regelungen/ (visited on 02/18/2022).

SEVGUV Senatsverwaltung für Gesundheit, Umwelt und Verbraucherschutz (2009). *Ergänzender Länderbericht Berlins zum Entwurf des Bewirtschaftungsplans für den deutschen Teil der Flussgebietseinheit Elbe*. Senatsverwaltung für Gesundheit, Umwelt und Verbraucherschutz, Referat II E. Red. Matthias Rehfeld-Klein. URL: https://nbn-resolving.de/urn:nbn:de:kobv:109-opus-80153.

Sieker, Ingenieurgesellschaft. (2022a). *Flächenversickerung*. URL: https://www.sieker.de/fachinformationen/regenwasserbewirtschaftung/versickerung/article/flaechenversickerung-155.html (visited on 01/03/2022).

— (2022b). *Konzept der dezentralen Regenwasser Bewirtschaftung*. URL: https://www.sieker.de/fachinformationen/umgang-mit-regenwasser/article/konzept-der-dezentralen-regenwasser-bewirtschaftung-76.html (visited on 01/03/2022).

— (2022c). *Water Balance*. URL: https://www.sieker.de/en/fachinformationen/article/wasserhaushalt-65.html (visited on 01/03/2022).

Sitterson, J., Knightes, C.D., Parmar, R., Wolfe, K., Avant, B., and Muche, M.E. (2018). *An Overview of Rainfall-Runoff Model Types*. U.S. Environmental Protection Agency.

Stapf, M. (2011). "Kalibrierung eines Schmutzfrachtmodells mit InfoWorks CS - Sensitivitätsanalyse und Kalibrierung". Diploma Thesis. Institut für Siedlungswasserbau, Wassergüte- und Abfallwirtschaft.

Sweetapple, C., Fu, G., and Butler, D. (2017). "Reliable, Robust, and Resilient System Design Framework with Application to Wastewater-Treatment Plant Control". In: *Journal of Environmental Engineering (United States)* 143.3. DOI: 10.1061/(ASCE)EE.1943-7870.0001171.

Trapp, J.H. and Winker, M. (2020). *Blau-grün-graue Infrastrukturen vernetzt planen und umsetzen. Ein Beitrag zur Klimaanpassung in Kommunen*. ISBN: 978-3-88118-660-5.

Trapp, J.H., Nenz, D., Rouault, P., Matzinger, A., Gunkel, M., and Reichmann, B. (2019). "Planungsprozesse in der wassersensiblen und klimagerechten Stadt – blau-grün-grau gekoppelte Infrastrukturen in der Planungspraxis am Beispiel Berlin". In: *KA Korrespondenz Abwasser, Abfall* 66.11, pp. 929–934.

Walker, B., Holling, C.s, Carpenter, S., and Kinzig, A. (Nov. 2003). "Resilience, Adaptability and Transformability in Social-Ecological Systems". In: *Ecol. Soc.* 9. doi: 10.5751/ES-00650-090205.

Westra, S., Fowler, H., Evans, J., Alexander, L., Berg, P., Johnson, F., Kendon, E.J., Lenderink, G., and Roberts, N. (Sept. 2014). "Future changes to the intensity and frequency of short-duration extreme rainfall: FUTURE INTENSITY OF SUB-DAILY RAINFALL". In: *Reviews of Geophysics* 52. doi: 10.1002/2014RG000464.

Zhou, Q. (2014). "A Review of Sustainable Urban Drainage Systems Considering the Climate Change and Urbanization Impacts". In: *Water* 6.4, pp. 976–992. doi: 10.3390/w6040976.

Zhou, Q., Leng, G., Su, J., and Ren, Y. (2018). "Comparison of urbanization and climate change impacts on urban flood volumes: Importance of urban planning and drainage adaptation". In: *Science of The Total Environment* 658. doi: 10.1016/j.scitotenv.2018.12.184.

A. Appendix

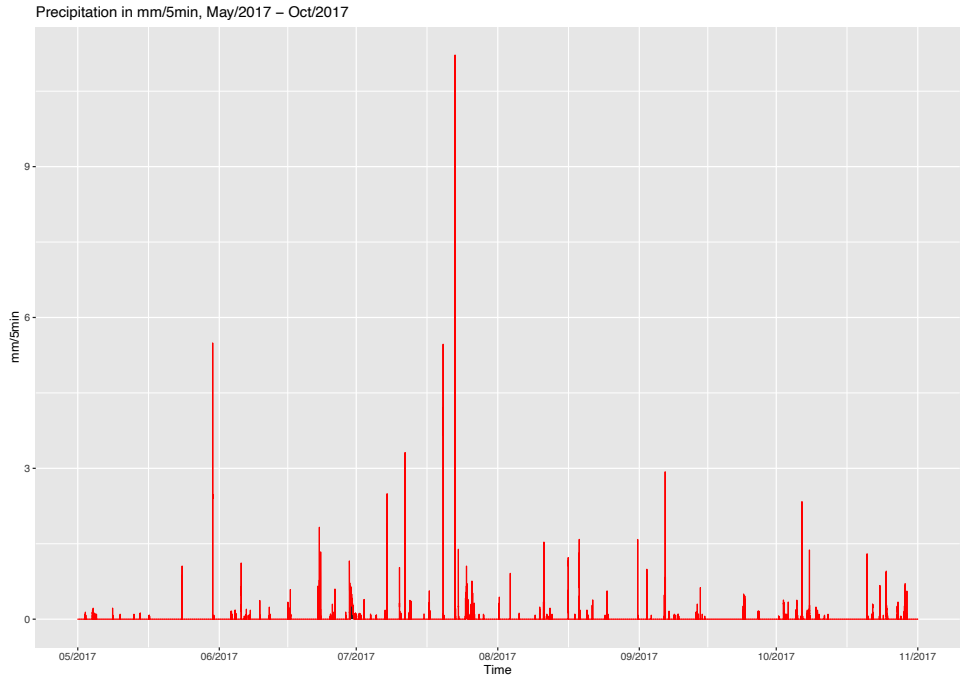

Figure A.1: Precipitation in mm/5min May/2017 - Oct/2017

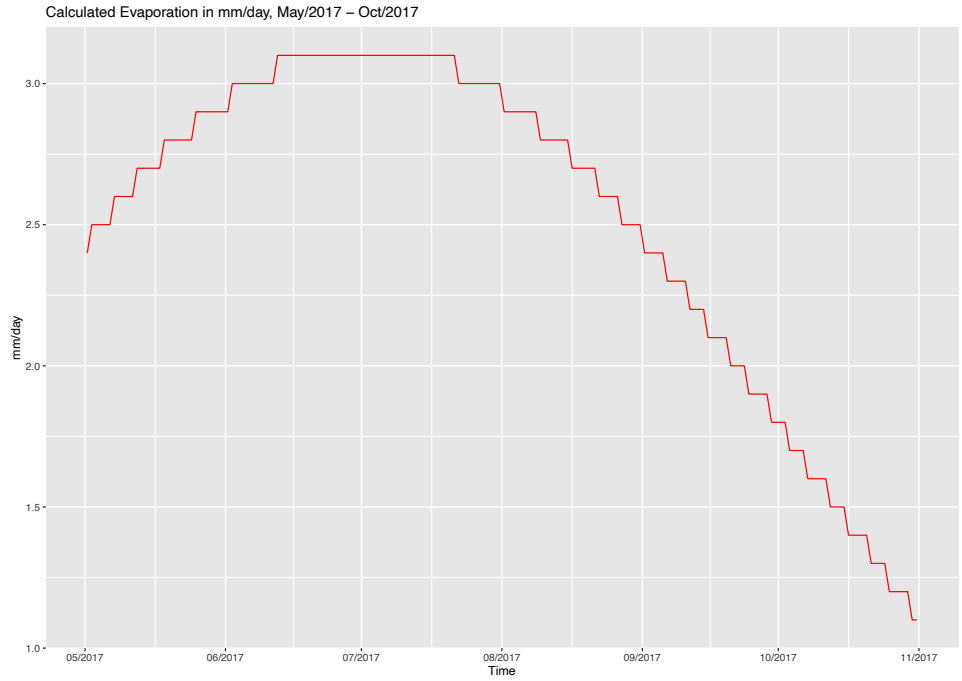

Figure A.2: Calculated Evaporation in mm/day

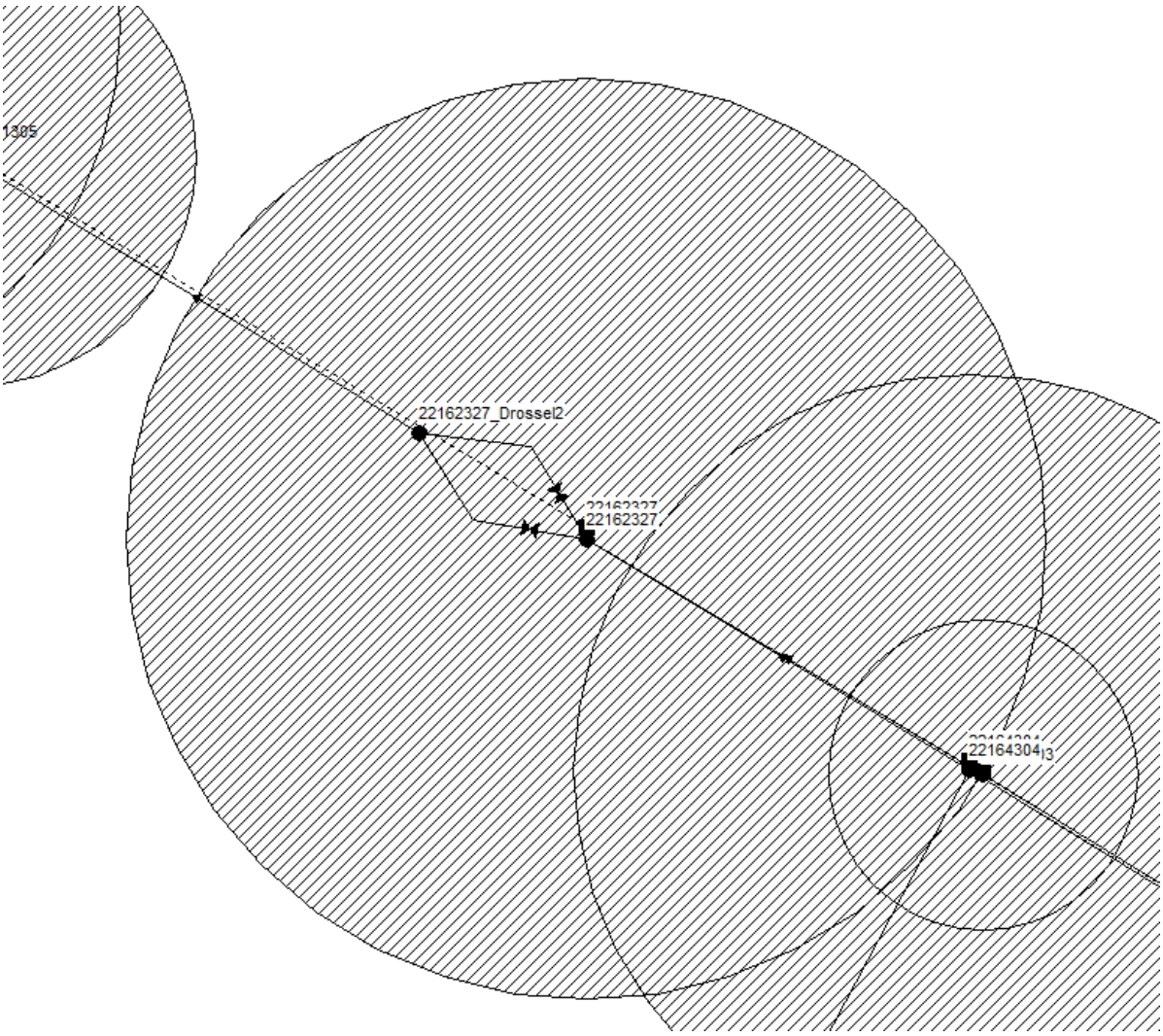

Figure A.3: Representation of the subcatchments in *SWMM*-model before the implementation of the LID chains

	Extensive Green Roof	Intensive Green Roof	Infiltration Swale	Infiltration Trench	Partially Sealed Area	Surface Infiltration
Surface Parameters						
Berm Height (mm)	5.0	10.0	300	300	1.0	100
Surface Roughness (Mannings n)	0.1	0.1	0.1	0.1	0.01	0.1
Surface Slope (%)	2.0	2.0	0.1	0.1	1.0	1.0
Soil Paramters						
Thickness (mm)	100	250	100	100	100	100
Porosity (Volume Fraction)	0.55	0.55	0.44	0.44	0.3	0.1
Field Capacity (Volume Fraction)	0.3	0.3	0.1	0.1	0.2	0.1
Wilting Point (Volume Fraction)	0.05	0.05	0.05	0.05	0.15	0.05
Conductivity (mm/hr)	70	70	3600	180	36	3600
Conductivity Slope	15	15	10	10	10	10
Sunction Head (mm)	58.8	58.8	58.8	58.8	3.5	58.8
Storage Parameters						
Thickness (mm)	100	100	100	1000	100	500
Void Ratio	0.633	0.633	0.2	0.35	0.633	0.2
Seepage Rate (mm/hr)	0.0	0.0	36	3.6	400	360
Underdrain Parameters						
Flow Coefficient (mm/hr)	200	200	0.0	0.0	0.0	0.0
Flow Exponent	0.5	0.5	0.0	0.0	0.0	0.0
Offset Height (mm)	0.0	0.0	0.0	0.0	0.0	0.0

Table A.1: LID parameters

	Flat Roof	**Fully Sealed Area**
% Slope (%)	3.0	1.0
% Imperv. (%)	100	100
N-Imperv (-)	0.01	0.01
Dstore-Imperv (mm)	1.0	2.5

Table A.2: LID parameters Flat Roof, Fully Sealed Area

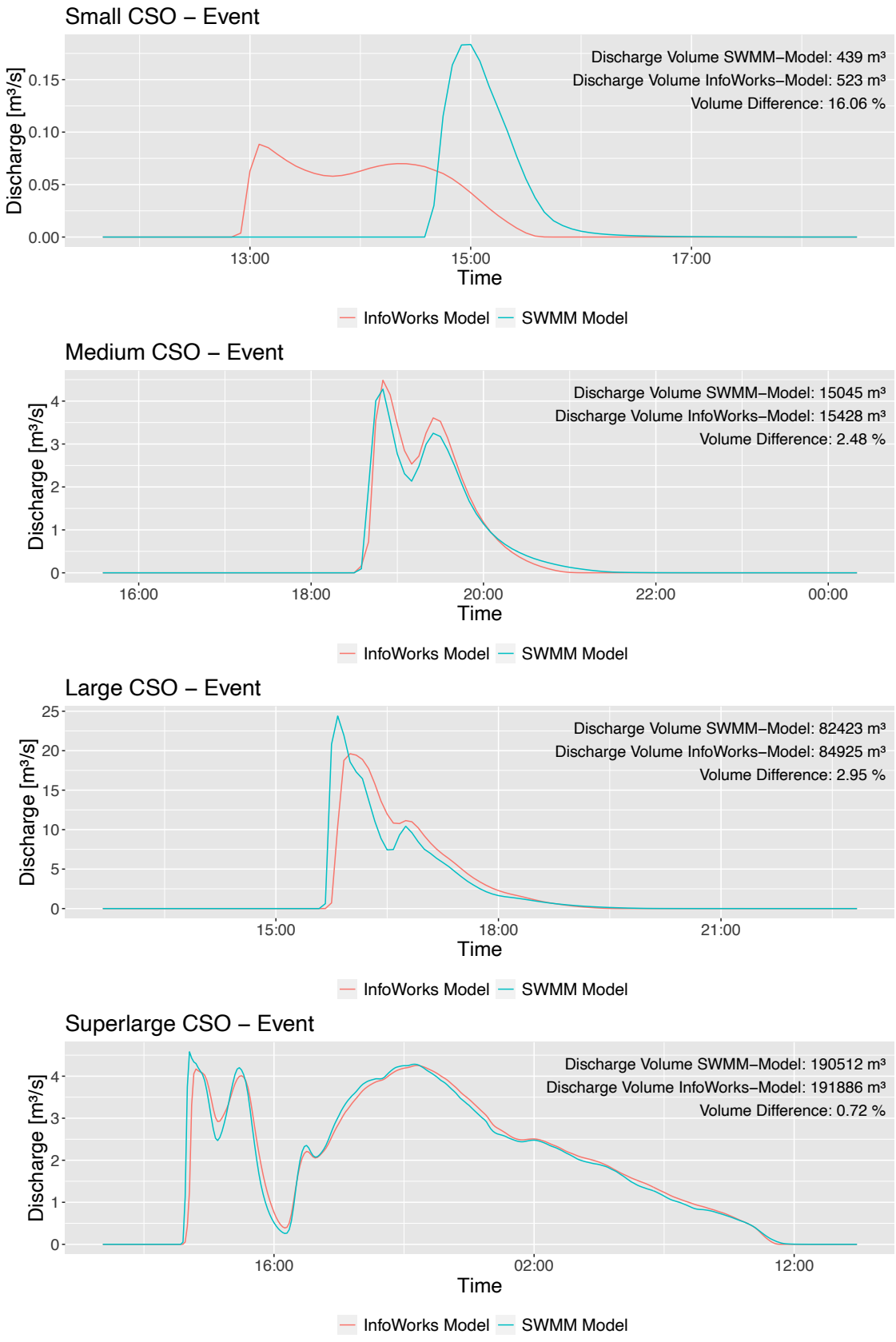

Figure A.4: Calibration shown on selected CSO events

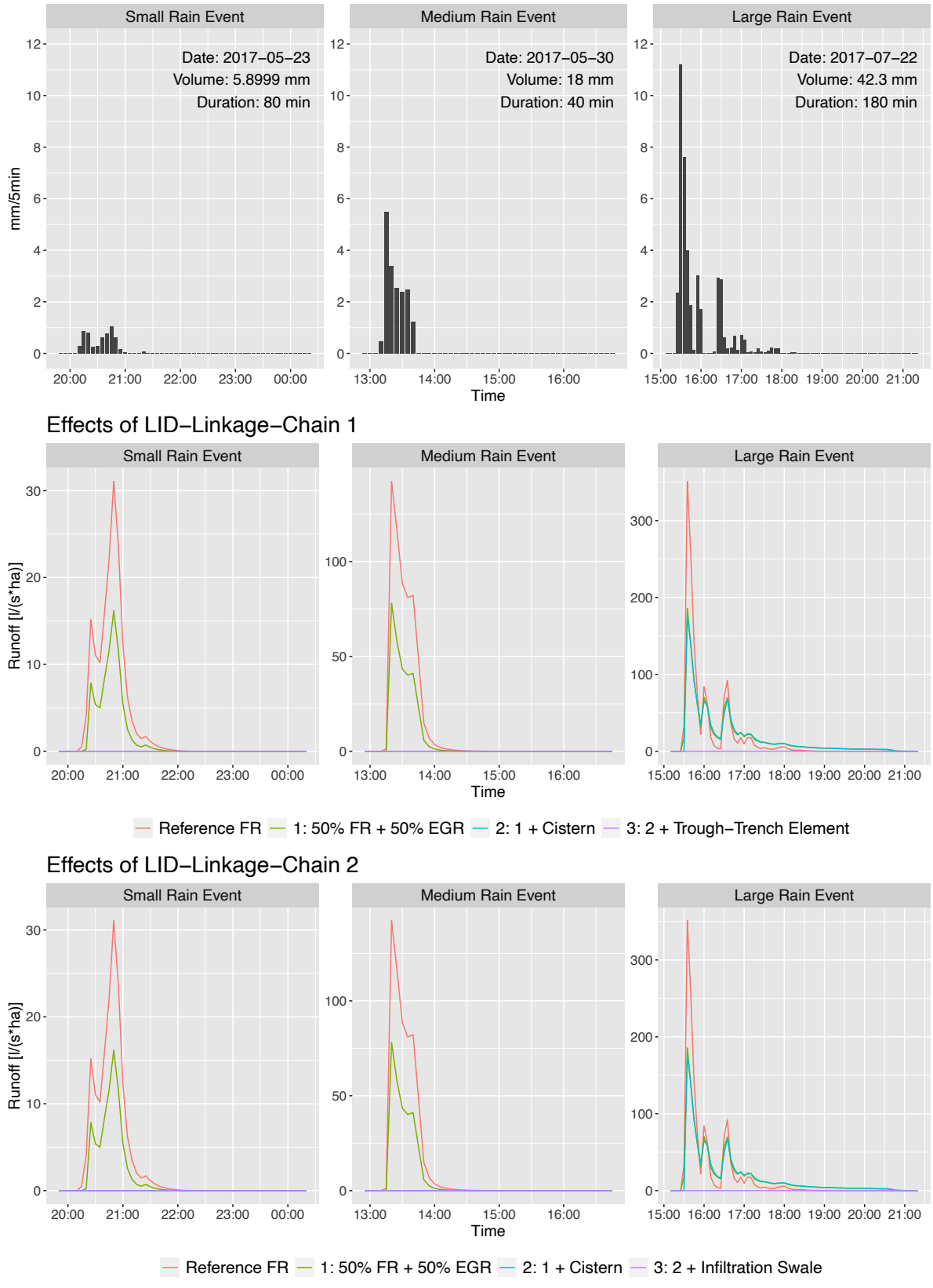

Figure A.5: Effects of Building-Chains 1 - 2

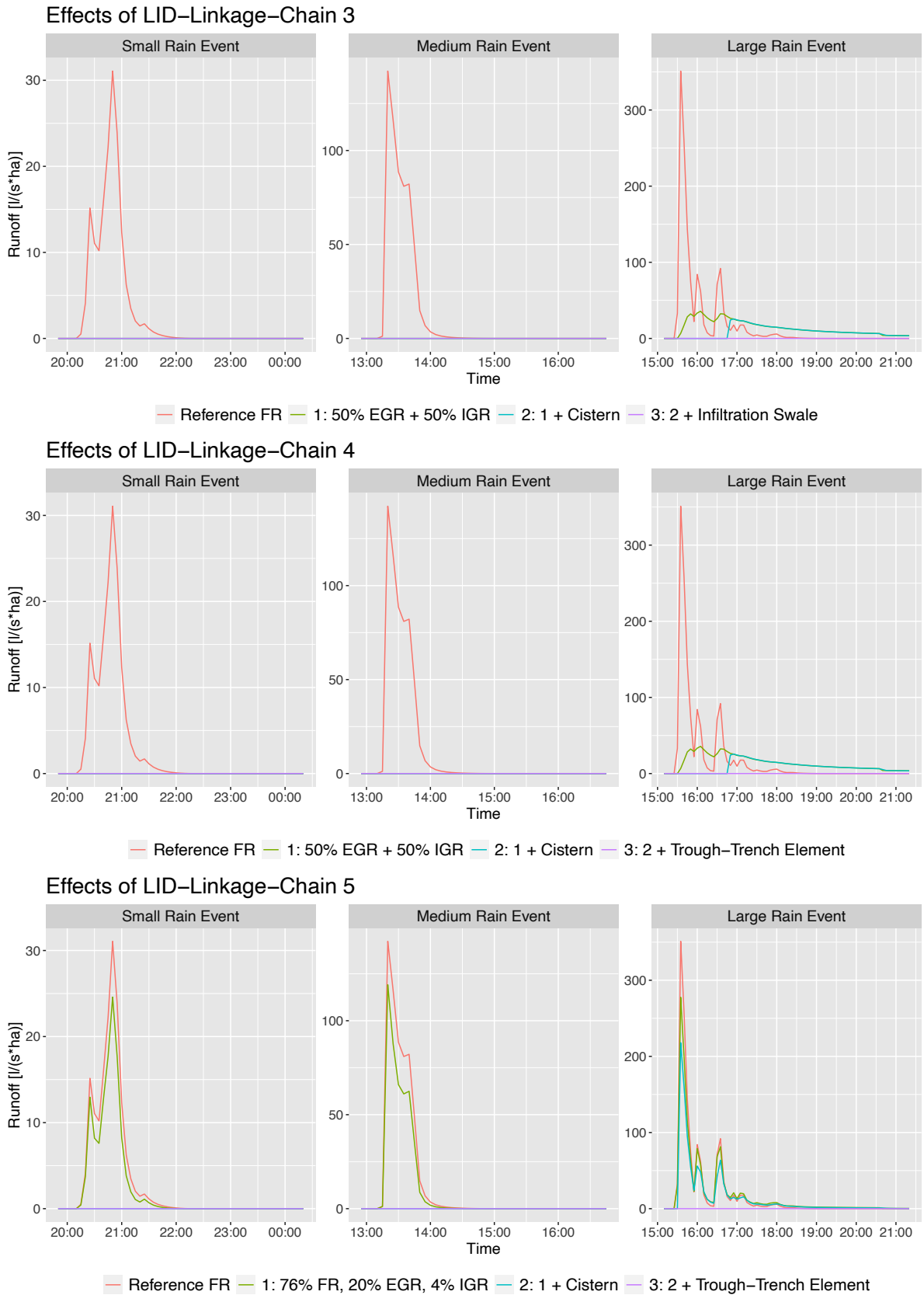

Figure A.6: Effects of Building-Chains 3 - 5

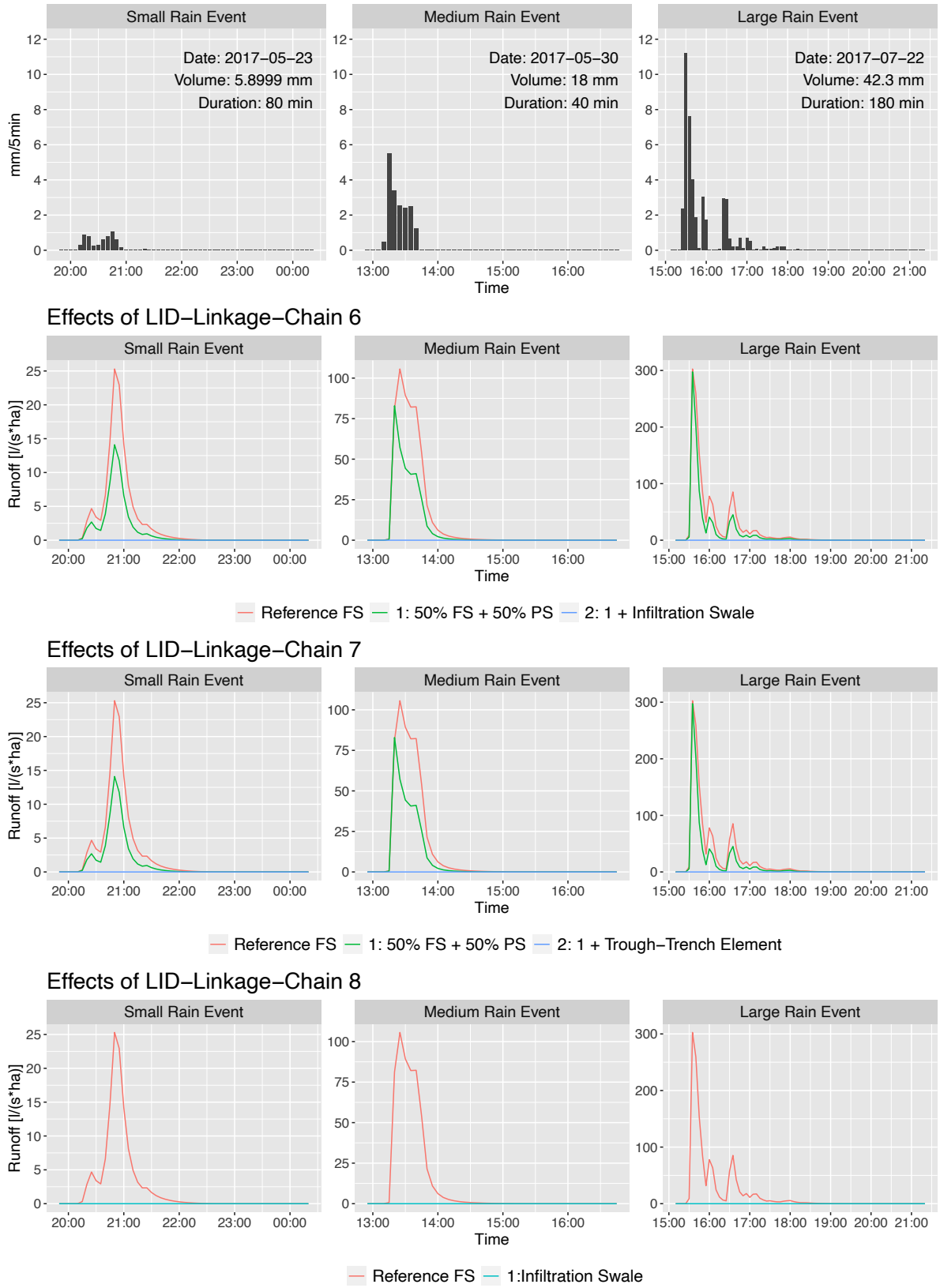

Figure A.7: Effects of Area-Chains 6 - 8

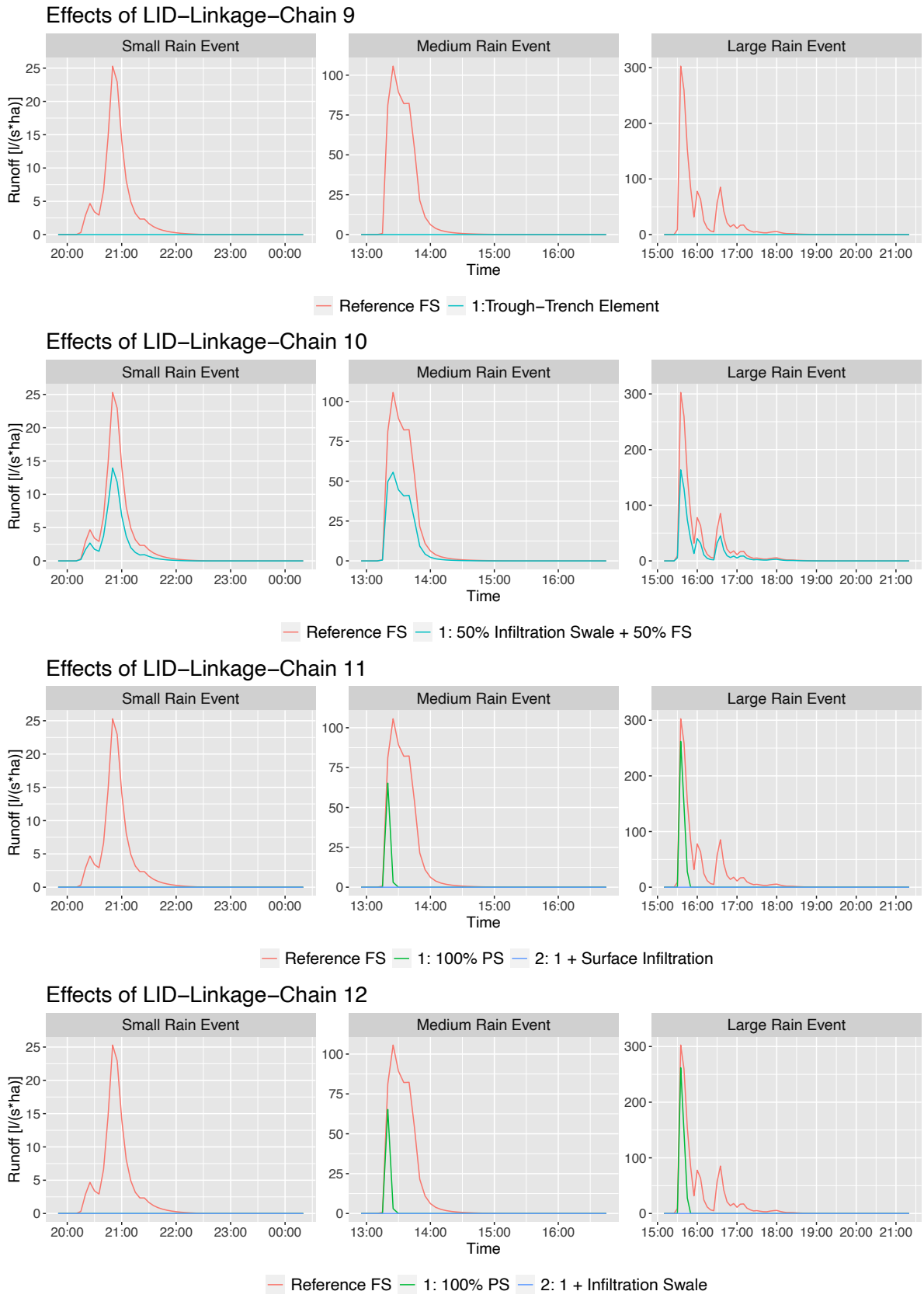

Figure A.8: Effects of Area-Chains 9 - 12

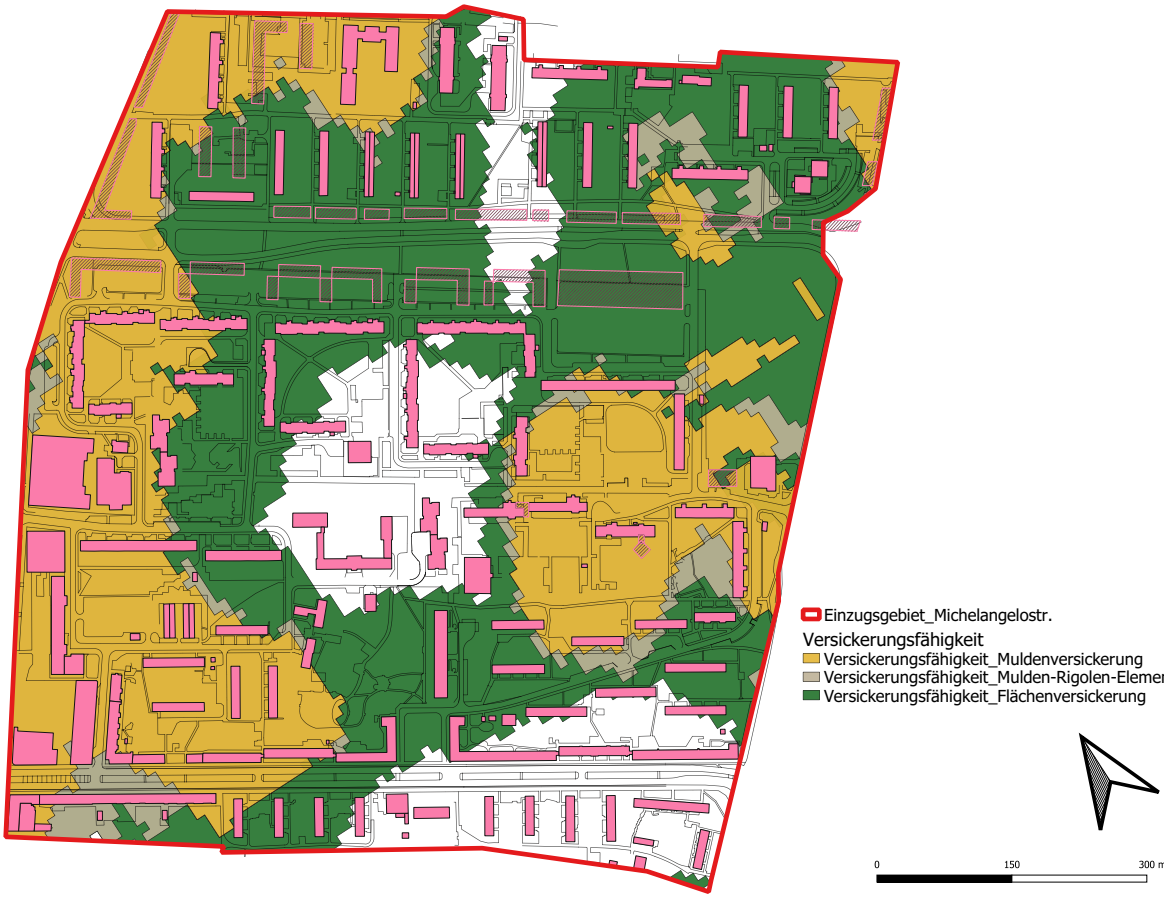

Figure A.9: Infiltration capacity URA Michelangelostraße [Kriegebaum, 2021]

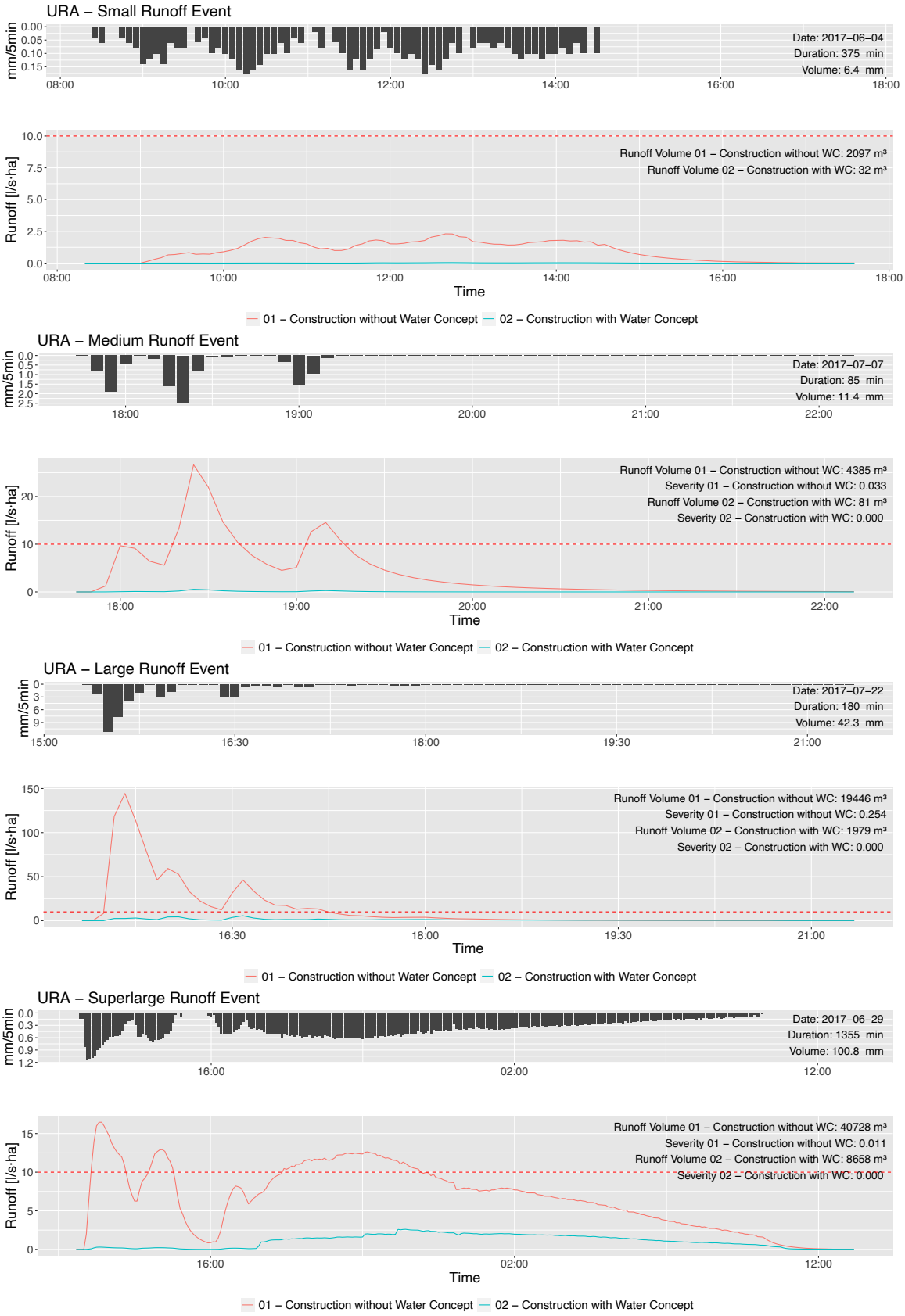

Figure A.10: Selected events - URA Runoff

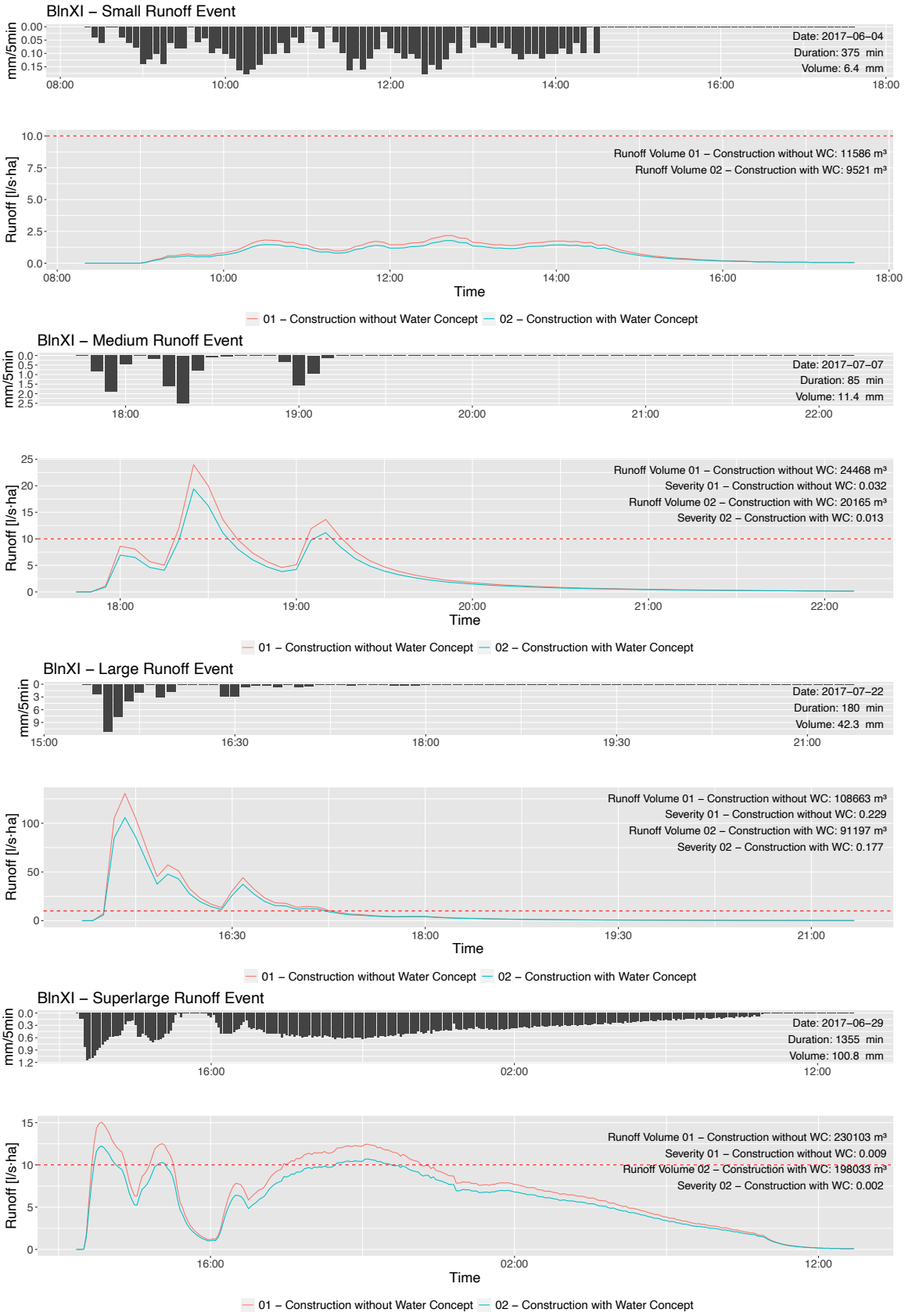

Figure A.11: Selected events - *BlnXI* Runoff

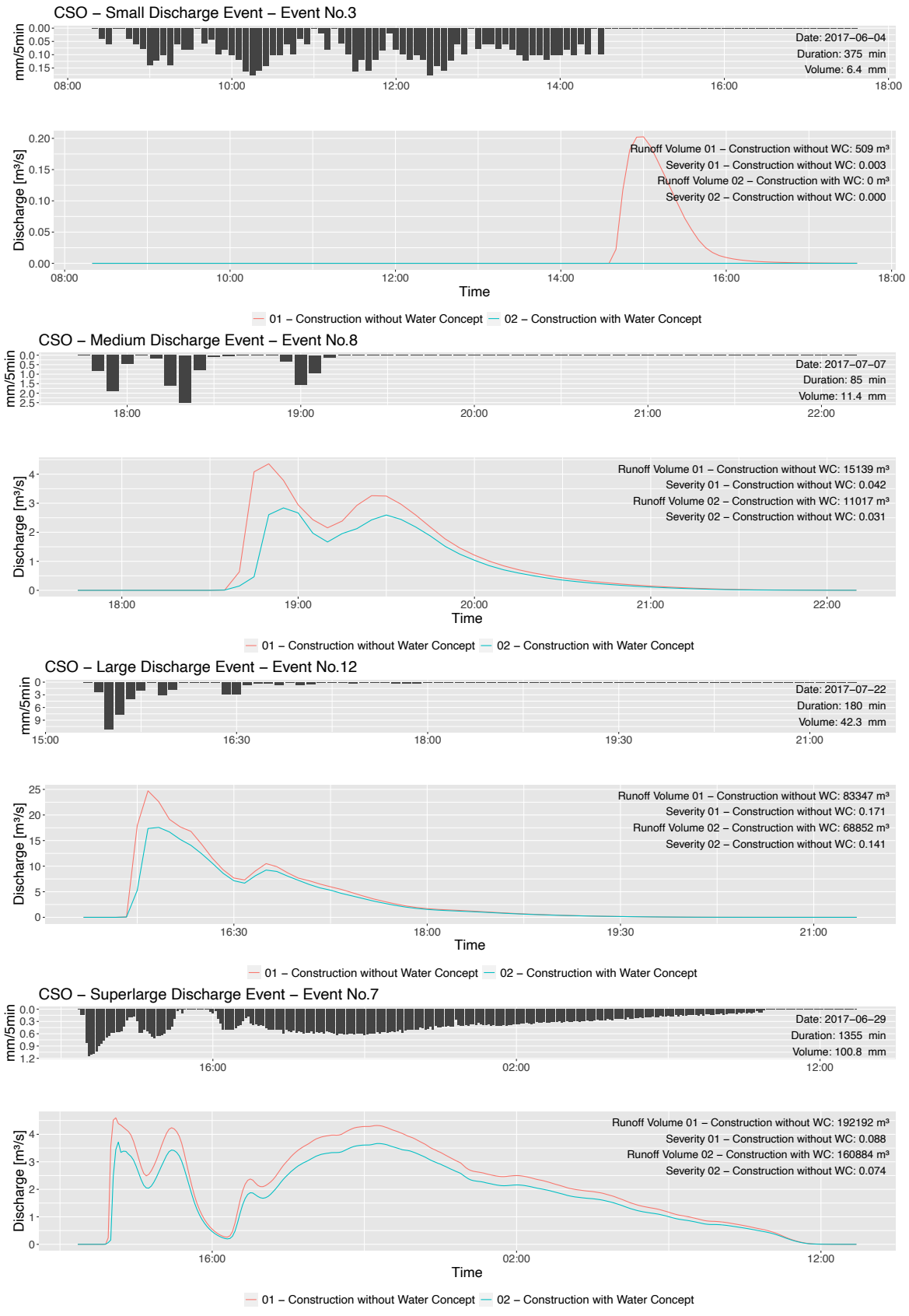

Figure A.12: Selected events - CSO Discharge

Event No.	Volume of Rain Event	Event Start	Event End	Event Duration (min)	CSO Volume - 01 Construction without WC (m^3)	CSO Volume - 02 Construction with WC (m^3)	Reduction of CSO Volume (%)
1	5.9	23.05.2017 21:15	24.05.2017 00:30	200	3829	1828	52.3
2	18	30.05.2017 13:30	30.05.2017 17:50	265	29874	23660	20.8
3	6.4	04.06.2017 14:40	04.06.2017 16:50	375	509	0	100
4	5.7	05.06.2017 20:00	05.06.2017 23:10	195	3295	1399	57.5
5	20	22.06.2017 22:55	23.06.2017 08:55	605	23860	16563	30.6
6	5.8	26.06.2017 09:05	26.06.2017 12:30	210	3047	1204	60.5
7	100.8	29.06.2017 12:30	30.06.2017 13:05	1355	192192	160884	16.3
8	11.4	07.07.2017 17:35	07.07.2017 19:20	85	15139	11017	27.2
9	5.1	10.07.2017 12:30	10.07.2017 15:35	190	1704	149	91.2
10	4.8	11.07.2017 17:30	11.07.2017 20:20	175	1614	98	93.9
11	21.3	20.07.2017 01:00	20.07.2017 07:25	390	35017	27659	21
12	42.3	22.07.2017 15:30	22.07.2017 18:30	180	83347	68852	17.4
13	4.9	23.07.2017 10:00	23.07.2017 13:05	190	1611	174	89.2
14	31.7	25.07.2017 01:40	25.07.2017 14:00	745	45433	36358	20
15	24.4	26.07.2017 08:40	26.07.2017 23:50	915	26957	20818	22.8
16	11.8	11.08.2017 02:50	11.08.2017 08:05	320	10193	6136	39.8
17	11.5	16.08.2017 10:45	16.08.2017 15:05	265	15759	11531	26.8
18	10.4	18.08.2017 20:45	19.08.2017 04:15	455	11431	7967	30.3
19	4.4	31.08.2017 16:35	31.08.2017 18:55	145	932	0	100
20	8.4	06.09.2017 16:35	06.09.2017 20:40	250	6588	4009	39.1
21	12.16	23.09.2017 21:30	24.09.2017 07:45	620	6210	2035	67.2
22	7.5	02.10.2017 16:05	02.10.2017 20:15	255	4471	1952	56.3
23	11.3	05.10.2017 10:10	05.10.2017 16:35	390	10192	6313	38.1
24	8.6	06.10.2017 15:30	06.10.2017 19:25	240	8846	5955	32.7
25	4.8	20.10.2017 22:35	21.10.2017 01:20	170	1600	77	95.2
26	16.1	25.10.2017 02:25	25.10.2017 07:55	335	19667	13950	29.1

Table A.3: Overview - CSO events